POLITECNICO DI TORINO

Master's Degree in Environmental Engineering for Climate Change

Mater's Degree Thesis

Estimation of volume, nutrient and carbon dioxide from a waste incinerator's flue gases as carbon source for an outdoor, continuous microalgae cultivation plant in south Sardinia.

Supervisors

Prof. Vincenzo Andrea RIGGIO

Prof. Deborah PANEPINTO

Candidate

Francesco Salvatore CORDA

20 March 2024

Contents

1 Abstract

In the present work, an outdoor continuous cultivation of the microalgae *Chlorella sp.* was dimensioned. The plant location was chosen as the Macchiareddu industrial area in South Sardinia (Italy). The choice was driven by the vicinity of Tecnocasic waste incinerator plant whose flue gases could represent a source of carbon. At first, a literature review concerning the best microalgae strains for gaseous CO_2 absorption was conducted. *Chlorella sp* was consequently selected as the microalgae species and Bubble Column was chosen as the photobioreactor type. Next, solar irradiance data were obtained from the European Photovoltaic Geographical Information System (PVGIS) for the chosen site. A model for irradiance control through the use of automated light-diffusive nets was developed to optimise the irradiance components at the surface of the reactors along the seasons. Then the Lambert-Beer law was used to model the light distribution inside the reactor volume for every hour of the year. The Molina growth model was consequently applied in order to estimate the biomass production as a function of irradiance. Finally, with the assumption that all the required carbon dioxide would be provided from the waste incinerator plant through an ammine capture system, the specific energy lost per ton of burned waste was computed. All the calculations were done in MATLAB. The technical cut off for the dimensioning of the plant was the harvesting flow rate, assumed in this case as 500l/h, for 16 hours per day 365 days per year. Results from the model showed a potential biomass productivity of 0.021 g/l d, an annual biomass production of 40 tons per year and a required operating volume of 7.139 m^3. The 84.8 tons of required carbon dioxide for growth of the microalgae would represent the 0.11% of what is emitted every year by the waste incinerator. The energetic impact of the carbon capture and carbon dioxide compression processes on the waste incinerator energy production was found as orders of magnitude lower than the specific energy production and therefore negligible.

List of Figures

List of Tables

2 Introduction

In the present era, the rising of carbon dioxide (CO_2) concentrations in the atmosphere is widely acknowledged as the most significant contributor to global warming. Terrestrial plants can capture atmospheric CO_2 through photosynthesis but are projected to mitigate only 3–6% of global CO_2 emissions. In contrast, the potential carbon dioxide uptake capacity of microalgae is reported to be 10 to 50 times higher than that of what the common sense recognise as "plants" [11].
Moreover, microalgae possess the capability to efficiently convert the biologically sequestered CO_2 into more complex organic compounds, ranging from lipids, to carbohydrates, to pigments and even hydrocarbons. Subsequently, the biomass of microalgae can be utilized as a valuable source of bio-polymers, as fertilizers, live feed, medicines, food supplements and many other high-value products which now days are already utilised in very specific market niches. These product can be, in some cases, substitutes of fossil-fuel based products making microalgae a possible tool for the neutralisation of certain sector's emissions.
While many microalgae cultivation plant are already operating around the world, bottlenecks in production costs make this kind of business economically sustainable only for very specific and high-valued end products and only in very specific locations.
Overall, being photosynthetic organisms, microalgae need light, carbon dioxide and nutrients to grow. The way of providing these three main requirements determines the type of cultivation and the type of plant. Despite certain microalgae species have been around earth for millions of years and are able to withstand a wide range of extreme conditions, the environment into which these organisms grow have to be carefully controlled in order to have a successful and economically sustainable production.
Several options have been historically experimented, with the most successful ones being open ponds and enclosed photobioreactor. Biomass production plant can both be artificially or naturally illuminated. Carbon dioxide can be uptaken from the atmosphere or directly injected at high concentration and fine grade into the cultivation to enhance the growth rate. Nutrients can be synthetic or provided through organic compounds commonly found in digestate, urea or waste streams.
The scope of this work is therefore to provide a method suitable for the first dimensioning of an outdoor, enclosed microalgae cultivation plant and to apply it into a real case scenario where part of the flue gases emitted from a waste incinerator plant in south Sardinia are used as carbon source for the cultivation of *Chlorella sp.*
A brief overview of the waste incineration topic is given with emphasis on related emissions and on how a cogenerative incineration plant works. Next, a selection of high-CO_2 tolerant species is done according to existing literature experiments. An overview on different types of microalgae cultivation plants and real world example of flue gas utilisation for cultivation purposes is also given. Related topics such as nutrients requirement, CO_2 supply, temperature and illumination are moreover detailed.
In order to calculate the biomass production in the chosen location, hourly local solar radiation data from European Photovoltaic Geographical Information System (PVGIS) are implemented in the Lambert-Beer law to model the irradiance distribution inside a generalized Bubble Column Photobioreactor. The Molina growth model is then applied to estimate the annual biomass production of a selected microalgae species considering a continuous culture with fixed centrifugation flow rate. Literature data re-

garding the max specific growth rate, the saturation irradiance and the light attenuation coefficient of selected strains are used. The microalgae is supposed to grow in an ideal environment where temperature, nutrient and mixing are always at the best setting for the growth.
Finally, given a specific elemental composition of the selected microalgae strain, annual carbon dioxide and nutrient requirement are found. All the carbon is provided at food grade following the capture of this latter from Tecnocasic waste incineration plant's flue gases. The capture of the required CO_2 is done by an monoethanolamine capture system whose energy demand, both in the form of electricity and heat, is completely full filled by the waste incinerator. Energy demand of carbon dioxide compression into a buffer-storage tank is also considered. Downsides of this energy uptake are computed in order to assess the possible impacts of such a method to the energetic balance of the waste incinerator.

3 Waste Production and Disposal

Any object which the holder discards or intends to discard can be called as "waste". Wastes produced in a domestic environment are recognized as municipal waste (MW), while other types of waste are classified as special waste (SW). These are product coming from any other general origin outside the domestic domain.
Waste is further classified as hazardous or non-hazardous based on its hazardous characteristics (content of certain substances, potential release of certain chemical species). The classification is done based on the codes listed inside the European Waste Catalogue (EWC).
Being the location of the present work south Sardinia, a more detailed focus on the waste management and production in italy and Europe will be given in following sections.

3.1 Generalities regarding waste production and disposal in Italy

Waste production and economic growth have been historically linked together by a positive correlation. In 2018, Italy produced about 30 million tons of urban waste, in line with the average of the last twenty years. By giving a look back at past decades in **Figure 1**, urban waste production grew rapidly from 2000 to 2006, then slowed down between 2006 and 2010 due to the economic crisis, and then decreased from 2010 to 2013. Since then, it has stabilized at around 29-30 million tons/yr, in line with the levels of the early 2000s. The positive correlation between Gross Domestic Product (GDP) and tons of produced wastes can again clearly be seen from **Figure 1**. The graph also shows household expenditure indicator, with reference to the year 2010 as further indicator.

3.1.1 The end of life of a waste

On very general terms there are 4 main end of life categories for wastes:

- **Recovery**. Wastes are used in substitution of other materials that would have otherwise been produced ex-novo for the same function.
- **Recycle**. Wastes are processed in a way to obtain products, material or substances which can be utilized for their original function or for secondary purposes.
- **Energy recovery**. Wastes are processed to burned in proper conditions in order to capture a part of their energy content and transform it in available electrical or thermal energy.
- **Disposal**. Wastes which cannot be recovered, recycled or burned are disposed in landfill under monitored conditions.

Upon specific classification of wastes, it is primarily possible to categorize them on the basis of the material which composes them. From here, by measuring the ratio between the amount of a specific material gone into recycle/recovery and the amount

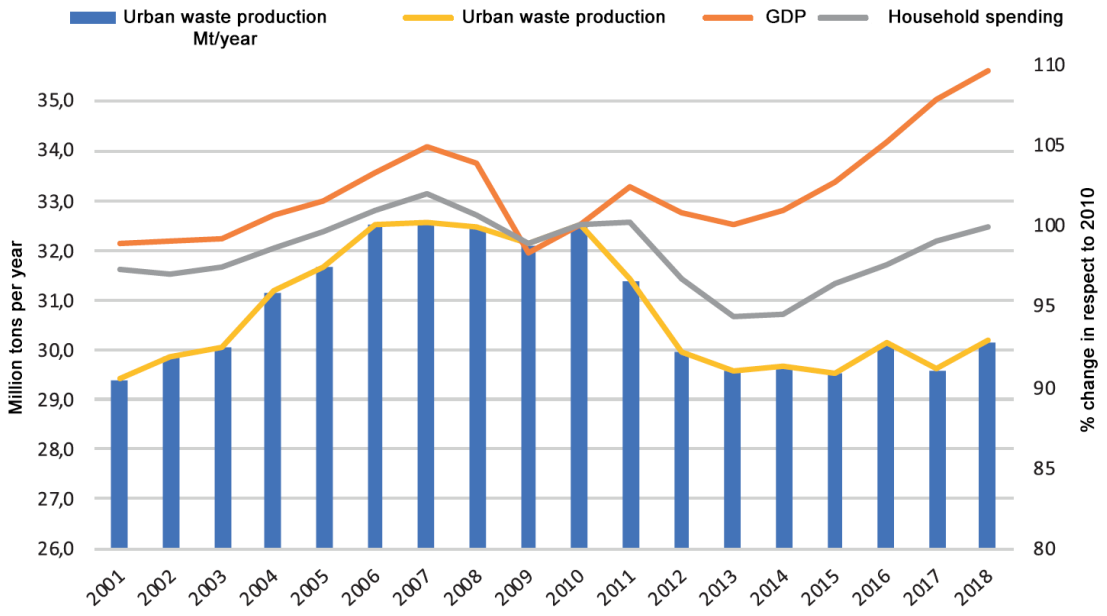

Figure 1: *Urban waste production in Italy from 2001 to 2018 (source of data: ISPRA Report on Urban Waste 2019) and corresponding concatenated trend values (references to the year 2010) of Italian GDP and household expenditure indicator (source of data: Eurostat). [79].*

of the same material introduced on the market during the same year, it is possible to retrieve the recycle/recover index of a certain material. The classification of different materials composing a waste is useful when the objective is the investigation of a precise the waste production, recovery/recycle or disposal of a particular service, activity or product.

3.1.2 Macroscopic origins of wastes in Italy

Waste processing is an activity whose intent is to select, separate and prepare different materials contained inside the municipal waste for ulterior processes. Wastes can belong to the most particular and detailed categories. In general, these categories are divided according to the type of material. Plastic, paper, organic fraction, the so called "Secondary Solid Fuel" (SSF) are the most common in Italy.

- **Wastes coming from processing of urban waste organic fraction**. This fraction is currently separately collected and sent to composting or anaerobic digestion plants. To ensure the efficiency of these processes, it is necessary to remove all non-compostable materials (NCM) erroneously disposed such as plastic, metals, and glass. It is also important to use bags compatible with the technology of the destination plant. However, many users still use bags made of unsuitable materials for the process. For this reason, some plants opt to remove all plastic or bioplastic bags regardless of their conformity at the head of the plant. The usual destination of all wastes generated during this phase is incineration or landfill.

- **Wastes coming from processing of plastic.** There have been lately multiple factors are affecting the quality of recycled plastic. The general upward pressure toward plastic recycling, together with the complexity of packaging and finally the Chinese block of plastic wastes import put in place in 2018 are all factors which influence the recycling system. The processing of plastic materials collected through separate waste collection generates a secondary stream called *Plasmix*. Despite being this mixed composition material suitable for energy recovery, it has seen a significant increase in landfill disposal in recent years. This increase may have been caused to the growing presence of non-recyclable foreign materials and the difficulty of finding outlets in energy recovery plants already saturated with flows of urban waste.

- **Wastes coming from proccessing of paper** On average, 6.5% of the materials entering the paper industry end up into recycling. These residues must be either sent to landfills or used for energy recovery. The stream mainly consists of pulper rejects, which are waste materials composed mostly of mixed plastic substances. In Italy, the amount of pulper rejects produced annually is 300,000 tons, and, in principle, it is a suitable material for energy recovery [79].

- **Wastes coming from production of Secondary Solid Fuel**. These are fluxes of materials coming from the conversion of residual fraction of municipal waste RMW into a fuel that can be burned or processed for energy recovery purposes. Being the residual municipal waste composed by all those material which could not be recycled, the processing of RMW generates secondary flows of wastes which varies depending on the quality and quantity of produced SSF. In general, the more work is done on the RMW to enhance its calorific value and quality, the larger will be these fluxes of secondary wastes. Disposal in landfill is the usual destination for these materials, even if this require further treatments such as bio stabilization.

3.2 Generalities regarding waste production and disposal in Europe

According to Eurostat [24], in 2021, a total of 2.135 million tonnes of urban and special waste were produced in the EU28, with the main contributions coming from Germany, France, and the United Kingdom. Italy contributed just over 6% of the total. The per capita production of waste widely varies from around 300 kgyear in Romania to around 835 kg/year in Austria. Italy places itself below the European average of 527 kg/year with a per capita production of 495 kg/year. The differences between countries can be linked to various socio-economic characteristics and waste classification methods.

3.2.1 The Waste Framework Directive, WFD

On the European level, the management of wastes is governed by the Waste Framework Directive (WFD - Dir. 2008/98/EC). The WFD is then received and implemented inside the national legislative framework of each country. In Italy, the directive is received and implemented inside the "Testo Unico Ambientale" (TUA, D.Lgs. 152/2006). Some fundamental definitions contained inside WFD regard the waste management

hierarchy. It states in order preferential path for wastes, starting from reducing the resources in use, preparation for reuse, recycling, other recoveries (such as energy recovery), and only as last solution, the disposal of it. The WFD allows for deviations from this hierarchy only in particular cases and only by demonstrating greater environmental benefit based on life cycle analysis.
In 2018, the "Circular Economy Package" was also introduced, which strengthens some concepts already contained in the WFD and introduces new objectives, such as increasing the percentage of preparation for reuse and recycling of urban waste, set at least as the 55% of MW by 2025 with annual increases of 1 percentage point until 2035. In Italy, these objectives overlap with those already set by Italian legislation in terms of separate collection of urban waste. The difference between the quantities of urban waste destined for preparation for reuse and recycling and those subject to separate collection is mainly in the selection/sorting residues produced by urban waste treatment processes.

3.3 Energy recovery from waste

3.3.1 Types of recovery

According to WDF, the preferential path for wastes should be to recycle and reuse. When these strategies are not applicable, energy recovery remain the only solution before landfill.
Now days, three main options are available to recover the energy contained inside residual fraction of municipal wastes.

- **Gasification** and **Pyrolisis**. Wastes are placed in a high temperature furnace with very low oxygene available (pyrolisis) or with no oxygen at all (gasification). Thanks to these anaerobic or anoxic condition, substances decompose to form simpler and high-energy content compounds. In case of pyrolisis, products are light oils or biochar while for gasification a mix of carbon monoxide, hydrogen and methane is obtained. These are all energy carriers which find application both in the chemical industry as in the energy generation.

- **Combustion** Wastes are burned inside a furnace with an excess of air. From a thermochemical point of view, the elements contained inside the organic compounds are oxydized at high temperature to generate simpler molecules at the gas state. Organic carbon is oxidized into CO and CO_2, hydrogen into H_20, sulphur into SO_x and nitrogen into NO_x. The inorganic matter is then removed as inert material.

Among these solutions, combustion has seen over time the largest adoption on an industrial scale. Several reasons are accountable for this largest adoption of incineration upon gasification and pyrolysys. A energy recovery plant which works with pyrolysis would require a relatively high purity of the MSW in order to have an high quality liquid fuel. Something that can be problematic when dealing with untreated and unsorted municipal waste. Moreover, the solid fraction of pyrolysis need as well to undergo an incineration process in order to be finally disposed. Gasification has

instead seen over the years a bottleneck in scales. At the current state, it can only be economically profitable in large scale plants which require significantly higher capital investment in comparison with incineration [5].

3.3.2 Waste incineration plants

As shown in a simplified representation in **Figure 2**, an incineration plant is made by several compartment. Starting from the head of the plants, wastes are processed, trimmed and transported into a combustion chamber. Here, hot flue gasses and inert ashes are produced at a temperature between 950-1000 °C with low concentration of oxygen (6-8%). The oxygen should however be enough to guarantee the complete oxydation of the organic matter during the combustion minimizing in this way the emissions of uncombusted products. Hot flue gasses then enter a heat recovery circuit while hashes are collected and opportunely disposed. One way to classify these plants is based on the type of combustion chamber. In *Fluidized bed incinerators* wastes are kept suspended upon an inert material (usually sand) and an air flow which constituted also the oxidizer is blown over them. In *Mechanical grate incinerators* air is instead blown from below a grate where wastes are poured.

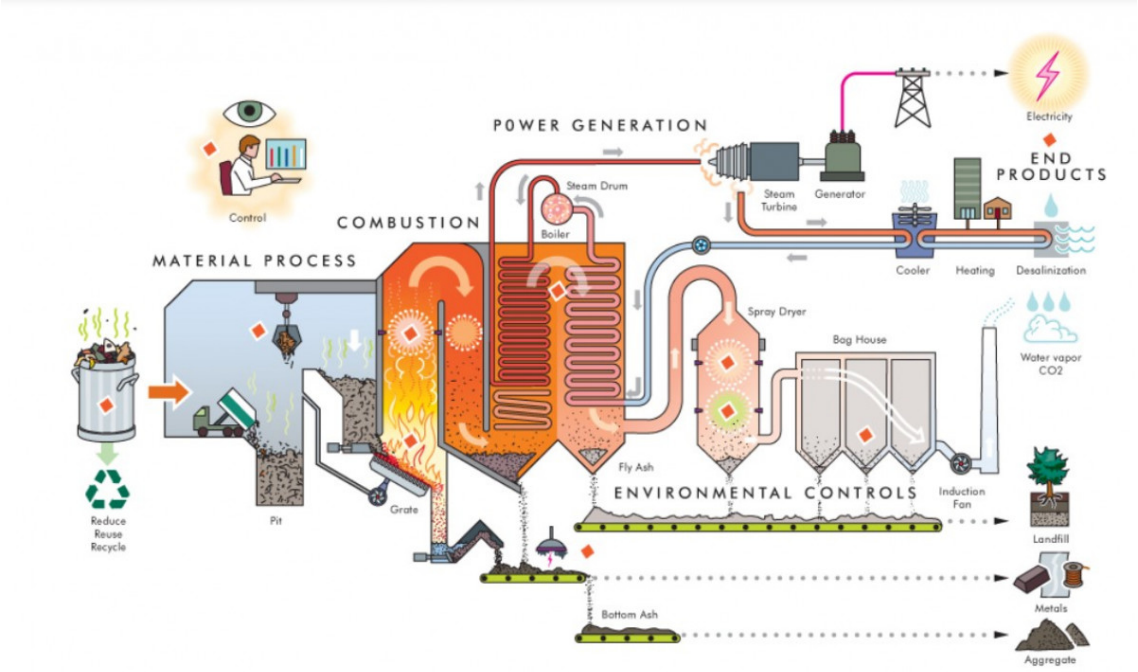

Figure 2: *Simplified cogenerative mechanical grate incineration plant. [81].*

Heat can be recovered from flue gasses through heat exchangers and used to produce electricity by warming up steam with consequent expansion in a turbine, or it can be used as source of heat for domestic or industrial purposes. Depending on the type of plant, the only electricity generation could be present or, in a a co-generative plant, both electricity and heat generation. Given an even input of material to both solutions, the co-generative approach remain the most efficient strategy for converting

energy with an efficiency that can reach 70% versus the 30% of a pure electicity generation [79].

3.3.3 Flue gas purification

On very general terms, an incineration plant produce three different types of emissions: one of solid type, regarding all the ashes and uncombusted material; one of liquids, since water is usually used to fix the ashes and finally the gaseous emissions. These last are composed by micro and macro components according to their concentration.
All those compounds whose concentration can be measured in order of mg/Nm^3can be considered as **macro pollutants**. In this category are contained dusts, nitrogen and suphur oxydes, carbon monoxide and halogen acids (mainly HCl and HF).
Micro pollutants are instead all those with much lower concentrations, in the order of $\mu g/Nm^3$. These are mainly inorganic substances such as heavy metals a(Cd, Cr, Hg, Pb) or organic ones such ax dioxines.
Finally, **Furans and polycyclic aromatic hydrocarbons**.
According to the current normative, emission reduction should be done by using the Best Available Techniques (BAT), as they are defined by IPCC Bureau document especially made for incineration plants.
Flue gases purification is however done in several step. Ashes and particulates are usually removed by a bag filters. Nitrous Oxide emissions require instead a denitrifying agent. This rose is usually taken by gaseous ammonia or urea. The agent is sprayed together with water and compressed air over the hot flue gasses reducing in this way nitrogen to its molecular state N_2. Micro contaminants like heavy metals, dioxines and furans are usually removed using active carbons or lime milk while acid gases (halogens and fluorinated) are sequestered by dry or wet washing.

3.3.4 Energy Recovery

It has already been said that waste incineration with energy recovery plants are capable to recover energy from the combustion of wastes in form of heat or electricity. As a matter of fact, in order to be considered "energy recovering", these plants have to satisfy certain parameters which distinguish them form an incineration only plant. In this perspective it is possible to quantify the goodness of a plant by comparing its energy performance with the one of a standard European power plant. This process is done by using Energy Efficiency R1 index, defined by the current EU normative and expressed as:

$$R1 = \frac{E_P - (E_F + E_I)}{0,97 \times (E_W - E_F)} \times CCF \tag{1}$$

where:

- E_P = Annual energy production in the form of electricity and/or heat;
- E_F = Energy supplied annually to the plant from fuels other than waste;

- E_W = Energy supplied annually to the plant from wastes;
- E_I = Annual energy importation other than that counted in EW and EF;
- 0.97 = correction coefficient. Considers losses from irradiation and slug discharge;
- "Climate Correction Factor", climate correction factor (currently in the range of 1.00-1.25; in the future between 1.00 and 1.12 depending on the local climate).

This index is not a proper physical efficiency but just a way to compare two different types of plants. Depending on the construction year of the waste incineration plant, it will be considered efficient or not. Plants built before 01/01/2009 are considered as "energy recovering" with a R1 equal or greater to 0.60, plants built after 31/12/2008 need to reach at least 0.65.

3.4 The environmental impact of waste incineration

The analysis of the environmental impact of waste incineration plants is based on two main criteria. The first regards the expected performance of the emission control system, expressed as the capacity to sequester pollutants according to the current normative. These emissions are also compared with the ones of nearby emitters intended as other point emitters or emission sectors. The second criteria is based on modeling simulation of local and regional concentration of pollutants. Simulation are performed in order to quantify the contribution of a particular incineration plant to the local atmospheric concentration of pollutants. The pollutants produced by combustion include both compounds typical of any combustion process such as acid gases NO_x and SO_2, particulates or various dimension, carbon monoxide and other organic carbon as well as specific substances typical of waste combustion, like heavy metals, other acid gasses such as HCl and HF and aromatic organic molecules. National sector legislation is based on emission limits at the chimney that cannot be exceeded and on indications contained in reference documents associated with the best available techniques in the sector (BREF). The latter describes the emission which would be expected from the application of the BAT. It represents an important reference for the Authorities responsible for authorization procedures. The intrinsic value of the BREF is therefore very significant in terms of applicability due to their informative content, periodically updated with extensive investigations on different types of plants and full-scale purification systems, which allows to capture technological and system capabilities in emissions control. The philosophy is that of "continuous improvement" of technologies and the consequent need for adaptation by all plants, with a view to continuously reducing impacts on the environment.

3.4.1 Emission at the chimney

As example to this, **Table 1**, shows Current emission limits in Europe (2010/75/EU) and concentration achievable with BAT [79]. It is possible to notice BAT tend to be more conservative then the limit them self. This is due to the use of advanced technologies for flue gas treatment, which are characterized by the almost exclusive use of

Pollutant	2010/75/EU, IED	BAT
Dusts	10	<2-5
HCl	10	<2-8
HF	1	<1
SO2	50	5-40
NOx	200	50-150
COT	10	<3-10
CO	50	10-50
Hg	0,05	0,001-0,02
Cd + Tl	0,05	0,005-0,02
Other metals	0,5	0,01-0,3
PCDD/F (ngTEQ/m3)	0,1	<0,01-0,08
NH3	–	2-10
IPA (μg/m3)	10	–

Table 1: *Current emission limits in Europe (2010/75/EU, Industrial Emissions Directive) and BAT emission interval (expressed in mg/m3 daily average)*

bag filters as the main dust removal unit, the widespread adoption of Selective Catalytic Reduction (SCR) for nitrogen oxide, and the wide diffusion of dry systems for the treatment of acidic gases integrated with the addition of powdered adsorbents for the removal of volatile toxic species such as mercury, dioxins, and furans. The double dust removal, with a preliminary stage also entrusted to electrostatic filters, contributes to further enhancing the performance of these systems. The dust concentrations in the gases emitted from the chimney are now of the order of magnitude of those measured in ambient air in urban contexts.

3.4.2 Emission contribution to atmospheric concentration

Emission data by sector are collected and published by the European commission every year thanks to the constant activity of monitoring and reporting done by each single country. In Italy, ISPRA is the organism in charge of the annual inventory of emissions. As **Table 2** shows, at the year 2021 the contribution of Waste incineration to Italian emissions was in most case inferior to every other sector's emissions. This is again the result of both strict normative regarding emission limits and of the "continuous improvement" approach.

Another way to look at single sector's contribution to atmospheric emission is to compare emission factors by source. The waste sector, particularly waste incineration, is minor but still significant contributor to various pollutants. In 2021 the sector was responsible for a 13.9% contribution to the total Italian dioxin emission. Other contributions were smaller but still considerable as shown in **Table 3**

	Combustion in energy and transformation industries	Non industrial combustion plants	Combustion - Industry	Production processes	Solvent and other product use	Road Transport	Other mobile sources and machinery	Waste treatment and disposal	Agricolture
SOx	9.9	9.8	27.6	19.1	0.005	0.4	7.6	4.1	0.1
NOx	35.8	85.1	49.6	10.4	0.1	254.3	120.5	2.3	52.7
NH3	0.1	1.3	1.2	0.4	0.3	5.3	0.0	9.2	332.6
NMVOC	3.5	175.4	7.3	56.2	319.8	117.4	21.7	10.6	125.4
CO	34.5	1310.5	99.6	69.5	3.8	357.9	114.1	42.2	11.7
PM10	0.6	97.9	7.7	29.8	5.8	20.5	8.1	6.0	23.1
PM2.5	0.5	96.6	6.4	8.7	4.4	13.5	8.1	5.6	5.3
Pb	1.5	14.4	81.0	72.6	1.2	38.5	0.8	0.2	0.02
Cd	0.1	0.5	1.3	1.2	0.3	0.5	0.0	0.4	0.1
Hg	0.49	0.49	1.74	3.11	0.0	0.18	0.0	0.10	0.02
PAH	0.4	52.9	0.5	8.5	0.0	2.5	0.3	1.1	0.4
Dioxin	4.0	104.7	62.1	90.8	0.01	8.0	1.0	43.7	0.1

Table 2: *Atmospheric emission contribution by economic sector in Italy [97].*

Pollutant	Municipal waste incineration contribution in National Total Emissions
Dioxin (D)	13.9%
Black Carbon (BC)	8.2%
Cadmium (Cd)	8.1%
Hexachlorobenzene (HCB)	7.0%
Ammonia (NH3)	2.6%
Carbon Monoxide (CO)	2.1%
Mercury (Hg)	1.7%
NMVOC	1.2%
PAH	1.6%
PM2.5	3.8%
PM10	3.0%

Table 3: *Waste Incineration contribution in Italy 2021 total emission, ISPRA 2023 [97].*

3.5 Tecnocasic incineration plant

Tecnocasic s.p.a. is a sardinian company entirely own by Cacip, namely the Industrial Consortium of the Province of Cagliari. Among the different activities brought up by Tecnocasic, waste incineration coupled with energy production is one of the most important. Tecnocasic waste incineration plant, shown in **Figure 3** is situated inside Machiareddu industrial area, just outside Cagliari, in south Sardinia. The sorrounding of Tecnicasic is represented by the wild and environmentally protected Santa Gilla lagoon. This lagoon represents a sanctuary for several and very rare volatile species in Sardinia such as pink flamingos, kentish plover and many others.

Figure 3: *Aerial view of Santa Gilla lagoon and Tecnocasic waste incineration plant in Macchiareddu industrial plane.*

In this controversial location, several firms operated in the sector of chemicals, waste management, metallurgy and energy.
Tecnocasic incineration plant receives municipal waste from the whole Cagliari province. Wastes are however well differentiated both at households and at the head of the plant so that only the dried residual waste fraction is sent to the incinerator. Currently, the waste-to-energy platform works on three different combustion lines and utilises the heat produced by the combustion of an annual 120,000 tons of dried municipal waste to generate high pressure steam. The steam is then sent into two separate turbines where its expansions drives an annual electricity production of about 40 GWh. The plant is however undergoing several upgrades. In the upcoming years the actual electricity generation system will be dismantled. The new system will have a 7 MW heat capacity output for district/industrial heating and in parallel an electricity generation capacity of 16 MW.

A schematic representation of the actual system is given in **Figure 4**.

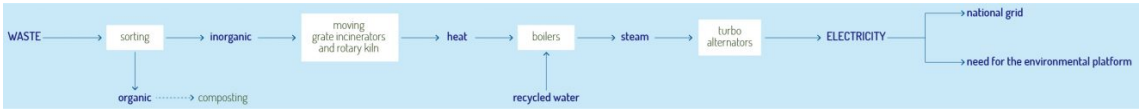

Figure 4: *Schematic representation of the electricity generation cycle*

The post-combustion chamber is supplied by a system for the controlled introduction of a mixture of water, compressed air and urea into the exhaust gases. This mixture acts for the reduction of NOx (nitrogen oxides) concentrations. The combustion gases, after passing through the steam generator (boiler), enter the first abatement system consisting of an electrofilter for coarse dust removal. Cooled through a heat exchanger, the gases are then directed to the upper part of a reactor where a dry mixture of lime and activated carbon is injected into the gas flow. The reaction allows for the reduction of most acid gases (HCl, HF, SO2), organic micropollutants, mercury, and any heavy metals. The remaining mixture of dust, salts, lime, and carbon within the gas flow is then sent to bag filters for further reduction of the aforementioned pollutants and for dust removal. In the scrubbing tower shown in **Figure 5**, the gases are first contacted with a mixture of water and soda (quench) recirculated from the bottom of the column. Subsequently, they undergo treatment with water and soda countercurrently in a first wet stage filled with highly adsorbent activated carbon-coated plastic material (ADIOX).

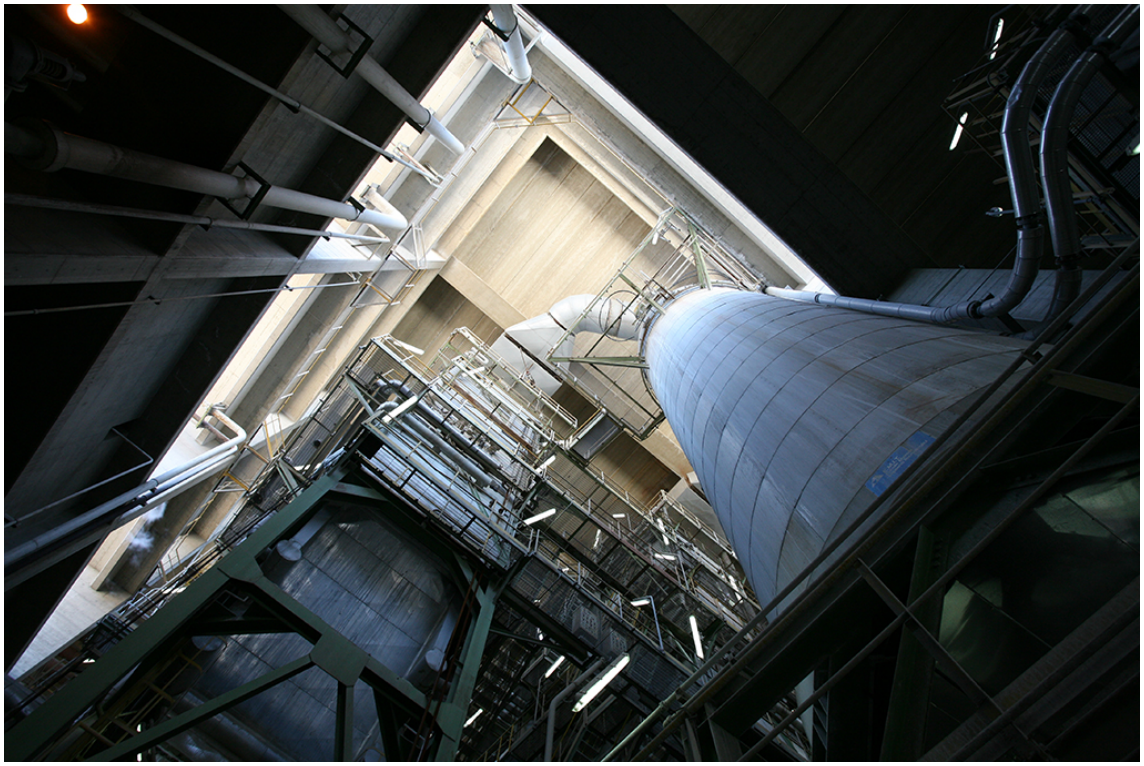

Figure 5: *The scrubbing tower seen from below, inside the plant.*

This column serves the dual purpose of cooling and reducing acid gases such as hydrochloric acid, hydrofluoric acid, and sulfur oxides, as well as removing micropol-

lutants. Two additional sections, also filled with ADIOX rings, follow for further removal of dioxins; one of the two sections can be used in both wet and dry modes. The saturated and clean gas flow leaving the scrubbing tower passes through the flue gas-to-flue gas heat exchanger to be heated and released into the atmosphere through a multi-channel chimney. The chimney consists of an external reinforced concrete chamber, inside of which a duct for conveying the exhaust gases to the Rotary Kiln line is installed.

Figure 6 shows the incineration plant from the satellite together with the possible location of the biomass production plant.

Figure 6: *Sentinel 2 satellite image of the waste incineration plant (in red) and the possible location of the microalgae production plant in Macchiareddu, south Sardinia.*

Figure 7 shows the complete scheme of Tecnocasic plant.

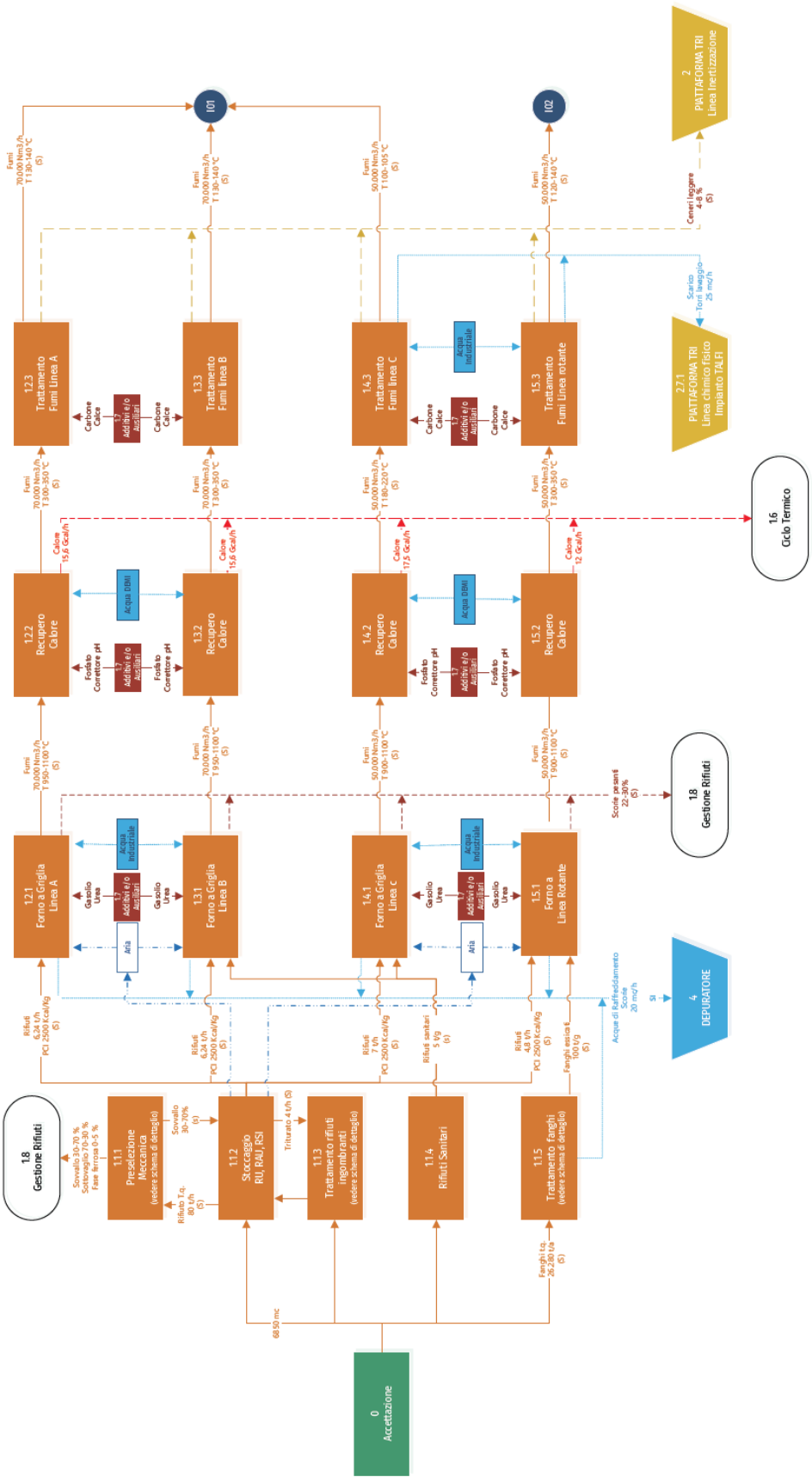

Figure 7: *Block scheme of plant's complete production cycle [137]*

4 Microalgae

Microalgae are microscopic, primitive and unicellular, organisms with a fundamental ecological role in our planet. They are responsible for the largest part of oxygen production and they serve as the base of the food chain, being a nutrition source for a wide range of animals and subsequently as well as people. In general terms, microalgae perform photosynthesis, converting in this way carbon dioxide into proteins, carbohydrates, lipids, minerals, and vitamins and other substances while releasing oxygen at the same time. Depending on the strain, these organism are able to survive and reproduce over a wide range of conditions in terms of pH, temperature, salinity of the water and gas concentration. All these features make them a potentially viable tool for carbon recycling. Since they are rich in minerals, vitamins, oils and fatty acid methyl esters, several value-added products and biofuels can be obtained from them as **Figure 8** shows.

Figure 8: *Microalgae as precursor to several secondary products [104].*

Moreover, their high tolerance to carbon dioxide makes them very advantageous in utilizing CO_2 from flue gases. They are fast growers with biomass volumes that under optimal conditions can double within 24 h [101].

Before going more in detail about microalgae production, harvesting and conversion of microalgae into valuable products, their main advantages are:

- natural solar energy is used with photosynthesis efficiency 10 to 15 times higher than the one of terrestrial plants. This means that microalgae can be used for applications where high fluxes of CO_2 need to be absorbed. [102].
- fast growing rate, as these microorganisms can double their concentration within 24 to 48 hours [102].
- adaptability of growing conditions. Microalgae living conditions are of the most diverse and distributed. They can tolerate high concentration of CO_2, they can be selected according to temperature, salinity, pH, and a wide variety of water sources can be used to constitute their growing environment (fresh, blackish, seawater and wastewater). For example, municipal wastewater and agroindustrial wastewater can be used as sources of nutrients to grow microalgae at low cost [103].
- high valuable types of microalgae can be cultivated and used for the making of food, animal and aquaculture feed, cosmetics, pharmaceuticals, fertilizers, and biofuels (e.g., biodiesel, biohydrogen, aviation oil, biomethane). These means that carbon dioxide can be recycled with an overall reduction of emission of the production chain of these products [104].

4.1 Eukaryotic and Prokaryotic

Despite the huge variability in microalgae strains and species, which can be counted in dozens of thousand, only a dramatic small percentage of these have been studied sufficiently. On a micro scale, cells are the basic unit for life. Many types of cells and therefore cells function exist. Cellular structure is one possible way to classify living organisms. If organelles inside the cell are well separated from the cytoplasm by mean of a membrane and so for the nucleus, these are *Eukaryotes* organisms. If instead there are no such separation the organisms are called *Prokaryotic*. In the first class fall cells found in human, plants, fungi and insects while bacteria are the main constituent for the latter. Among the multitude of microalgae strains, some belong to *Eukaryotes* and some to the *Prokatyotes* class. Common strains like *Spirulina* are so-called cyanobacterias, prokaryotic algae which among many other pigments, mainly contain chlorophyill **a**. Since cellulose is lacking in these bacteria digestion is also facilitated, making them a possible food source for human and animal consumption. Eukaryotes "green algae" and "red-algae" such as *Chlorella*, *Dunaliella* and *Porphyridium* contains instead different pigments like chlorophyll **a**, chlorophyll **b**, carotenoids, starch, amylose, amylopectin and other substances. The classification of microalgae is now day based on the kind of pigment, chemical nature of storage product and cell wall constituents. Thanks to this variability in cell components, microalgae find a wide range of application in several different sector [98].

4.2 High CO_2 tolerant microalgae species

The selection of the microalgae species to grow must be done according to the purpose of the cultivation. If the goal is to recycle the largest amount of carbon emit-

ted by a nearby source, species with a good tolerance to gaseous CO_2 should be preferred in those case where maximising the gaseous carbon uptake is a priority. At the same time, living conditions for these species should imply pH certainly below 7, in an range where gaseous carbon dioxide is the prevalent carbon source as will be shown in **Section 4.5.3**. Arun et al. (2018), Van Den Hende et. al (2012) and Salih et al. (2011) provided separately a wide review of more than 80 experiments concerning the cultivation of microalgae with the common intention of investigating significant species for flue gas carbon capture and remediation [3], [8], [21]. From these resources have been selected only species whose experiments utilized CO_2 concentrations above 10% vol and where the pH of the culture was equal or below 7. Results of the selection are reported in **Table 4**.

Species	Reactor type	V (l)	Light Intensity	Light/dark (h)	Outdoor	T(C°)	CO_2 (%)	pH	CO_2 fixation rate (g l-1 d-1)	Biomass production			Ref
										Value	U. of measure	g l-1 d-1	
Anabaena sp.	BCPB	5	250 [b]	12:12	no	35	10	5.9	1.01	2.09	g/d	0.418	[6]
Botryococcus braunii	PB	3	150 [b]	24:00	no	25	20	7	1.10	2.31	g/l (25 days)	0.092	[12]
Chlorella sp.	BCPB	1	84 [b]	12:12	no	18	10	6	0.5	0.27	g l-1 d-1	0.268	[76]
Chlorella pyrenoidosa	EF	-	180 [b]	24:00	no	25	10	7	0.260	1.55	g/l (14 days)	0.111	[14]
Chlorella pyrenoidosa	SB	4.2	4500 [d]	24:00	no	-	15	6.5	-	0.95	g l-1 d-1	0.950	[16]
Chlorella vulgaris	CF	0.1	165 [b]	24:00	no	22	10	6.0	0.522	0.480	g l-1 d-1	0.480	[39]
Euglena gracilis	PB	1000	-	-	yes	28	7.5	3.5	-	0.710	g/l (5 days)	0.142	[56]
Euglena gracilis	CF	0.5	100 [b]	24:00	no	24	15	4.0	0.234	1.32	g/l (7 days)	0.189	[22]
Nannochloripsis Oculata	BCPB	0.8	300 [b]	24:00	no	26	15	7.0	-	0.372	g l-1 d-1	0.372	[65]
Nannochloripsis sp	CF	1.0	10000 [d]	24:00	no	25	11	6.3	-	0.510	g/l (8 days)	0.064	[42]
Nannochloripsis sp	EF	0.5	60 [b]	24:00	no	30	10	6.7	0.256	-	-	-	[48]
Scenedesmus sp	PB	0.3	100 [b]	24:00	no	28	10	6.1-7.3	0.91	3.92	g/l (8 days)	0.490	[80]
Scenedesmus obliquus	EF	-	180 [b]	-	no	25	10	7	0.288	1.84	g/l (14 days)	0.131	[14]
Scenedesmus obliquus	BCPB	2	150 [b]	-	no	28	10	-	-	-	-	-	[64]
Scenedesmus obliquus	EF	-	5496 [d]	12:12	no	25	13	7	0.106	0.056	g l-1 d-1	0.056	[50]

Table 4: *Selected experiments where CO_2 concentration in feed gas was above 10% (vol/vol) and pH was equal or below 7. APB: air-lift photobioreactor, BC: bubble column photobioreactor, CF: conical flask, EF: Erlenmeyer flask, FBC: feed batch cultivation, FM: fermenter, FPB: flat-type photobioreactor, PB: photobioreactor, SAT: spraying absorption tower, SB:sequential bioreactor. [b] In $\mu mol m^2 s^-1$. [c] In $\mu Em^2 s^-1$. [d] In lux. [e] In $\mu Em^2 s^-1$*

In the next paragraph will be performed an overview of each one of these species highlighting experimental results, possible use and application and already existing cultivation plants.

4.2.1 Anabaena sp

Anabaena sp is a filamentous cyanobacteria whose filaments can count 100 and more identical vegetative cells. Together with some other cyanobacteria this microalgae is able to perform not only oxygenic photosynthesis but also nitrogen fixation [58]. Moreover, studies demonstrated how *Anabaena sp* can be used to produce phycobiliproteins, a group of water soluble protein responsible for light-absorption in cyanobacteria. Some of these phycobiliproteins find several application in food and cosmetic industries as colorant since they are non-toxic nor carcinogenic, but also as anti-oxidant,

anti-carcinogenic, anti-proliferative, anti-inflammatory and even as chemical tracer in medical diagnosis and treatment of diseases [59], [60]. These are therefore high valuable products. The price of 10 mg of pure phycocyanin, one of the phycobiliproteins group, can reach up 250 $ on the market [57].
Chang et al. 2011 showed instead a good tolerance of *Anabaena sp* at a volumetric concentration of 15% CO_2 and pH as low as 5.65. The culture was grown in Arnon medium with no carbon source other than CO_2. Indicated specific growth rates at 5%, 10% and 15% CO_2 level were respectively 0.27 ± 0.08, 0.24 ± 0.14 and 0.13 ± 0.07 d^-1 and specific CO_2 sequestration rate reached its maximum value of 1.01 $g\mathrm{CO}_2\ \mathrm{L}^{-1}day^{-1}$ in the 10% CO_2 level batch experiment. Authors of this study claimed that "this strain would achieve CO_2 reductions with injection of power-plant flue gas directly into photobioreactor to simplify CO_2 sequestration system" [6].
In 1991 Wang et al. published the results of a 3 year long large scale cultivation experiment of several strains of *Anabaena sp* in a continental subtropical region of China. The cultivation was a greenhouse open pond type with 5170 m2 of extension an 10-12 cm deep. Biogas (CH4 70%, CO_2 30% etc.) was injected into the ponds from a nearby methane generating pit. The average biomass productivity days reached 7-11 $gm^{-2}d^{-1}$ showing productivity peaks of 22 $gm^{-2}d^{-1}$ during optimal growth conditions in July and August. Protein content was 35-40% of dry weight [11].
A view of *Anabaena sp* under micrscope is provided in **Figure 9**.

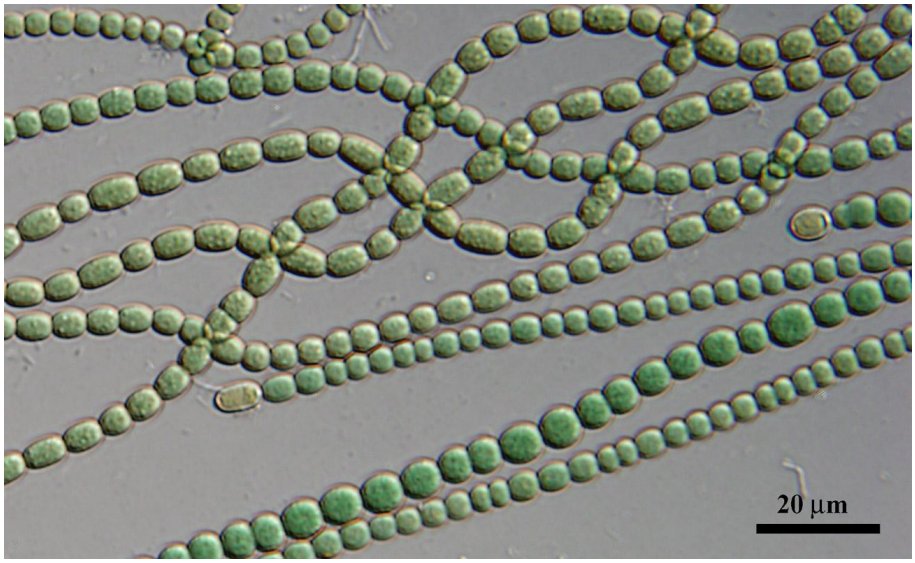

Figure 9: *Filamentous Anabaena sp. under the microscope [10].*

4.2.2 Chlorella

Chlorella is a green algae measuring in a range between 2μm and 10μm. Can be found in both fresh and marine water habitats and its presence of the earth is dated back to 2,5 billion of years ago. Once dry, this algae claims an high lipid and protein content, respectively ranging between 42 to 58% and 5 to 40% depending on growing conditions. The optimal pH for these species ranges between 6.5 and 7.5 while, despite

a good tolerance for temperature variation, a cultivation should always stay between 25 and 35°C in order to ensure proper growing condition and do not fall into inhibition of cell reproduction [98].

Zhao et al. 2015 successfully grew *Chlorella sp* under different CO_2% concentration finding the 10% vol as the best one in terms of biomass concentration , specific growth rate and CO_2 fixation rate. As the concentration of carbon dioxide increased, all performance parameters decreased. Despite this, even at 20% vol CO_2 and pH 5.5 *Chlorella* continued to grow. Specific growth rate, biomass production rate and carbon fixation rate changed respectively in 0.375-0.263 d^{-1}, 0.274-0.114 $gL^{-1}d^{-1}$ and 0.503-0.209 $gL^{-1}d^{-1}$ when shifting from 10% to 20% CO_2 [76]. Park et al. 2020 found instead an optimal growing condition for *Chlorella sp* at 15% CO_2 concentration with 43.2 $LL^{-1}d^{-1}$ loading rate and pH between 8-9. With these growing parameters *Chlorella* reached 1.785 $gL^{-1}d^{-1}$ CO_2 fixation rate and a 0.621 $gL^{-1}d^{-1}$ biomass productivity [77]. Among *Chlorella* more common strains, *Chlorella pyrenoidosa* was found to be more CO_2 tolerant than *Chlorella vulgaris* [8]. A sample of *Chlorella* under microscope is shown in **Figure 10**.

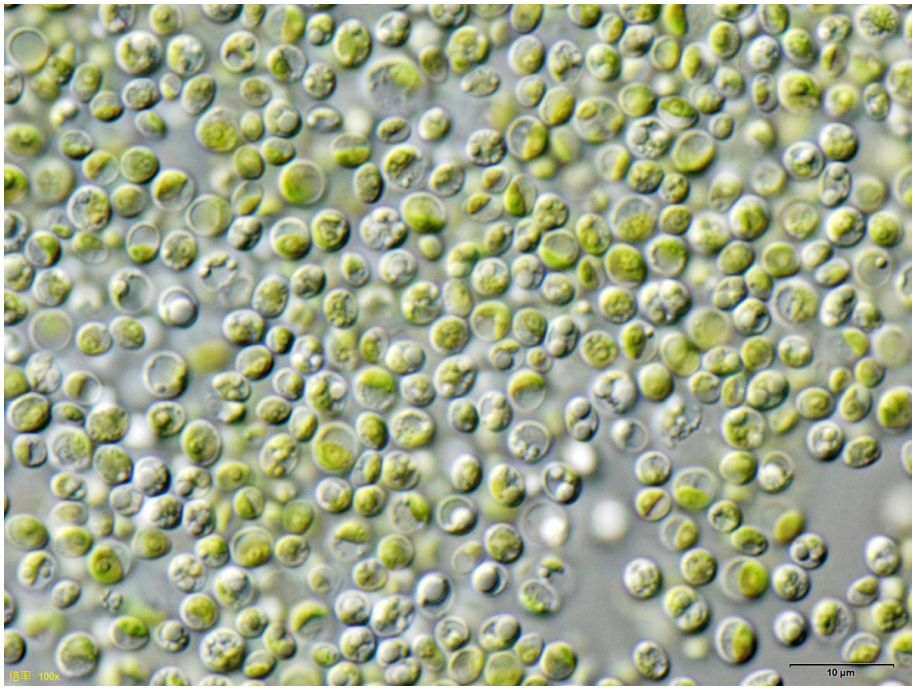

Figure 10: *Chlorella vulgaris under the microscope [90].*

For what concerns its potential on the market, since *Chlorella* is already widely recognized source of food integration compounds and a wide variety of products are already available and commercialized. *Chlorella* products are rich in essential nutrients, such as high-quality protein, dietary fibers, and polyunsaturated fatty acids, including alpha-linolenic and linoleic acids. Moreover they contain vitamins D2 and B12 which are usually not found in other plant based food. Its protein content is higher than soybeans and beyond that the amino acid composition profiles are evaluated as protein for human nutrition. Daily *Chlorella* consumption is also believed to be bene-

ficial thanks to a substance called b-1,3-glucan, which is an active immunostimulator and has many other functions such as reducer of blood lipids [15].

The largest producer of *Chlorella* is Taiwan Chlorella Manufacturing and Co., located in Taipei, Taiwan. This company produces an impressive 400 tonnes of dried *Chlorella* biomass per year. Another significant *Chlorella* production site is located in Klötze, Germany, where a tubular photobioreactor is used to produce 130-150 tonnes of dry biomass per year. Shown in **Figure 11**, this photobioreactor is made up of horizontally arranged glass tubes that run vertically and have a combined length of 500 km, with a total volume of 700 m3. According to a survey on european microalgae producers conducted by Araújo et al. (2020), Business to Business values (on dry weight) for *Chlorella sp.* varies between 25–50 €/kg. In contrast, Business to Consumer values range between 150 and 280 €/kg due to higher values for small package sizes and finished products. The global *Chlorella* market generates annual sales exceeding US$38 billion [37].

Figure 11: *Roquette Klötze GmbH & Co. KG Chlorella vulgaris cultivation plant [32]*

4.2.3 Botryococcus braunii

B. braunii is a green colonial microalga belonging to the member Trebouxiophyceae. Widely distributed on all continents, can be found in freshwater, brackish and saline lakes, reservoirs, and even in small pools. That thanks to its unique chemical synthesizing capabilities has an immense potential as biofeedstocks for various

industries related to biofuels, pharmaceuticals, nutraceuticals, and nanometer materials. This microalgae can be considered as a real bio-factory of hydrocarbons. In fact, its main three races "A", "B", and "L" are named according on the type of synthesized hydrocarbon. Differently from other microalgae who accumulate lipids mainly under stress condition such as nitrogen deficiency, *B. braunii* can continuously produce them during whole logarithmic growth phase. Moreover about 70% of hydrocarbons from *B. braunii* are contained in the extracellular matrix, thus the energy input and costs in extraction hydrocarbon from *B. braunii* are significantly reduced compared to other microalgae where lipids are contained inside the citoplasm [19]. Apart from hydrocarbon production, *B.braunii* is also a rich source of caroteoids. In particulare, B and L species of this alga produce α and β-carotenes, echinenone, canthaxanthin, lutein, violaxanthin, loroxanthin, and neoxanthin, with lutein in dominant position among all others. Luteinis already implemented several products sold on different markets among which are present: animal feed, functional foods, pigment for aquaculture and prevention of generative disorders. Doubling time of *B. braunii* is usually 6-7 days in natural condition but this time is lowered to 3-5 days when cultivated in optimal condition [17].
Yaming at al. 2010 conduncted an experiment where *B. braunii* was cultivated with continous illumination in a 3 L photobioreactor at different CO_2 concentrations. Among all the conditions, the maximum algal biomass was 2.31 gL^{-1} on day 25 with 20% CO_2 and pH as low as 6.3 [18].
Wan et al. 2019 conducted an experiment where the *B. braunii* was initially cultivated heterotrophically in a 3L reactor on CHU 13 medium enriched with 2 gL^{-1} glucose at pH 7.5. This first phase was conducted with the intention of developing a method to enhance the concentration of inoculums which were then used to start different photoautotrophic coltures. The final dry cell weight reached 37.02 gL^{-1} on the 28th day, a quantity that is reported to be the highest in literature. Despite this high-density heterotrophic culture of *B. braunii* provided a large quantity of biomass as seeds for the following photoautotrophic stage, inopportune weather condition probably caused a limitation of grow potentialities. The final dry cell weight were 0.57 gL^{-1}, 0.52 gL^{-1}, and 0.43 gL^{-1} in 1 L column, 3 L flat panel photo-bioreactor and 120 L circle pond respectively which were all located outdoors [19]. A cluster of *B. braunii* under microscope is shown in **Figure 12**.

4.2.4 Euglena gracilis

Euglena gracilis is a unicellular phototrophic organism common in freshwater environment. One of the remarkable features of *E. gracilis* is its ability to grow in different modes, including photoautotrophic, heterotrophic, and mixotropic growth. This microalgae can synthesize a range of commercially important bioproducts that contain proteins with essential amino acids, lipids, and the polysaccharide paramylon, which has been shown to have immunostimulatory and antimicrobial bioactivities [28].

Euglena gracilis is also capable of tolerating a range of external stresses, including acidic growth. Xin et al. (2022) grew *Euglena gracilis* photoautotrophically at different pH and CO_2 concentration. In 7 days the dried biomass yield increased by 21% from 1.09 g/L (wild-type strain) to 1.32 g/L with CO_2 to 15% CO_2 and pH 3-5. The study also

Figure 12: *A typical colony morphology of* Botryococcus braunii *on the left and the hydrocarbon matrix (white arrow) in which the colony is embedded on the right [20]*

evaluated a method were *E. gracilis* was domesticated to increasing CO_2 concentration step by step and successfully grew *Euglena* at 99% vol CO_2 and pH 4.5 even with not competitive dry weight (0.3 g/L after 7 days) [22].
Chae et al. (2006) found that the best initial pH, temperature, and CO_2 concentration for *Euglena* were respectively 3.5, 27°C, and 5–10%. A final biomass concentration of 0.71 g/l was collected after 5 days of cultivation in a 1000 liters pilot scale photobioreactor with simulated flue gas [56].

Although the mode of cultivation has a significant impact on the total protein content of *E. gracilis* and heterotrophic growth conditions yield the highest protein content, photoautotrophiccaly grown *Euglena* showed a protein content of 0.5 g/g dry weight against 0.7 g/g of heterotrophically grown one. These values make *E. gracilis* a potential competitor of animal based protein, also considering that animal products such as beef, chicken or fish, usually does not exceed 0.4 g/g protein content after cooking [28].

Euglena gracilis can moreover accumulate large amounts of the reserve polysaccharide paramylon. Paramylon and other b-1,3-glucans have been shown to lower cholesterol levels, exhibit antidiabetic, antihypoglycemic and hepatoprotective activities and have also been used for the treatment of colorectal and gastric cancers. This makes *E. gracilis* a promising source for the production of various bioproducts with potential biomedical applications [28]. Photoautotrophic growth conditions maximize the production of protective pigments such as b-carotene, which is essential for warding off photooxidative damage to chloroplasts [30] while heterotrophic are believed to be more beneficial for the accumulation of paramylon and b-1,3 glucans [69].
Takeyama et al. (1997) showed how *Euglena gracilis* grown in photoheterotrophic conditions produced a larger amount of biomass but contained a lower level of antioxidant vitamins compared to cultures grown in photoautotrophic conditions. To optimize vitamin production, a two-step culture was employed where cells were first grown in photoheterotrophic conditions and then transferred to photoautotrophic conditions. In a fed-batch culture under photoheterotrophic conditions, *E. gracilis* Z cells reached

a density of 19 g/L after 6 days. The subsequent transfer to photoautotrophic conditions increased the vitamin content, resulting in a total vitamin yield of 71.0 mg/L of β-carotene, 30.1 mg/L of vitamin E, and 86.5 mg/L of vitamin C. These content of vitamins are exceptionally high, even in comparison with vegetables that are known to be high in b-carotene and competitive with other strains commonly used for b-carotene and vitamins production like *Dunaniella tertiolecta and salina* [23]. Few commercial large-scale cultivation of *Euglena* exist in the world. One is located in Japan, on the Ishigaki Island in Okinawa prefecture. As seen from **Figure 13** The Euglena Co. Ltd grown this microalgae in 30 m diameter circular open ponds and has been continuously operating on food, food integration and cosmetic japanese market since 2007. Other *Euglena* production plant are located in US (Valensa International, Algaeon Inc) and produce biomass for micronutrients and β-1,3-glucan extraction [69]. Regarding possible food application in Europe. the dried whole cell of *Euglena gracilis* has been recently accepted as safe for human consumption [26]. A view of *E. gracilis* under microscope is provided in **Figure 14**.

Figure 13: *Euglena Co Ltd cultivation facilities at Ishigaki Island (as of 2010) [25].*

4.2.5 Nannochloropsis

Nannochloropsis species are marine microalgae capable of accumulating great amount of lipids inside their cell and as often occurs with microalgae, lipids accumulation can be influenced by environmental stress such as nutrient deficiency or salt stress [65]. Rodolfi et al. (2008) evaluated the lipid production of *Nannochloropsis sp. F&M-M24* under nitrogen deficiency and nitrogen sufficiency cultivating it outdoor in

Figure 14: *Euglena gracilis under microscope [27].*

a 110 L Green Wall Panel PBR. When fed with nutrient deficient media 60% lipid content was reached in respect to 32% of the control sample. The lipids production rate were respectively 117 mg/L/day (with an average biomass productivity of 0.36 g/ L/-day) and 204 mg/L/day (with an average biomass productivity of 0.30 g/L/day). The authors of this study claim that this algae could be grown to produce 20 tons of lipid per hectare in the Mediterranean climate and more than 30 tons of lipid per hectare in sunny tropical areas [66]. Thawechai et al. (2016) evaluated the synergistic effects of light intensity, photoperiod and CO_2 concentration on *Nannochloropsis sp* Culture medium were adjusted to a pH of 6.7 and the highest biomass concentration after 7 days were all achieved at 10% CO_2, with values varying between 1.37 and 1.23 gL^{-1} depending on flow rate and initial cell concentration [48]. Chiu et al. (2008) investigated *N. oculata NCTU-3* culturing in semicontinuous mode and found instead 2% CO_2 concentration as the best one for long-term biomass and lipid yield. Increasing CO_2 content till 15% caused a drop of pH from 7.8 to 7 and a decrease of biomass productivity from 0.48 ± 0.029 $gL^{-1}d^{-1}$ at 2% CO_2 to 0.372 ± 0.022 $gL^{-1}d^{-1}$ at 15% CO_2 [65].
Negoro et al. (1999) grew *Nannochloropsis sp. NANNP-2* in a raceway-type cultivator by injecting actual flue gas from a boiler containing 10–12 % vol CO_2, SO_2 and NO_x in concentration of respectively 70–90 ppm and 70–90 ppm observing no specific effect of the flue gas on algal growth [42].

The high content of Eicosapentaenoic acid (EPA), makes this algae suitable as food supplement. In fact several companies in UE are currently producing *Nannochloropsis* as biomass for aquaculture but its potential may apply also to livestock [35]. However, few *Nannochloropsis* products for human consumption such as oil and dry algae are currently commercialized and still unavailable in Europe due to the pending status of *Nannochloropsis* as food ingrendient [33]. For the most relevant *Nannochloripsis* species cultivated for feed purposes, B2B price values are in the range of 30–110 €/kg and B2C market value (as marine phytoplankton) can go up to 1000€/kg [36]. There are several *Nannochloropsis sp* cultivation plant in Europe, among which Allmicroalgae –

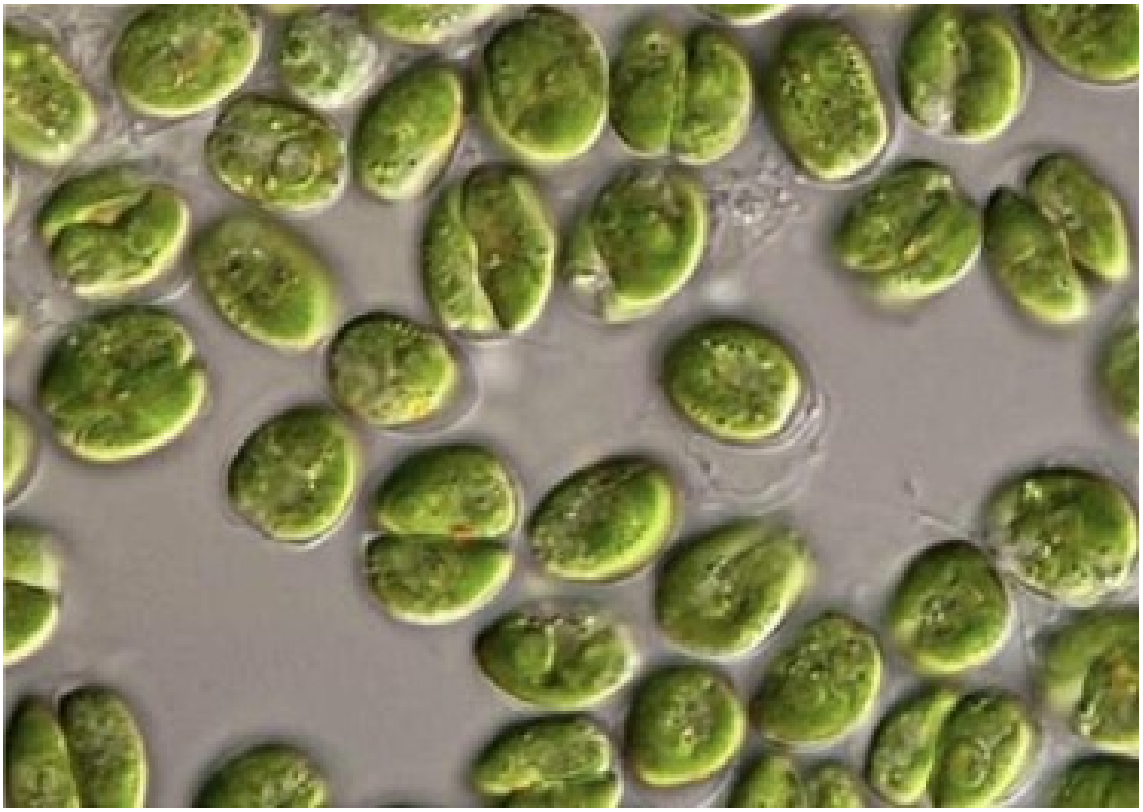

Figure 15: Nannochloropsis oculata. *Image from Malakootian, Hatami, Dowlatshahi, and Rajabizadeh (2016) licensed under the terms of the Creative Commons Attribution License [34]*

Natural Products S.A. shown in **Figure 16** and AlgaSpring producing *Nannochloropsis gaditana* in Flevoland, Netherlands are among the biggest.

Figure 16: *Allmicroalgae cultivation facility in Pataias (Portugal). [68]*

4.2.6 Scenedesmus

Scenedesmus is a family of green algae which usually can be found in freshwater sources as lakes or rivers. Spherical shaped, this organism can grow on a wide variety of environmental conditions with pH ranging from 6.5 to 9 and temperatures going from 10 to 40 °C depending on the species. *Scenedesmus* cell can accumulate high amount of lipids and carboydrates, reaching percentage as 60% of the total dry weight for lipids and 50% of it for carbohydrates. Because of this, *Scenedesmus* is a viable candidate for bio-diesel and bio-ethanol production [98].
Huang et al. 2020 experimented *Scenedesmus sp* growth under different CO_2 concentrations ranging from 1 to 70% vol. After 8 days results showed maximum biomass production of 3.92 gL^{-1} at 10% CO_2 and 2. 75 gL^{-1} at 20% [80]. Tang et al. (2010) found the best growing condition of *Scenedesmus obliquus SJTU-3* at 10% CO_2. Maximum biomass concentration achieved in 14 days and maximum CO_2 biofixation rate were respectively 1.84 gL^{-1} and 0.288 $gL^{-1}d^{-1}$. Higher level of carbon dioxide were instead favorable for the accumulation of lipids and polyunsaturated fatty acids [63]. For what concern *Scenedesmus* food potential, Vendruscolo et al. (2022) evaluated the composition of *Scenedesmus obliquus* in terms of proteins, pigments and lipids resulting from being grown at different CO_2 concentration. Results of this experiment showed that *S. obliquus* protein content was 57.8 and 57.2 % of the total mass for CO_2 concentration of 5 and 10%. An increase of CO_2 caused slightly decrease of protein content while increased total lipids. The production peak of carotenoids was obtained at 3% CO_2, even if at 5 and 10% the production was still significant. Carotenoids content was 25.3 ± 0.5, 22.7 ± 0.1 and 18.1 ± 1.0 mgg^{-1} at respectively 3,5 and 10% CO_2. A further increase in CO_2 caused strong decrease in carotenoid production. According to the authors of this study, treatment with CO_2 from 3 to 10% produced a biomass with a high potential for application in food and food integration [64].

4.3 Microalgae Cultivation

Microalgae have been living on earth for billions of years and there are historical evidences of microalgae use as food source as early as 700 years ago along both Africa and America [98].This consumption was however mainly based on research and collection of natural blooming, while a proper microalgae industry oriented to selection, production and processing of them only developed in the last few decades. Since a wide variety of living condition is possible for these organism, many types of cultivation techniques are plausible. In general terms, the the type of cultivation to settle for a commercial production depends on the type of microalgae, on the site where cultivation is located, on the type of final product and on the required quality of it. Before going into the details, it may be useful to distinguish some basic differences among all possible cultivation methods. The main distinction is done according to the nutrients and sunlight availability in three main categories as shown in **Figure 17**:

- **autotrophic cultivation**: sunlight constitutes the energy source and CO_2 is absorbed directly from the air. Despite the low operational costs, this method can have the downside of insufficient CO_2 input, restriction of the growth due to sunlight limitation, water evaporation.

- **heterotrophic cultivation**: microalgae are grown in a dark room with an artificial light source and an organic carbon source. High density culture, short growth cycle, and high oleaginous algae content are some of the advantages of these cultivation. However, limited algae species can be used for this type of cultivation, costs are higher and energy consumption rises [104].
- **mixed cultivation**: the organisms are fed by an organic carbon source but this time over the direct sunlight.

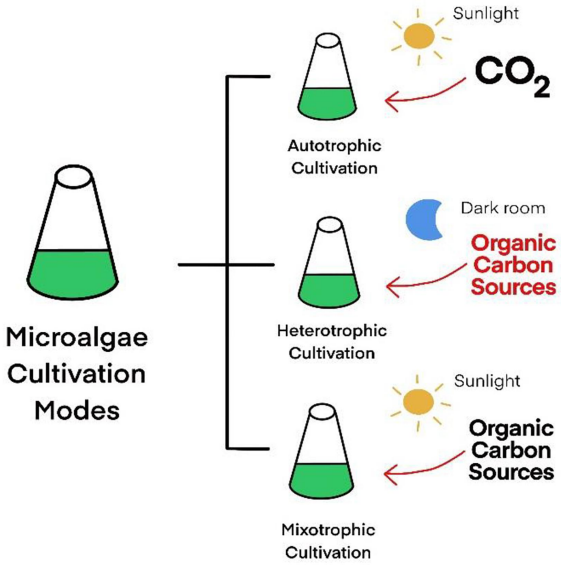

Figure 17: *Microalgae cultivation methods [104].*

4.3.1 Types of plants and reactors

All cultivation systems for microalgae can be classified at first into two main families: open and closed systems. This distrinction only regards the very general type of structure where microalgae are located and refers to the direct on not direct contact that they have with open air. Apart from this difference, all microalgae cultivation requires in general the same need such as: a proper mixing mechanism, or by mechanical way or by turbulent mixing of air bubbling, illumination, temperature control and feeding mechanism. All these options together shows why microalgae cultivation is a very flexible and adaptable activity to develop.

Open systems consists in large ponds, usually made up by concrete or soil and sealed with plastic. These ponds are exposed to open air and direct sunlight. The water is always kept in motion by a paddle wheel so that regular mixing and no sedimentation occurs. Being the mechanical energy of the rotating wheel the only significant electrical energy consumption, these plants have low operational costs.

However due to the direct contact between open air and growing medium it is nearly impossible to reach an optimal growing condition. This happens mainly since, being the system not enclosed, injected CO_2 rapidly tends to excape from the growing

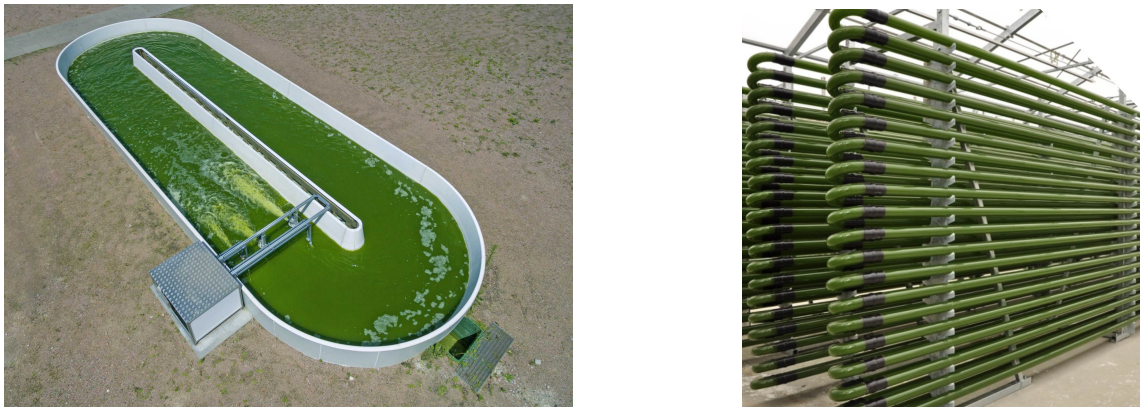

Figure 18: *A raceway open pond system (on the left) and a tubular photobioreactor (on the right)*

Figure 19: *Livegreen Srl Spirulina open pond cultivation in Oristano, Sardinia. [1].*

medium by exchange with the surroundig air. In another case, if the only exchange is directly from the air with no injection, it would be impossible to fully reach the maximum biomass production. Moreover, being under the direct sunlight with no other illumination sources means that in case of cloudy days production drops. Another issue with these plants concerns the contamination of the culture by organisms coming from the outside since little or no protection at all is given. In general these systems are mainly remunerative in very large scale where natural temperature and illumination fluctuation are trustful enough for a commercial cultivation to operate. [100].

Closed systems are usually composed by several enclosed volumes of water. The con-

tainers of this water can be cylindrical or planar. These systems are called photobioreactors (PBRs). PBRs show higher efficiency in comparison with open pond systems since all parameters can be easily controlled. This is a strong advantage for this technology since it could potentially host the growth of a vast amoung of species at high productivity rates. Moreover, being enclosed in transparent containers, microalgae can be fed by sunlight or artificial light more equally. CO_2 has no escape and therefore no or very small leaks happens in PBRs. Despite these advantages, closed systems have an higher cost than open ones. Injection of CO_2 into the medium requires compressed air, a fine tuned circulation system for nutrient mixing and a temperature control unit in order to keep the cultivation at its best growing condition [100]. Other disadvantages regard the higher maintenance cost for these reactors. Possible formation of musilage on the inside of pipes requires programmed cleaning procedures with possible revenue loss. Moreover due to constant exposition to direct light degradation of the pipes could develop over time, with subsequent higher costs on the long term. In general, these systems are preferred for high selective and high quality productions.

4.3.2 Temperature and illumination

Microalgae are quite sensible both to the type of illumination and to the temperature of the culture. Despite be a very adaptable organism, temperature of the medium is one of the main driving parameters for aglae cultivation. In general, the optimal range for microalgae cultivation should be between 15 and 30°C, but much depends on the cultivated species. Outside this range, microalgae tends significantly slow down their growth or even to die [102]. This constitutes a disadvantage for the majority of open ponds system which are exposed to direct air and therefore cannot control the temperature of the medium nor have a perfect uniform distribution of it. Closed system can instead rely on temperature control units, despite this significantly increases their energy demand in terms of heat or electricity. For what concerns illumination, researches have shown that when continuous illumination is provided through artificial light, the carbon sequestration capacity of microalgae reaches 99.69%, but the cell density and growth of some microalgae decreases when the photoperiod is too long. Light intensity shows also a fundamental role. Photosynthetic activity, an so biomass production, can therefore be described and linked to the irradiance and three main region of activity can be recognized as shown in a qualitative way in **Figure 20**. In the light saturated region, photosynthetic activity can be linked with irradiance using a linear relation so that its slope can be described as:

$$\alpha = \frac{P_{max}}{I_s}$$

where:

- P_{max} = light saturated rate of photosynthesis
- I_s = saturation light intensity (μ mol photons $m^{-}2s^{-}1$)

When irradiance is around the saturation zone the optimum range for photosynthetic activity is reached. Following this region, if irradiance increases photoinibition

occurs. This is a situation in which the cell cannot sustain anymore the use of incoming photons and its activity starts to decline. Below the so saturation irradiance the organism is still performing photosynthesis but at slower rates. An important detail is that for irradiance equal to zero, photorespiration occurs. This is a process where the organism use its own biomass to survive instead of accounting on solar energy.

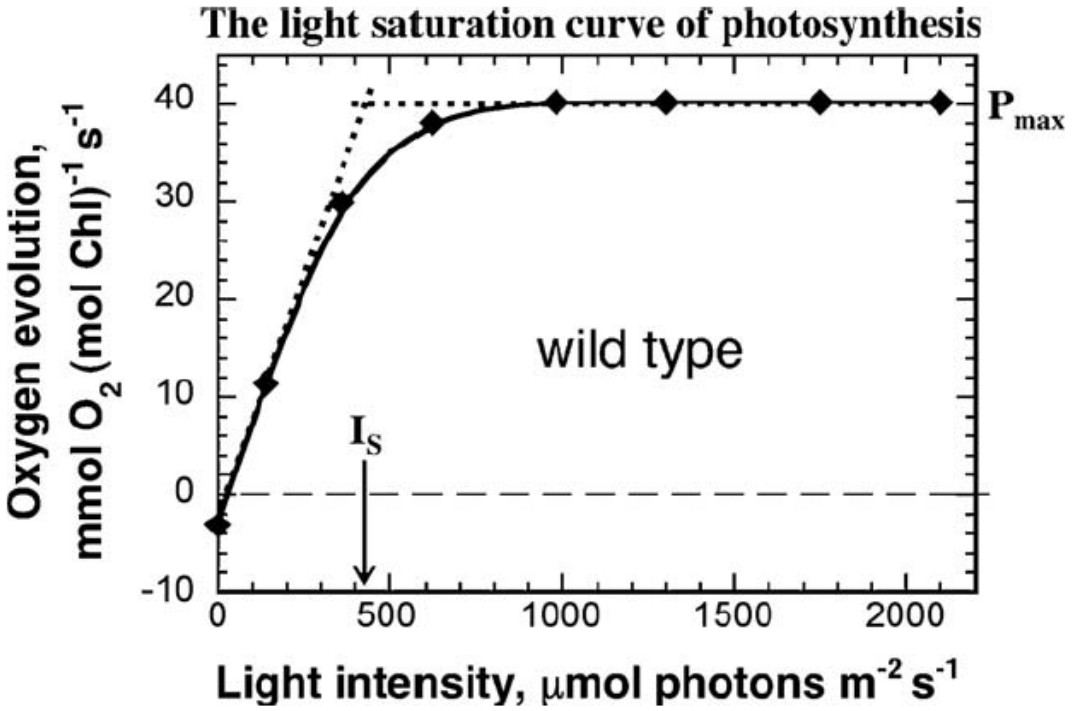

Figure 20: *A diagram of Oxygen evolution, representative of photosynthesis, versus irradiance I. The diagram shows the approximate values for a wild type microalgae. The light-saturated rate is denoted Pmax [43].*

Now days, LED systems are taking more and more space in this field thanks to their high emission uniformity, the possibility of real time intensity and spectrum variation and a lower energy consumption than fluorescent light. Moreover, studies suggest that certain frequencies, such as red and blue light, can significantly promote the growth of some species [102].

4.3.3 Nutrients requirement

The necessity of supplying mineral nutrients and other growth requirements to algae in culture has been known for a long time. Depending on their metabolism, algae can be divided into two categories:
Autotrophic (phototrophic) organisms which derive their energy from light energy absorption and use it to reduce CO_2 by oxidating the substrate, mainly water, with O2 release. Heterotrophic organisms which obtain their material and energy needs from organic compounds produced by other organisms. Inorganic mineral ions are the only

requirements for photoautotrophic organisms, Mixotrophic or amphitrophic organism are those whose metabolism is equivalent to autotrophy and heterotrophy, where growth is achieved through both organic compounds and CO_2 [98]. Regarless these differences, the main necessities and aspects which are at the base of an adequate cultivation medium, intended as the substrate where microalgae grow, can be summarized as:

- The medium total salt content. Mainly determined by the algae's original environment.
- The cell composition requirements of ions components such as K^2+, Mg^2+, Na^2+, Ca^2+, SO_4^- and Cl.
- A nitrogen sources, usually achieved with ammonia, urea or nitrates.
- A carbon source. Depending on the metabolic route, the options could be to provide it as organic using for example acetic acid, glucose and fructose or as inorganic, as CO_2 or carbonates.
- The pH of the medium.
- Vitamins.

Moreover, the purpose for which the alage are cultivated is also an aspect to consider when programming nutrient feeding. Studies have shown how lipid and carotenoids accumulation can be induced by the stress conditions such as nutrient limitation or exposure to the damaging physical factors [96]. These practices have to be carefully tuned and are often implemented though a two phase growing strategies in which the algae biomass first develops in a normal environment and only after having achieved a robust concentration undergo nutritional depletion in a second reactor [85].

Among all nutrients, a distinction can be made between micro and macro nutrients, regarding which the concentrations are measured at the order of mg/l for the first while g/l for the latter.
Another aspect to consider is that water used for the cultivation should be filtered and cleared to prevent any type of contamination, avoid the intrusion of alien algae or chlorine in case of domestic water.
Table 5 shows different common mediums composition.

Substance	BG11	Modified Allen's	Bold's Basal	Sorokin/ Krauss	Zarrouck	Ben-Amotz and Avron
NaNO3	1.5	1.5	0.25	2.5	-	
KNO3	-	-	-	-	1.25	0.505
K2HPO4 $\cdot 3H_2O$	0.04	0.039	0.075	-	0.5	0.014
KH2PO4	-	-	0.175	1.25	-	
MgSO4 $\cdot 7H_2O$	0.075	0.075	0.075	1.0	0.2	1.2
MgCl2 $\cdot 4H_2O$	-	-	-	-	-	0.1
CaCl2 $\cdot 2H_2O$	0.036	0.025	0.084	0.04	0.08	0.033
Ca(NO3)2 $\cdot 4H_2O$	-	0.02	-	-	-	
Na2SiO3 $\cdot 9H_2O$	-	0.058	-	-	-	
Citric acid	0.006	0.006	-	-	-	-
Fe-Ammonium citrate	0.006	-	-	-		
FeCl3	0.002	-	-	-	-	-
FeSO4 $\cdot 7H_2O$	-	-	0.00498	0.05	0.01	-
EDTA, 2Na-Mg salt	0.001	0.001	0.05	0.5	0.01	-
NaHCO3	-	-	-	-	16.8	1.7
Na2CO3	0.02	0.02	-	-	-	
NaCl	-	-	0.025	-	1.0	117.0
K2SO4	-	-	-	-	1.0	-
KOH	-	-	0.031	-	-	-
Tris-HCl	-	-	-	-	6	
H3BO4 (mg l^{-1})	2.86	2.86	11.42	114	2.86 6	
MnCl2 $\cdot 4H_2O$ (mg l^{-1})	1.81	1.81	1.44	14	1.81	-
ZnSO4 $\cdot 7H_2O$ (mg l^{-1})	0.222	0.222	8.82	88	0.222	-
ZnCl2	-	-	-	-	-	14
Na2MoO4 $\cdot 2H_2O$ (mg l^{-1})	0.391	-	-	-	-	
CuSO4 $\cdot 5H_2O$ (mg l^{-1}	0.079	0.079	1.57	16 0.08	-	
Co(NO3)2 $\cdot 6H_2O$ (mg l^{-1}	0.0494	0.0494	0.49	5	-	
CoCl2 $\cdot 6H_2O$ (mg l^{-1}	-	-	-	-	-	4.8
MoO3 (mg l^{-1}	-	-	0.71	7 0.01	-	
Ajust final pH	7.4	7.8	-	6.8	-	-

Table 5: *Composition of some of the most commercially diffused mediums. Concentrations are expressed in g/L, unless indicated otherwise. [98]*

4.4 Microalgae preparation and harvesting

After algae have grown inside the cultivation system, they need to be collected, separated from water and prepared for the following downstream processes. The end product of the harvesting phase is a wet or dry paste as can be shown in **Figure 21**. The frequency and amount of volume collected every time depends on the production strategy.

In **batch harvesting** all the biomass present in the cultivation is removed at once, separated from the medium that is then re-injected into the ponds or the reactor to

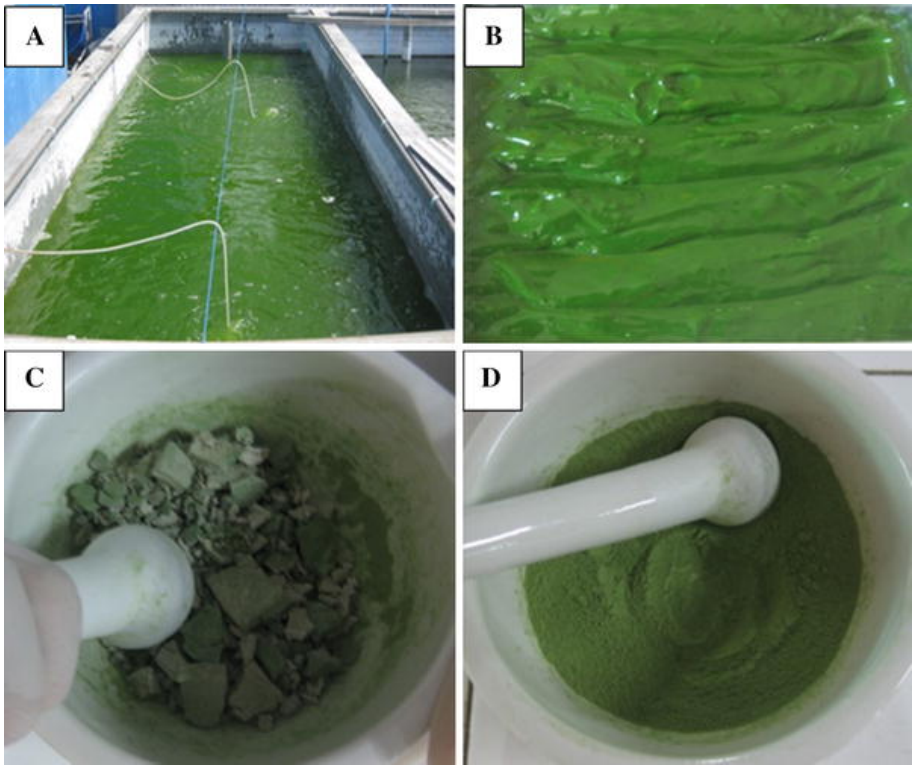

Figure 21: *The cultivation pond (a), the biomass sediment (b), the dried biomass chunk (c), and biomass powder (d) of Nannochloropsis oculata [51]*

start a new growing cycle. This technique has the disadvantage of shutting down the plant for at least some days per year.
In **continuous harvesting** a relative small percentage of the total medium volume is removed constantly over time. The biomass is then harvested and the medium is immediately re injected into the cultivation. In this way the growing phase does not stop with all consequent advantages. Principles of continuous flow culture will be analyzed more deeply into **5.1**.

The main methods for microalgae harvesting include filtration, centrifugation, sedimentation and flotation.

Filtration methods are quite simple but problematic for the largest part of commonly cultivated microalgae. This is mainly due to the small dimension of the algae (3-30 μm) and to their low concentration in the medium. Both factors influence the efficiency of filtration. The method is anyway usually implemented in for *Spirulina* algae only [98]. A membrane is used to keep the solid part while the liquid one is able to flow through it. A suction pump may be used to force the accumulation of solid on the filter. This process, despite been simple, require a constant cleaning and maintenance of the filter in order to prevent any type of clogging [98].

Centrifugation is done by using a rotating device filled with water and algae. As the device rotates, microalgae are collected in a sedimentation tank. The centrifuge forces acts in a way to sediment the biomass while separating it from water. Efficiency

of centrifugation is strictly linked with the applied centrifugal force. These forces can range from 1300 to 13 000 g. Harvest efficiency of 95% is only obtained at the maximum centrifugation force of 13 000 g, while at 6000 g it has already decreased to 60% and to 40% at 1300 g. This method is however expensive for the not negligible energy demand but represent a suit able option for long-term commercial and industrial scale plants [98].

Flocculation is a technique where chemicals (flocculants) are added to the water with the intention to aggregate single cells into bigger clusters. Aggregation can be reached both by the addition of polymers or electrolytes. The addition of flocculats cause a reduction of repulsive forces between the cells walls enabling in this way the aggregation of them. As they come together, they either float or sink [91]. Flocculation processes are however still problematic in all those cases where biomass is produced for food consumption purposes. This is due to the toxicity of polymers and salts used for this process.

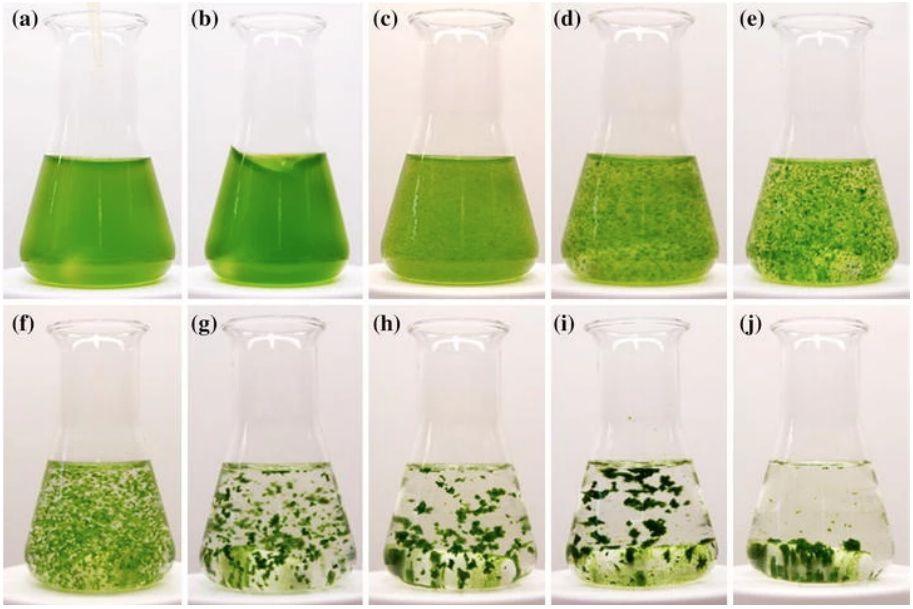

Figure 22: *Example of flocculation on a lab sample of microalgae [91].*

4.4.1 Drying

Once the microalgae have been collected, it is necessary to dry them up. Since their water content is high, a large amount of energy enters in this phase making the drying one of the most energy demanding step in microalgae cultivation. Hot air can be recovered in case of power plants and used for this purpose. Another cheap option is to dry the biomass directly in open air, option that requires large spaces and long time. Finally, dry can also be performed by using cold dryers. And since refrigeration does not damage in any way the cell contrary to what could happen by heat exposure, this method is recommended for whatever post use of the algae requires the preservation of the pigments and of all other substances contained inside the cell walls.

4.4.2 Extraction and separation

The last phase of microalgae cultivation is the extraction of cellular components from the biomass. Extraction techniques for microalgae are similar to those used by terrestrial biomasses. Among all the possible methods, a distinction can be made as: mechanical, chemical and enzymatic extraction. The cellular structure presents an excellent and durable barrier. Because of that, independently from following processes, the biomass is usually broken down mechanically. Enzymatic extraction then uses enzymes to degrade cell walls.

4.5 Flue gases from power plants as carbon source

Till now it has been said that phototropic microalgae are photosynthetic organisms whose requirements include light, a carbon source and some nutrients. Depending on the type of cultivation, carbon can be provided by injection of CO_2 into the medium with consequent dissolution, absorption and eventually dispersion or it can be provided through inorganic or organic sources directly into the medium.
Since microalgae are good carbon utilizers, it has recently took more and more place the idea to use them as carbon fixation tool inside a more general carbon recycling prospective. Microalgae seem to adapt well to this job. According to Li et al., about 1.8 g of CO_2 are required per 1 g of biomass produced [105].
In a climate change mitigation prospective, the idea of using microalgae for carbon fixing belongs to the field of carbon neutral technologies. The carbon fixed by the algae will ultimately end up into the atmosphere again closing the emission-uptake circle. However, if products which currently have a positive emission impact could be substituted by equivalent products made using the algal biomass, the emission reduction could become positive compared to the business as usual scenario.
This perspective poses some challenges. In fact, such a strategy would be feasible on a large scale only by placing microalgae cultivation plant near single point emitters capable of providing a reliable CO_2 source. Among all carbon dioxide point emitters, the ones which can claim large and constant volume emitted are recognizable mostly as power or chemical plants.

4.5.1 Microalgae cultivation plant using flue gases

Despite microalgae have been cultivated worldwide since decades, only few projects use flue gas as carbon source. Moreover, among those that already operate, few information are available to the public. At the knowledge of the author of this work there is only one existing plant that capture CO_2 from an incineration plant and use it as carbon source for microalgae cultivation. The plant, located in Saga City, Japan, is able to sequester about 10 tons of CO_2 per day. Part of the captured CO_2 is directly transferred into a nearby microalgae indoor greenhouse cultivation plant operated by **Alvita Corporation** while the rest is utilized by other nearby greenhouses. The company cultivates *Hoematoccoccus pluvialis* with the specific intention to produce astaxantine, one of the most powerful natural anti-oxidant. The carbon capture system was developed by Toshiba Corporation. According to the head of the project, Engineer Hideo

Kitamura, the largest difficulty was to tune the system in order to not be compromised by the high concentration of hydrogen chloride that is released by waste incineration. The CO_2 is absorbed by an amine solution into an absorber tower and released in a stripper tower at a food grade purity. Heat from the incineration plant is used to regenerate the solvent. No information about other technical details are available [46]. The system is shown in **Figure 23**.

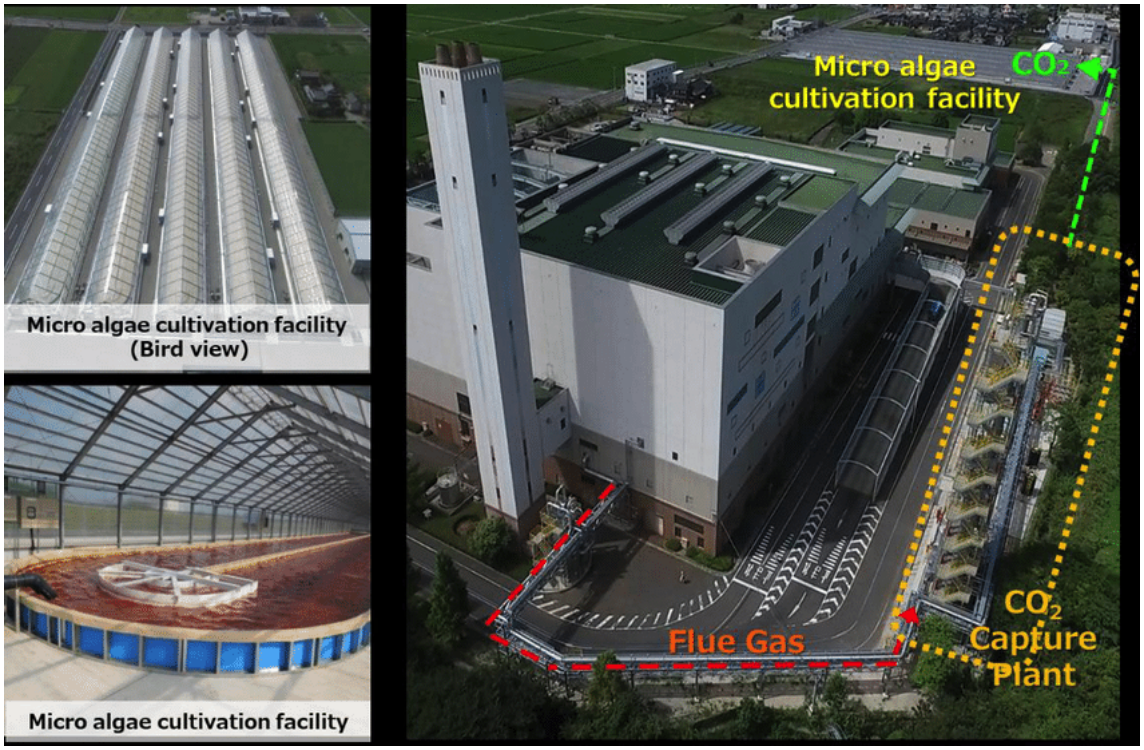

Figure 23: *CO_2 capture plant and micro algae cultivation facility in Saga-city, Japan [47].*

Another example of commercial microalgae cultivation fed with flue gases is **Seambiotic Ltd**. Based in Israel, the company currently grows microalgae using flue gas coming from a nearby coal power station (Rutenberg Power Station). The plant is located 100–150 m apart from the coal power station in order to minimize transportation cost of the gas and has been operating from 2006. Cultivated species are *Nannochloropsis sp., Phaeodactylum tricornutum, Amphora sp., Navicula sp., Dunaliella sp., Chlorococcum sp. and Tetraselmis sp.* The cultivation is shown in **Figure 24**. Open pond type, this plant occupies around 1000 m2 as surface area. Around 180 m3 of flue gas are injected into the ponds every hour, constituting only a very small fraction of the 1.7 million m3 of flue gasses emitted every hour by the nearby power plant.

For what concerns the feeding of flue gas to the cultivation plant, **Figure 25** shows how the deviation from the chimneys to the cultivation is done. Flue gasses are initially collected between the Flue Gas Desulfurization system (FGD or scrubber) and the chimney at 50°C. Water is slightly separated by a buffer vessel where flow speed decreases and pressure increases leading to a partial condensation of some of the gas. A 2.2 kW 500 mm water column blower provide the necessary pressure to collect the feed the gas into a buffer thank and then directly to the algae cultivation ponds located

Figure 24: *Aerial view of Seambiotic Plant in Ashkelon, Israel. [61]*

100-150 m apart from the power station. The blower is activated only during daytime. Apart from electrostatic precipitation (ESP) and desulfurization, the flue gas does not undergo any other cleaning or cooling procedures, arriving at 12% concentration of CO_2 and at ambient temperature to the cultivation ponds where it is redistributed into the medium using underwater bubble aerators or diffusers. The plant also receives cooling seawater while neither steam nor other thermal feed is supplied. Harvesting is done continuously when algae concentration reach approximately 0.5 g/L by removing 10% of the largest pond volume each day. This procedure is done using a Westphalia centrifuge, model NA7-06-076 (8520 rpm; 4 kW) which increases the algae concentration from an initial 0.1% to approximately 15–18% solids guarantying a production of 20 g biomass/m2/day. This biomass is then utilized mainly sold for research purposes [61].

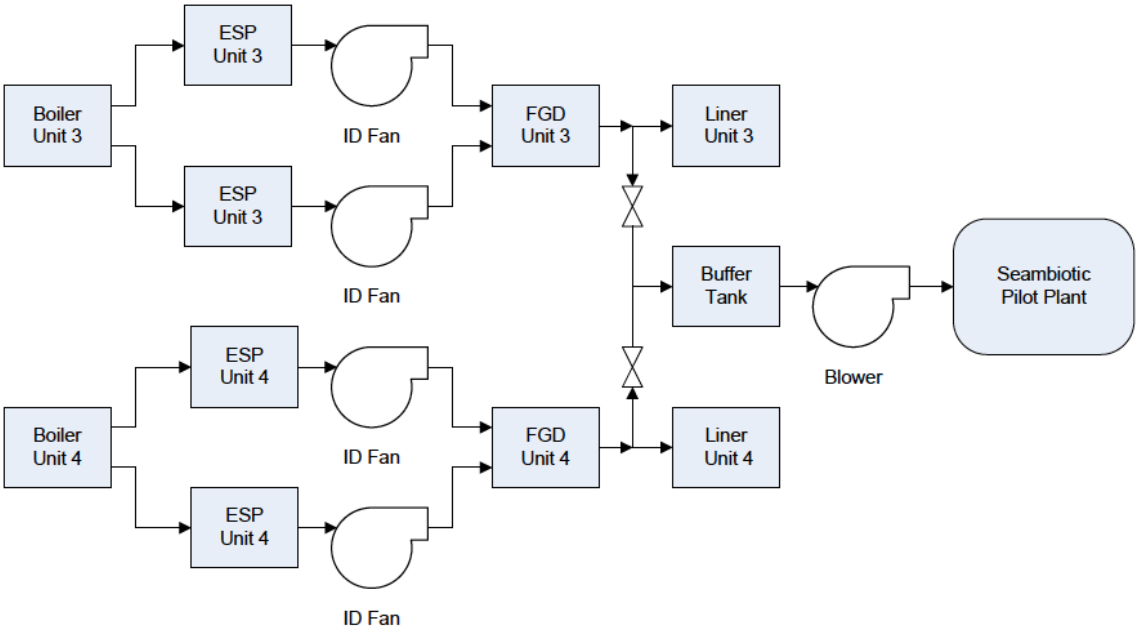

Figure 25: *Seambiotic Ltd f Flue Gases Supply System Diagram. ESP = electrostatic precipitator. FDS = Flue Gas Desulfurization System. [61].*

Another significant experiment regarding large scale cultivation of *Spirulina* fed with flue gases was conducted in **Dalin coal fired power** plant in southern Taiwan. The cultivation shown in **Figure 26** was a 30 m^3 closed system which successfully fixed 2,234 kg of CO_2 in one year. According to the estimation made by Chen et al. [84], the cultivation could be scaled up to a potential fixing rate of 74 tons/ha per year.

Figure 26: *External view of Dalin's power plant photobioreactor [84]*

Another example of flue gas utilization for microalgae feeding was developed by **Novagreen Projekt-management GmbH** in Niederaussem, near Cologne, Germany. As shown in **Figure 27** the system is composed by several V-shaped photobioreactors located inside a 600m2 greenhouse.

Figure 27: *Hanging bags in the greenhouse at Niederaussem power station [72]*

Although is not clear the end use of the cultivated biomass, the owner of the plant, RWE company, claims to be able to fix around 12 tons of CO_2 per year by producing 6 tons of dry algal biomass. Few information are however available for this plant [72]. These and other real case examples are collected in **Table 6**.

Project	**Reactor type/size**	**CO_2 source**	**CO_2 fixation**	**Biomass production**	**Ref**
Bergheim-Niederaussem	PBR 600 m^2	coal-fired power plant	12 t/y	6 t/y	[72]
Da-Lin, Taiwan	PBR/30240 L	coal-fired power plant	2234 kg/y	-	[84]
Seambiotic Ltd	OP 1000 m^2	coal-fired power plant	-	20 g biomass/m^2/day	[61]
Global Algae Innovations, Hawaii	OP 3.2 ha	fossil fuel power plant	240 t/y	-	[3]
Penglai facility, PR China	open pond/1191 m^2	coal-fired power plant		18.4–40.7 g/m^2/day	[3]
CO_2ALGAEFIX Project	PBR/85000 L	Combined Cycle power plant	120 kg/d	60 kg/d	[**?**]

Table 6: *Cultivation plants which use flue gases as carbon and nutrient source*

4.5.2 Challenges of using flue gasses

Feeding microalgae with flue gasses poses some challenges. As a matter of fact, these gasses come out of the source (power plant or waste incineration plant) at high temperatures, with variable concentration of gasses and before being used for any purpose they need to be filtered, cooled and, depending on the final use, gas components need to be separated. In fact, these gas contains nitric oxide, nitrogen dioxide, sulfur oxides, fine particles, heavy metals, and other contaminants that could damage the cultivation. However, opportune concentration of some of these compounds could enhance and favourite the microalgae growing [89]. Because of this reason,it is fundamental to understand possible negative and positive effects of these compounds on microalgae. A schematic representation of microalgal-based carbon capture scheme is shown in **Figure 28**.

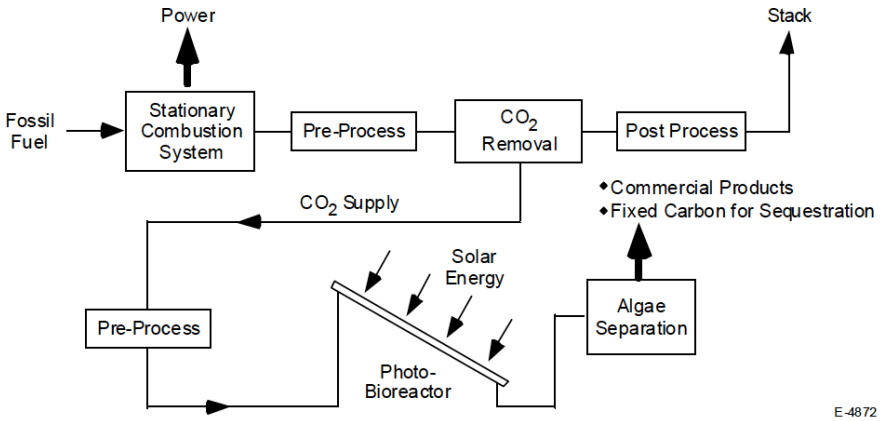

Figure 28: *Schematic representation of a microalgae cultivation fed with CO_2 captured from flue gasses of a fossil fuel power plant. [45].*

Despite flue gases from fossil fueled power plants contains many components, the brief focus in this work will be on CO_2, NO_x and SO_x. Nevertheless, it is important to remember that many other substances such as unburned hydrocarbons, O2, N2, CxHx, H_2O, CO, aerosols, heavy metals, and particulate matter are contained in untreated flue gasses and therefore a filtration and purification of the gases is mandatory in those cases where the biomass is expected to be used in fine-grade applications.

4.5.3 Carbon dioxide gas from industrial source

The use of CO_2 from flue gas for microalgae cultivation offers advantages over atmospheric CO_2 since diffusion of CO_2 from the atmosphere into the microalgal culture is not sufficient to obtain high biomass productivity [88]. Carbon dioxide can be injected using various systems and depending on the type of reactor in use. The priority is however always to promote the maximum mass transfer between the flue gas and the algae. Because of this, gas supply velocity and mechanical mixing should be settled in a way to provide a turbulent region inside the reactor and bubbles distribution should optimize the volume to area ratio of the bubbles [102]. However, the main

problem with direct CO_2 injection into the medium regards the pH of the medium itself. As carbon dioxide is injected into water, it dissolves to form carbonic acid $H_2CO_3^-$ through the following chemical reaction:

$$CO_2 + H_2O \rightarrow H_2CO_3 \tag{2}$$

The newly formed carbonic acid can then dissociates into hydrogen ions (H^+) and bicarbonate ions (HCO_3^-). Then bicarbone ions can subsequentely dissociate again in carbonic acid (CO_3^{-2}) and hydrogen ions as shown in the following reactions:

$$H_2CO_3 \rightarrow H^+ + HCO_3^- \tag{3}$$

$$HCO_3^- \rightarrow H^+ + CO_3^{-2} \tag{4}$$

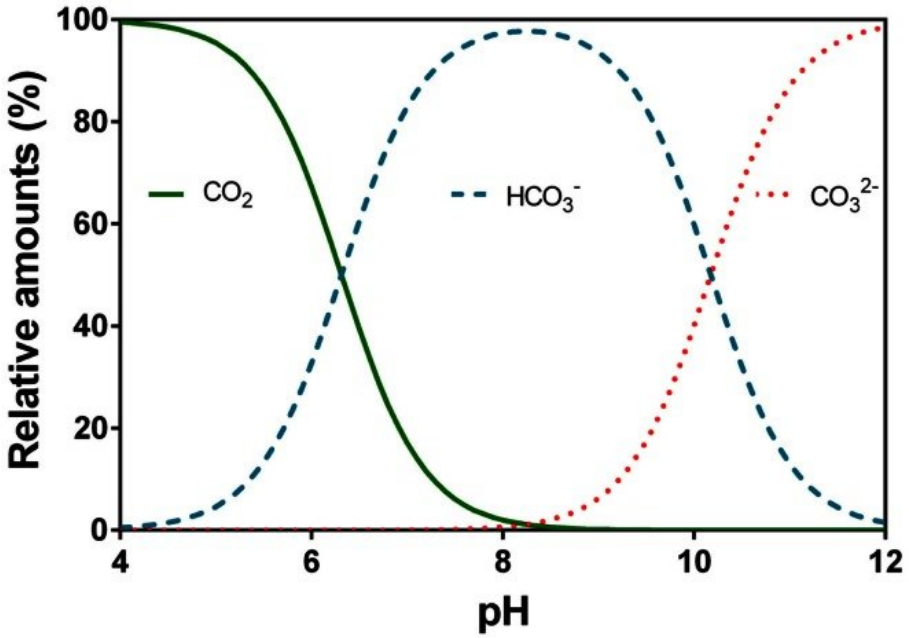

Figure 29: *Relative speciation (%) of carbon dioxide (CO_2), bicarbonate (HCO_3^-), and carbonate (CO_3^{-2}) in water as a function of pH [71].*

As shown in **Figure 29**, depending on the pH of the medium it will be possible to find dissolved inorganic carbon in form of CO_2 , HCO_3^-, CO_3^{2-} and H_2CO_3. According to these consideration, the injection of carbon dioxide with consequent hydrogen ion release can be responsible for the acidification of the medium. The acidification caused by elevated concentration of CO_2 may consequently limit microalgal growth and reduce the efficiency of photosynthesis. These reduced growth rates under high CO_2 concentrations are generally linked to the inactivation of key enzymes in the Calvin-Benson cycle [3]. To overcome this, microalgal strains with high CO_2 tolerance need to be screened.
Another possible road to enhance the uptake of carbon dioxide by these organisms is the addition of CO_2 absorbers such as amines into the cultivation medium. A wide variety of carbon capture methods based on chemical absorbers and adsorbers are already operating at industrial scales.

The distinction between absorption and adsorption is based on the state difference between the captured and the capturing compound. Absorption happens when a gas in fixed in a liquid, while in adsorption the fixing medium is a solid. While capture requires low temperature and high pressure, the opposite is true for desorption [87].
Garam et al. [82] conducted an experiment where *Scenedesmus sp* was grown by adding to a BG-11 medium four alkanolamine adsorbents, respectivey *monoethanolamine* (MEA), *diethanolamine* (DEA), *triethanolamine* (TEA) and *2-amino-2-methyl-1-propanol* (AMP) separately. CO_2 was then injected as the only carbon source in a 1L tubular reactor artificially illuminated. In comparison with the cultivation where no adsorbent was added, the molar CO_2 absorption ratio was 0.70, 0.90, 1.02 and 1.54 for MEA, AMP, DEA and TEA, respectively. The enhancement of the growth rate was about 12.2% and 22.8% with 2 mM DEA and TEA, respectively.
Another experiment conducted by Choi et al. [75] went ever far by comparing two different *Scenedesmus sp* 1L tubular reactor cultivations. One where MEA was enriched with carbon dioxide before being injected into the medium in what can be called *ex-situ* adsorption, and a second one where pristine MEA was added into the medium and then CO_2 was injected, *in-situ* adsorption. The scope of the experiment was to investigate if having free-MEA and CO_2-enriched-MEA in the same solution could affect cell growth. The culture was then supplied with a 5% (v/v) CO_2 at 0.1 vvm. Results showed how MEA addition to BG-11 brought the Dissolved organic carbon to a concentration 6 times higher than CO_2 saturated solubility limit in BG-11 of 8.6 mg/L, bringing it to a 51mg/L concentration. Moreover, it was understood that CO_2-enriched-MEA was beneficial for the algae only on the range 0-100 mg/L, above which inhibition of photosynthetic activity occurs, probably due to the formation of an intermediate carbamate in the medium. Pristine MEA was instead beneficial till 300mg/L. Both cell growth rate and final cell density were enhanced compared to when no MEA was added. The cell growth rate reached 288.6 mg/L/d, which was equivalent to 539.6 mg-CO_2/L/d as a CO_2-fixation rate and enhancement of about 63.0% compared to not adding MEA. Chlorophyll-a content and nitrate consumption rate increased correspondingly.
Another method that has been studied is the absorption of CO_2 into calcium oxide (CaO), also known as limestone.

$$CaO + H_2O \rightarrow Ca(OH)_2 \tag{5}$$

$$Ca(OH)_2 + CO_2 \rightarrow CaCO_3 \tag{6}$$

$$Ca(OH)_2 + CO_2 \rightarrow Ca(HCO_3)_2 \tag{7}$$

When dissolved in water, calcium oxide produces the solution of calcium hydroxide which can be the effective absorbing material for CO_2. Consequently as CO_2 is flushed into calcium hydroxide medium calcium carbonate precipitate forms at first and, if an excess of CO_2 is still available, calcium bicarbonate is formed as a colorless liquid.
Once reached the equilibrium the aqueous solution now contains calcium bicarbonate and carbon-ate ions together with dissolved carbon dioxide. These three components enhance the ability of the liquid solution to dissolve more solute molecule. Zawar et al. [74] conducted a comparative experiment using limestone as CO_2 fixer and then fed two different microalgal cultures viz. Chlorella sorokiniana PAZ and Arthrospira sp. VSJ with Zarrouck's medium enriched with bicarbonates. Results shows how the rate of bicarbonate utilization by C. sorokiniana PAZ was higher when CO_2 was trapped in the

presence of 2.67 mM calcium oxide (CaO) than in the presence of 10 mM sodium hydroxide ($Na(OH)$) and with direct addition of 10 mM sodium bicarbonate ($NaHCO_3$). For Arthrospira sp. VSJ the bicarbonate utilization was 92.37%, 88.34% and 59.23% for the medium containing CaO, NaOH and $NaHCO_3$, respectively.
Although all these studies represent a good promise for microalgae cultivation's future developments, none of these solution has ever been implemented on large scale. Moreover there is a lack of studies regarding a possible industrial implementation of these methods and it's therefore impossible to state the economical and environmental sustainability of using mediums with enhanced CO_2 absorbing capacity. As consequent consideration to this, the most promising strategy for a large scale implementation of flue gases as carbon source remains the selection of CO_2 tolerant microalgae strains.

4.5.4 NO_x

Nitrogen Oxide and Nitrogen Dioxide are usually the two most common species of nitrogen compound found is flue gasses [80]. Their respective concentration can vary between 90-95 vol % for NO and about 5-10% for NO_2. The solubility of NO in water is quite low, (0.032 gL^-1 at 25°C) while NO_2 can be absorbed much more easily (213.0 gL^-1 at 25°C) [86]. The dissolution of NO_x in water is described trough the following equations:

$$NO_{aq} + H_2O \rightarrow HNO_2 \tag{8}$$

$$2NO_{aq} + H_2O \rightarrow HNO_2 + HNO_3 \tag{9}$$

$$3HNO_2 \rightarrow HNO_3 + 2NO_{aq} + H_2O \tag{10}$$

Nitrogen can be consumed by microalgae in various forms such as

$$NO_2$$

$^{-1}$, N2, $NH4^+$, NO, and $NO3^{-1}$. The reduction of nitrate and nitrite is however strongly influenced by the energy supply from extrinsic organic carbon or by photosynthetic electron transfer [3]. Microalgae tolerance to NO_x stricly depends on the species. Some studies have shown how concentration of NO below 300 ppm are not harmful for microalgae [41]. Moreover, the removal of NO from the flue gases depends on the dissolution of NO into the aqueous solution and is often considered to be the rate-limiting step.

4.5.5 SO_x

Sulphur oxides, together with NO_x are another typical component found in flue gases. The solubility of sulphur dioxide is hight in water (22.971 g/100 g H_2O at 0°C, lowering to 5.881 g/100 g H20 at 40°C). The dissolution of sulphur dioxide is described through the following reaction:

$$SO_{2(g)} + H_2O_{(aq)} \rightarrow H_2SO_{3(aq)} \tag{11}$$

$$H_2SO_{3(aq)} \rightarrow HSO_3^- + H^+ \tag{12}$$

$$HSO_3^- \rightarrow H^+ + SO_3^{-2} \tag{13}$$

The main form is SO_3^2 (sulphite) at pH 6 or above while HSO_3 (bisulphite) is prominent at pH from 2 to 6 (25 °C and 1 atm [8]. An accumulation of SO_x, even if present in small concentration in the flue gas, could lead to a pH reduction over time with further influences on bicarbonates as stated in **Figure 29**. Moreover, the toxicity of bisoulphite is enhanced in acicid condition [13], therefore the injection of CO_2 into the medium could lead to a its toxicity increase. High SO_2 concentrations is also thought to be detrimental for pigments and protein. For these reasons, gases with concentration of SO_2 above 60 ppm should be avoided [9].

4.6 Cost of microalgae production

Despite the great potential of microalgae as novel food, the high cost of production is still a limiting factor for large scale cultivations [36]. Because of this reason, microalgae biomass is currently produced mainly for high-value applications such as food integration, nutraceuticals, cosmetics, and pharmaceuticals.
The first step to determine production cost is to define a flowchart of the process and calculate the mass and energy balances in order to scale the systems on a a certain biomass production capacity. The major equipment and consumables needed are identified (such as cultivation medium and CO_2) and their costs are determined using information from suppliers or databases. Among the various expenses it is possible to distinguish the fixed capital, which is the total cost of the major equipment plus costs related to installation, piping, cabling, and land arrangement, and the operational costs, concerning the consumable utilities, the energy cost and the workforce cost. As for any other type of industrial plant, depreciation cost over the lifetime of the process need to be assessed. The lifetime can range from 5 to 15 years in the biotechnology field. In the case of microalgae, a conservative value of 5 years is recommended due to the higher risks involved. The depreciation cost includes the amortization of fixed capital as well as property tax, insurance, and purchase tax, and is the first contribution to the annual cost.
Norsek et al. (2014) theoretically evaluated production cost of dry microalgae powder in the three main cultivation plants: raceway ponds, tubular photobioreactor and flat panel photobioreactor and for 2 main sizes: 1 ha and 100 ha [53]. [36].
The analysis was done by setting Eindhoven in Netherlands as the plant location. The productivity of the plant was settled to 21 ton ha-1 year-1 for the raceway pond, 41 ton ha-1 year-1 for the tubular photobioreactor and 64 ton ha-1 year-1 for the flat panel photobioreactor. Biomass production rate for a 12 h production day were set respectively to 0.003 kg m-3 h-1, 0.021 kg m-3 h-1 and 0.025 kg m-3 h-1. Results of this analysis are presented in **Table 7**. Since the research was done in 2011, all costs were corrected according to an actualization factor of 1,25 as indicated from Italian Istituto Nazionale di Statistica ISTAT website for 2011-2023 € actualization [52]. Despite Norsek et al. extended their analysis till an extension of 100 ha, it is however important to point out how this was a theoretical analysis and that despite the generous reduction in costs coming from an up scaling of the plants, in reality the largest plant producing Spirulina, the most largely commercialized microalgae, is only 44 ha, therefore much less than the 100 ha hypothesized extension.

(Base case)	Raceway ponds cts kg^-1 DW		Tubulars cts kg^-1 DW		Flat panels cts kg^-1 DW	
	1 ha	100 ha	1 ha	100 ha	1 ha	100 ha
Major equipment + power						
PVC liner	61.7	56.3				
Centrifuge	148.3	55.6	54.1	11.9	48.3	9.0
Power	21.3	23.9	4.6	5.0	3.2	3.7
Medium preparation	101.6	55.8	36.6	11.6	24.1	8.8
Power	4.8	5.3	1.1	1.0	0.8	0.8
Harvest buffer tank	31.4	23.6	7.9	4.9	5.0	3.7
Culture circulation pump			92.2	91.7		
Power			58.8	58.8		
Steel framework					14.7	14.7
Blower/paddle wheel	5.7	5.7	8.6	1.2	91.9	86.6
Power	4.0	4.0	7.3	7.2	300.8	300.8
Other capital						
Installation costs	52.3	28.7	59.8	36.4	55.2	36.8
Instrumentation costs	34.9	19.1	19.9	12.1	18.4	12.3
Piping	104.6	57.4	59.8	36.4	55.2	36.8
Buildings	104.6	57.4	59.8	36.4	55.2	36.8
Variable costs (ex. power) Polyethyene tubing/sheet			16.0	16.0	12.2	12.2
Culture medium	55.0	55.0	55.0	55.0	55.0	55.0
Carbon dioxide	42.1	42.1	42.1	42.1	42.1	42.1
Medium filters	55.5	55.5	23.0	23.0	17.4	17.4
Labour	724.4	15.7	362.2	7.9	235.7	5.1
Salary overhead	181.1	3.9	90.6	2.0	58.9	1.3
Maintenance	53.6	29.4	61.3	37.3	56.7	37.8
General plat overheads	427.9	24.8	116.7	21.4	160.8	23.6
Sum	**2215**	**619**	**1237**	**519**	**1312**	**745**

Table 7: *Actualized production cost (in cts, eurocents) for a unit of dried biomass from various capital and operating cost elements for raceway ponds, tubular photobioreactors and flat panel photobioreactors [53].*

4.7 Microalgae Market

It has been already pointed out how the high production cost of microalgae is still now days a limiting factor for large scale cultivation. The production cost for microalgae is also strictly linked to the safety requirements of the final product. In fact, being these organisms suitable for a wide range of application, there are solid difference between the optimal selling price in one or another market.
Fernandex et al. (2019) conducted a wide review on market size and price of microalgae-based products as a function of safety requirement of the end products [44]. Results of this review are showed in **Figure 30**, even if some of these data probably already went under some evolution due to the rapid increase of global microalgae market size.

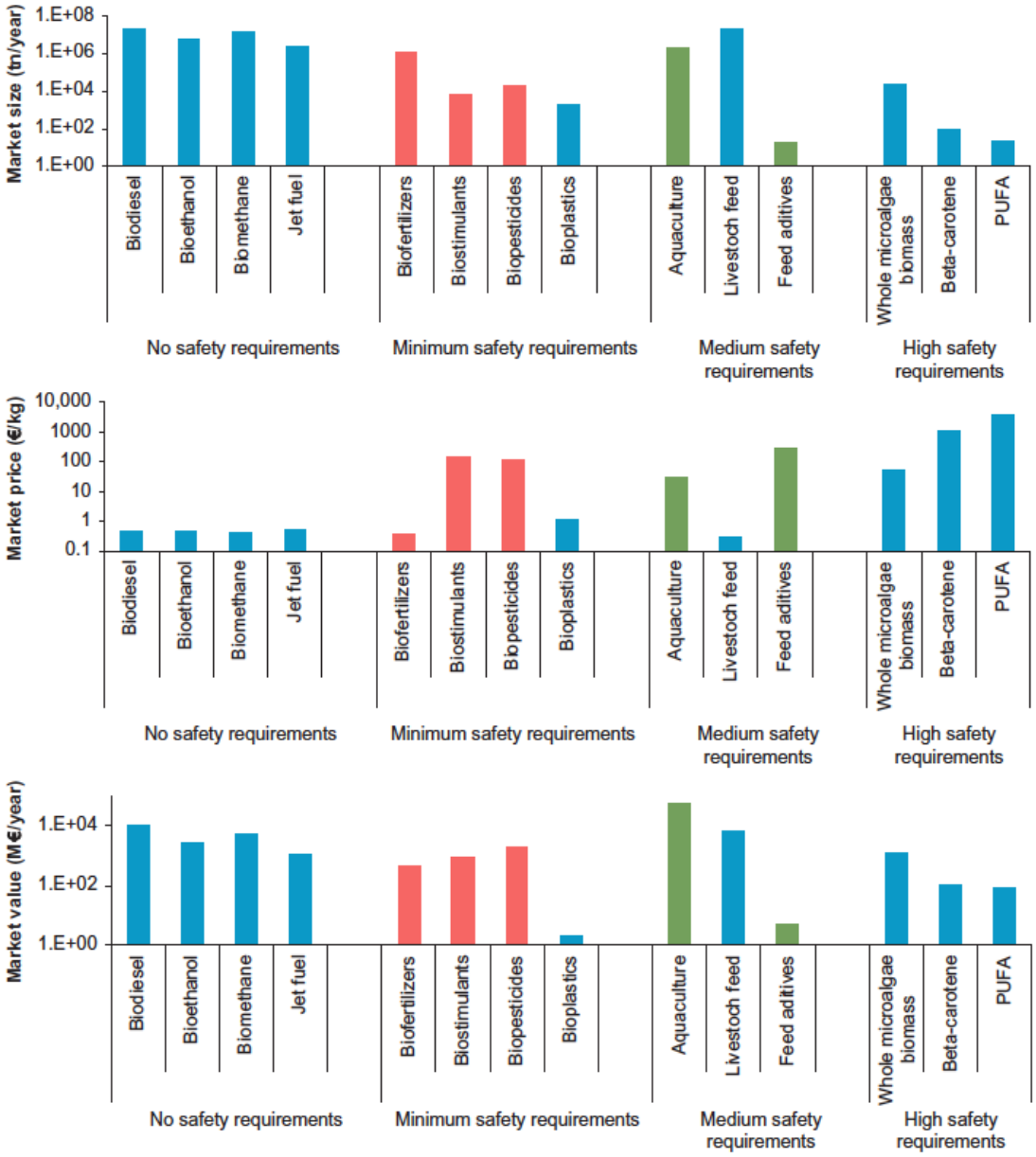

Figure 30: *Market size, market price and market value of microalgae based products according to their required level of safety [44].*

In the market with no safety requirements, the main end products are biofuels. Although this market is large, the production cost needs to be very low (below 1 €/kg), which is currently not achievable with existing technology. The next market with minimum safety requirements includes biofertilizers, biostimulants, biopesticides, and bioplastics, as well as commodities for industry. While the size of these markets is also substantial, the market price of biomass is higher (ranging from 1 to 100 €/kg) compared to biofuels. For markets with medium safety requirements, microalgae biomass is used in aquaculture, animal feeding, and feed additives. The sizes of these markets are similar to the previous category, but higher quality raw materials and technologies are required, resulting in higher production costs. The most relevant markets for microalgae biomass are those related to human applications, including food, nutraceuticals, and high-value compounds such as antioxidants and PUFAs (polyunsaturated fatty acids). Although these markets are smaller, the price of biomass is significantly higher (up to 1000 €/kg). However, producing biomass for these markets involves strict regulatory and safety requirements, limiting the number of strains that can be used. The best strategy to expand the commercial applications of microalgae is to focus on producing low-cost biomass in large quantities (below 10 €/kg and more than 1000 t/year). This would allow producers to enter emerging markets with medium and minimum safety requirements, such as aquaculture, animal feeding, agriculture applications, and commodities.

5 Plant design principles

Now that several microalgae strains have been selected according to their capability to grown in low pH and to absorb high concentration of gaseous CO_2, it is time to apply these experimental results in a real case scenario. The goal of this first plant design phase will be to roughly estimate the daily produced biomass, the daily CO_2 requirement and the volume of the whole plant. One of the most important step is to decide if the harvesting should work continuously or in batch. Advantages and disadvantages of both strategies have already been pointed out in section **4.4**. In this case a plant in which harvesting is done continuously for 16 hours per day 365 per year will be considered. The cut-off criteria for the design of the plant will be the nominal flow capacity of the centrifuge used to harvest microalgae. For this case, the use of a 500 l/h centrifuge will be assumed. This information is provided by DIATI microalgae cultivation laboratories in Politecnico di Torino. However, some more information about continuous cultivation are needed.

5.1 Principles of continuous flow culture

In cultures with continuous flow, a new batch of culture medium is introduced to the evenly mixed culture, while the culture itself is either continuously or periodically removed. This method is founded on the understanding that as cells grow, the available nutrients diminish and the produced substances accumulate. Eventually, cell growth stops because either the essential nutrient is depleted or an inhibitory substance builds up. To maintain cell growth, it is necessary to replenish the nutrient that limits growth and eliminate or dilute the inhibitory substance by introducing fresh culture medium.
As first step, we can assume that the medium feed rate and the rate of removal of culture medium (F) is the same, and the culture volume V is a constant. We can express the net increase in biomass in the culture as follows:

Net increase in biomass = Growth - Biomass removal

The equation can be rewritten for an infinitely small time interval dt, and the balance of the culture can be written as:

$$V dx = V \mu X dt - F X dt \tag{14}$$

where:

- V = culture medium (l)
- dx = Increase in biomass concentration ($g l^{-}1$),
- μ = Specific Growth rate ($1 h^{-}1$),
- X = Biomass concentration ($g l^{-}1$),
- dt = Infinitely small time interval (h)

- F = Culture flow rate ($lh^{-}1$) [98].

  Rearranging the previous equation is possible to obtain:

$$dx/dt = (\mu - F/V)X \tag{15}$$

The term F/V is called the rate of dilution of the culture and can be expressed as D, therefore:

$$dx/dt = (\mu - D)X \tag{16}$$

Considering a steady state, or a state were there is no increase nor decrease of biomass concentration, $\frac{dx}{dt} = 0$, and therefore $\mu = D$. If biomass is continuously harvested like in our case, the cultivation is reuquired to reach this steady state. Therefore, by knowing the Specific Growth rate μ ($1h^{-}1$) and the Culture flow rate F ($lh^{-}1$) it is possible to retrieve what should be the volume of the plant for each specific algae in order to maintain a constant biomass concentration. The volume will be expressed as:

$$V = F/\mu \tag{17}$$

Following these consideration, in theory, any concentration of biomass is suitable for continuous harvesting method, but to be effective some consideration based on the optimal production rate need to be done.

5.1.1 Consideration on microalgae selection

The selection of the most suitable microalgae species to grow has to be done according to the purpose of the cultivation. For the sake of this work, since the main objective is to fix the highest possible amount of carbon dioxide, the first step was to select microalgae species with an high fixation rate and biomass production. Secondly, since available literature on enhanced microalgae growth through high CO_2 concentration is wide, a selection of the most promising and adaptable experiment is necessary. As a first consequence, all biomass production values have to be normalized to a standard unit of measure, in this case grams of dry biomass produced over liter of medium per day ($gl^{-1}d^{-1}$). Among selected experiment, those which presented a concentration of biomass as g/l have been adapted to $gl^{-1}d^{-1}$ by dividing the final concentration for the number of days the experiment has been running. By doing so, a comparison between experiments is possible.
Another consequence of the wide availability of information is that many of these experiment were performed in controlled, artificially illuminated indoor lab condition. This detail could result in unbalanced application of lab data to this case, where microalgae are supposed to be grown in a outdoor, naturally illuminated plant. Therefore, only those experiments conducted outdoor with natural light or those conducted in artificial light but with a photoperiod (the light/dark cycle duration) which resemble the one of natural light, that is to say 12:12 dark/light will be considered. Consequentely, experiment with photoperiod of 24:00 will be discarded for now.
Following these considerations, many of the experiment previously reported in **Table 4**, Section 4.2, will be neglected as not applicable for an outdoor scenario.

5.1.2 Biomass production and CO_2 requirement estimation

Following previous considerations we were able to select four most adaptable experiments which could possibly be applicable to an outdoor scenario. These experiments concerned *Anabaena sp, Chlorella sp, Euglena gracilis and Scenedesmus obliquus*.
In the following step, considering a culture flow rate of 500 l/h and a 24 hours per day harvesting, the volume of daily processed culture medium was calculated as:

$$Daily flow rate = 500(l/h) * 24(h) = 12000 l/d \tag{18}$$

Using this daily flow rate and the biomass production rate from literature we were able to retrieve the daily biomass production as:

$$M_B = R_B \cdot Q_d = kg_{biomass}/day \tag{19}$$

where M_B is the biomass production, R_B is the biomass production rate and Q_d is the daily flow rate. The theoretical and the experimental CO_2 daily requirement were obtained using the theoretical 1,8 gCO_2/gBiomass and the experimental CO_2 fixation rate expressed by each experiment. Results of these calculation for the selected experiments are reported in **Table 8**.

Species	**Biomass production**		**Carbon Dioxide**			
			Experimental CO_2 **fixation rate**	**Theoretical** CO_2 **fixation rate**	**Experimental** CO_2 **requirement**	**Theoretical** CO_2 **requirement**
	($gl^{-}1d^{-}1$)	**(kg/d)**	**(g l-1 d-1)**	**(gCO_2/gBiomass)**	**(kg/d)**	**(kg/d)**
Anabaena sp.	0,418	5,0	1,01	1,8	12,1	9,0
Chlorella sp.	0,268	3,2	0,5	1,8	6,0	5,8
Euglena gracilis	0,142	1,7	-	1,8	-	3,1
Scenedesmus obliquus	0,141	0,7	0,106	1,8	1,3	1,2

Table 8: *Daily biomass production, theoretical and experimental daily CO_2 requirements for selected microalgae.*

Results shows the largest CO_2 requirement for Anabaena sp. This species also accounts for the highest daily biomass production. It is also possible to notice how theoretical and experimental CO_2 requirement are very similar.
The following step is to roughly calculate what should be the volume of the plant in order to continuously harvest the biomass using a 500 l/h centrifuge if the microalgae were growing with their maximum specific growing rate. The reasoning behind these calculation has already been explained in section **5.1** and results are collected in **Table 9**.

Species	**Max growth rate (d-1)**	**Culture flow rate (l d-1)**	**Theoretical plant volume (l)**
Anabaena sp.	0,24	12000	50000
Chlorella sp.	0,37	12000	32432
Euglena gracilis	0,72	12000	16667
Scenedesmus obliquus	0,63	12000	19048

Table 9: *Volumes required in order to continuously harvest biomass at a flow rate of 500 l/h with max growing rate*

Despite these results may look promising, it is necessary to remember that the maximum growing rate is not the average. Therefore, the volumes previously reported are certainly underestimated. A more precise computation would require the estimation of an average growing rate based on the light availability in the location selected to host the cultivation plant. In this way, a proper volume could be found based on the biomass production modeled on site. This process will be adopted to dimension the plant in **Section 6**.

5.2 Feeding CO_2 to the culture

Once the carbon dioxide has been collected and separated from other gasses at the source, many option are available. If the source is continuously emitting and the cultivation plant is naturally illuminated, carbon dioxide can be stored in proper tanks so that a controlled reserve is always available as the photosynthesis only happens during the day. This strategy could be beneficial is all the cases were the source is of an intermittent type. Moreover it can enhance the resilience of the cultivation in cases of any type of malfunctioning at the source. Another option is to activate the feeding system only during the day like **Seambiotic Ltd** does on their cultivation fed with unsaturated flue gasses. Therefore, once separated, carbon dioxide can be compressed in order to be stored in proper tanks.

5.2.1 Details about CO_2 supply system

Once the CO_2 has been stored the injection of it inside the microalgae culture at precise concentration can be more easily controlled. As for many lab experiment [6, 12, 56, 76], CO_2 is released from the storage tank where it is stored as pure. While it passes thought a valve and a flow meter a second gaseous source which is usually air or nitrogen is used to complement the flow in order to obtained the required volumetric concentration of carbon dioxide for the type of cultivated algae. Both the CO_2 and the air source have their own dedicated expansion valve and flow meter. The two gas components (CO_2 and air) are then injected into a gas mixer and consequently filtered in order to lower the risk of clogging the air sparger inside the reactor. A CO_2 sensor is also placed in between the mixer and the air sparger in order to double check the concentration. The gas mixture is then injected into the reactor where microalgae can finally utilize the carbon dioxide for their photosynthetic activity. Since oxygen is a photosynthesis product, an air outlet is also necessary for the release in order avoid oxygen accumulation which could lead to a photorespiration condition. An excessive amount of dissolved oxygen in the culture could result in decreased yields of cell mass as well as in pigment content. Moreover, under unfavorable conditions it could promote photo inhibition and photo oxidation resulting in quick culture death [98]. Because of this reason, a dissolved oxygen meter and a gas mass flow meter are usually implemented respectively inside the reactor and at its gaseous outlet. An example of these systems is shown in **Figure 31**.

Once the gas mixture has been opportunely mixed, it has to be injected into the reactor.

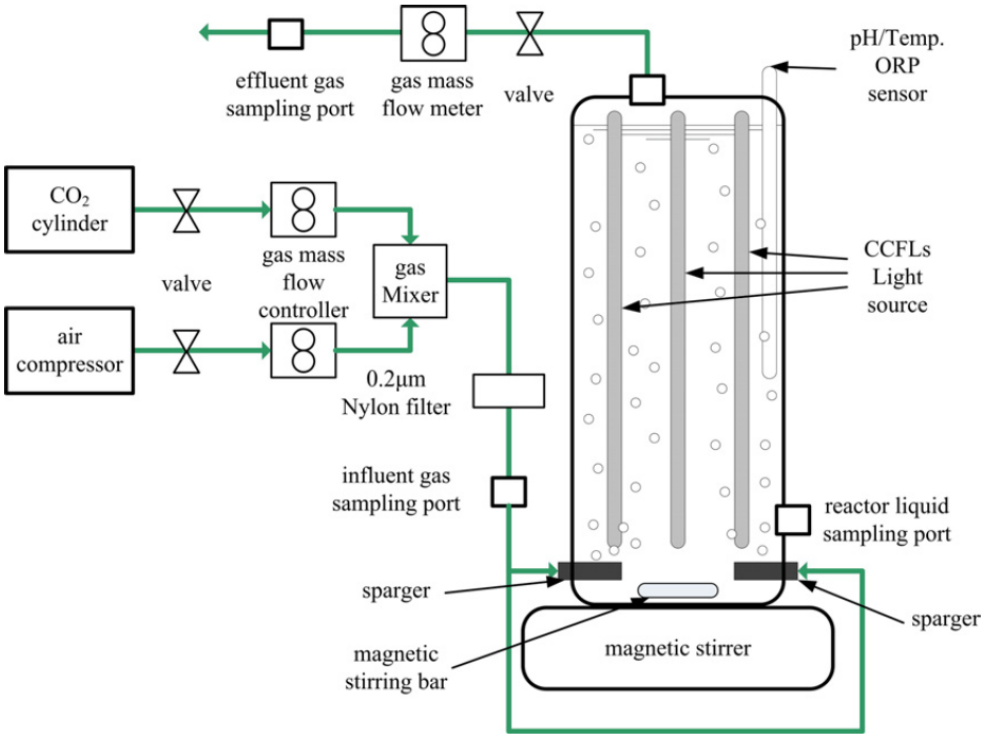

Figure 31: *Schematic representation of an experimental setup and instrumentation with two separated CO_2 and air sources, gas mass flow controllers, gas mixer and gas outlet [6].*

5.2.2 Photobioreactor types and air sparging system

Among the many aspects of CO_2 feeding, one of the most important is that the same system providing carbon dioxide is also partially responsible for the mixing of the culture. Turbulent mixing is fundamental in order to distribute cells into the illuminated portion of the reactor and for an even mixing of needed substances as well. Nevertheless, turbulent mixing could also result is an unsustainable shear stress for cell's membrane, leading in this way to a damage of the culture. This happens mostly during bubble formation, bubble rising and bubble brake up. Depending on the mixing strategy and on the geometry it is possible to divide photobioreactors into different categories. The most diffused are: bubble column, tubular, airlift and bag types.
Bubble column photobioreactors, also known as bubble column PBRs, are vertical tubes designed for chemical reactions. Gas is introduced at the bottom of the reactor, creating bubbles that rise through the reactor and exit from the top. This uniform sparging of gas ensures even distribution of bubbles throughout the reactor's cross-sectional area, inducing radial mixing of the growth medium. However, limitations arise as carbon dioxide is depleted and oxygen increases during the upward movement, restricting the height of the PBR. Furthermore, light penetration from the outer surface diminishes, reducing the reactor's diameter and compromising the uniformity of the growth medium. Illuminating the bubble column from all sides concentrates light towards the center, compensating for the decrease in surface area and maintaining uniform light

intensity throughout the column.

Airlift photobioreactors, another type of vertical tubular PBR, exhibit distinct vertical flows called risers and downcomers. These reactors feature physical barriers that separate the riser from the downcomer but don't extend to the top or bottom of the reactor. Air is introduced into the riser through a sparger, entraining the growth medium in the bubble flow. The medium travels up to the surface where air exits, while the growth medium turns laterally into the downcomer, moving vertically down the reactor. Carbon dioxide is concentrated in the riser due to the sparged gas, facilitating photosynthesis. Rectangular-shaped airlift PBRs can be constructed without a physical barrier between the riser and downcomer, offering improved gas exchange. However, scaling up these reactors can be challenging due to their fragility, height limitations, light penetration issues, capital costs, cleaning requirements, and concerns related to bubble bursting, gas holdup, gas transfer, and temperature control.

Tubular photobioreactors can be vertical, horizontal, or sloped, with varying tube sizes. They are composed by transparent pipers usually between 10 mm to 60mm diameter with variable length between 10-100m. They rely on a gas exchange system to remove oxygen and add carbon dioxide to the growth medium. Horizontal or inclined cylinders pose challenges for gas sparging, as the gas tends to collect at the top without effectively exchanging oxygen and carbon dioxide. Establishing perpendicular flow patterns in circular cross-sections is also difficult, but static mixers, injected gas, pumps, or turbines can induce mixing. Pumps are used to move the growth medium through vertically aligned tubes. For mass cultivation the medium is usually let flow at velocities between 0.2 m/s to 0.5 m/s in order to guarantee a proper mixing and a low mechanical stress on the cells [133]. Since the cells travel for the entire length of the pipes these systems have the disadvantage of accumulation of dissolved oxygen. Therefore a good system must be designed in a way that the time interval between two gassing point is enough to guarantee a good utilization of the injected carbon dioxide without reaching an excessive accumulation of dissolved oxygen. This time is denoted by the pumping velocity and the tube length and is called *dispersion time*. Due instead to the uneven distribution of light happening in the radial direction, the mixing time in this direction should not significantly exceed 1 s so that cells are not left in the bright front areas or the dark rear areas for too long [107]. High temperature, high pH, CO_2 and O2 gradients are also issues to take into consideration with these systems.

Bag photobioreactors are widely used for microalgae cultivation in the aquaculture industry, typically with volumes around 1-3 L. Sterilizing the bags, often made of polyethylene (PE), presents challenges, as autoclaving may not be feasible, and alternative sterilization methods are costly. Disposable bags that require periodic replacement can mitigate sterilization needs but contribute to plastic waste. Bag PBRs are adaptable, simple, and cost-effective, but optimization is necessary for scaling up and addressing the environmental impact of plastic waste. They are best suited for cultivation processes that don't require sterility, similar to open-pond systems. While bag PBRs show promise for large-scale microalgae cultivation, further refinement is needed to achieve industrial feasibility [78]. A schematic representation of these reactor types is given in **Figure 32**.

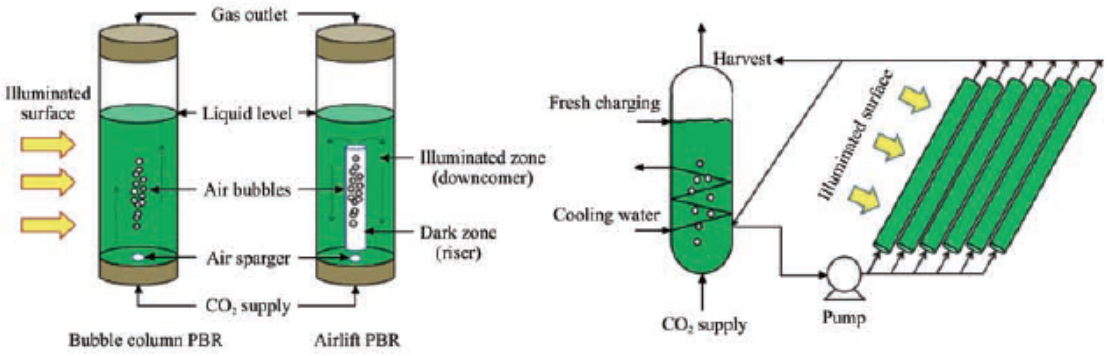

Figure 32: *Schematic representation of different types of PBRs for microalgae cultivation [106].*

5.2.3 Types of air spargers

It has already been explained how there are several types of different option for the configuration of a PBR. These differences mainly regard the geometry but also how the mixing of the medium is accomplished. The device which provides the gas into the culture medium is called sparger. This device is made up by a large number of small orifices that transfers a gas mixture into the microalgae growth medium through bubbles. The design of the sparger, including its geometry, diameter, spacing, orifice size, and number, is critical for efficient operation. Poor sparger design can result in an inefficient photobioreactor system. An example of four types of air spargers is given in **Figure 33**.

Design considerations include preventing weeping (when the gas pressure is lower than the medium pressure, causing the medium to enter the sparger) and minimizing the extent of non-uniformity (ENU) in gas transfer. Weeping is influenced by factors like pressure drop, liquid height, and surface tension. ENU occurs when gas transfer along the sparger is uneven, leading to high pressure drop and potential clogging. The amount of gas transferred to the photobioreactor affects flow patterns. Bubble diameter and flow pattern play significant roles in sparger and photobioreactor performance. Spargers consider three types of bubbles: small (volume equivalent diameter < 0.1 mm, spherical), intermediate (ellipsoidal), and large (diameters > 18 mm, cap-shaped with volume > 3cm3). Small bubbles decrease algae growth and productivity due to their similarity in size to the organisms, resulting in limited light penetration. Microalgae and cyanobacteria trapped in bubbles can be damaged when the bubbles burst due to the energy released. Large bubble diameters reduce the contact area between the air and medium, decreasing mass transfer. Optimal sparger design includes bubble diameters ranging from 3mm to 7mm and a flow rate that suspends microalgae, while maintaining a superficial gas velocity for homogeneous flow, especially during scale-up [133].

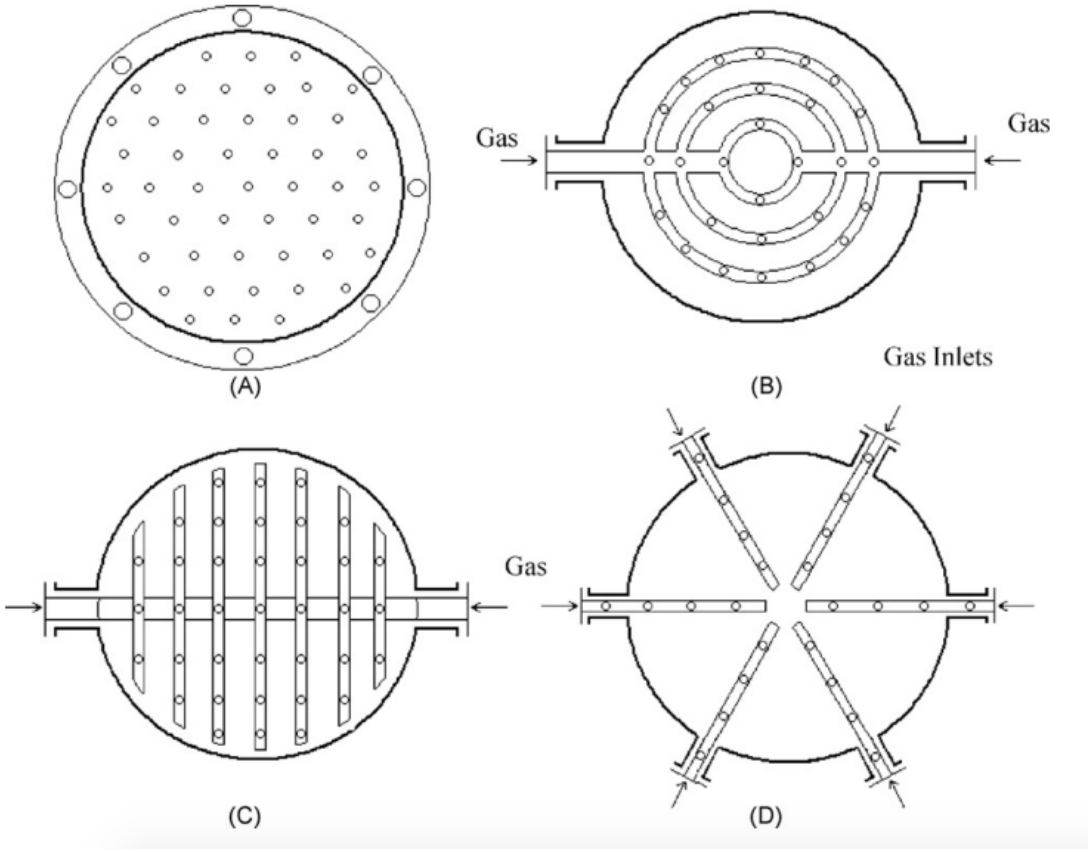

Figure 33: *Different sparger designs for bubble column reactor: (A) sieve plate sparger, (B) multiple ring spargers, (C) spider, and (D) pipe sparger [108].*

5.3 Technical parameters

The productivity of biomass in any culture system is heavily influenced by how closely the culture conditions align with the requirements of the selected strain. In a microalgal mass culture, mineral nutrient limitation can be easily avoided, making light availability and temperature the primary factors for achieving optimal system profitability. When the temperature is maintained within appropriate ranges, light availability becomes the sole determinant of growth. The incident solar radiation, which is influenced by the climatic and geographic parameters of the facility's location, as well as the design and orientation of the photobioreactor, determines the maximum energy available for growth. Due to mutual cell shading within the culture caused by the photobioreactor's geometry and the biomass concentration, a heterogeneous light profile emerges along the photobioreactor's cross section. The cell metabolism adapts to this light availability, influencing the biochemical composition and growth rate. Additionally, the fluid dynamics of the photobioreactor affect mass transfer and the light regime experienced by the cells. This light regime is influenced by the time cells spend in zones with different irradiance levels and the frequency of movement between those zones. It significantly impacts the behavior of the cells and their efficiency in utilizing solar radiation. Moreover, the design of tubular photobioreactors must also consider the transfer of gases between the liquid and gas phases and the dynamics of fluid flow. The introduction of carbon dioxide gas is essential for transporting inorganic carbon into the aqueous medium and maintaining the desired pH level of the culture. When the conditions remain constant, the inorganic carbon provided is assimilated into cells at a rate that is directly proportional to the intensity of photosynthesis. Likewise, oxygen is generated at a specific rate and transferred from the culture to the gas phase.

5.3.1 The volumetric mass transfer coefficient

The parameter which describes the capability of the reactor to transfer mass from the gaseous phase to the liquid phase and vice versa is called *volumetric mass transfer coefficient* and is the product between the mass transfer coefficient "K_L" and the interfacial area per unit volume of the aerated reactor "a". The mass transfer coefficient is indicated as $K_L a$ and measured in $[s^-1]$. This coefficient mainly depends on the geometry of the reactor, on the air sparging system type, on the properties of the liquid medium and on the mixing velocity. Each reactor as its own specific $K_L a$ for every gas component (CO_2 and O2) and despite several models have been proposed to evaluate the coefficient arithmetically, one of the simplest way is to directly measure the coefficient on site through the gassing-out method [109]. The estimation is done by filling the reactor with distilled water, hence in absence of any possible biomass interference, and by then blowing pure CO_2 into the reactor. A probe is then used to measure the concentration of CO_2 over time. The dissolved CO_2 concentration over time can be therefore describes as:

$$\frac{dC}{dt} = K_L a \cdot (C^* - C) \tag{20}$$

By integrating the equation for $C = C_0$ at t=0 it is possible to obtain:

$$\ln(\frac{C^* - C}{C^* - C_0}) = -K_L a \cdot t \tag{21}$$

From the previous equations, C_0 is the initial CO_2 concentration $[mgL^-1]$, C is the dissolved CO_2 concentration $[mgL^-1]$ at time t and C* is the CO_2 saturation concentration in water $[mgL^-1]$. The lower the mass transfer coefficient, the more efficient is the reactor in exchanging CO_2 from the gaseous to the liquid phase. Since the mass transfer coefficient has a strict dependency on several parameters of the reactor, giving average values can be controversial. Nevertheless, average values of $K_L a$ for different types of reactors vary between 10^-2 to $10^-5 s^-1$. [109], [110].

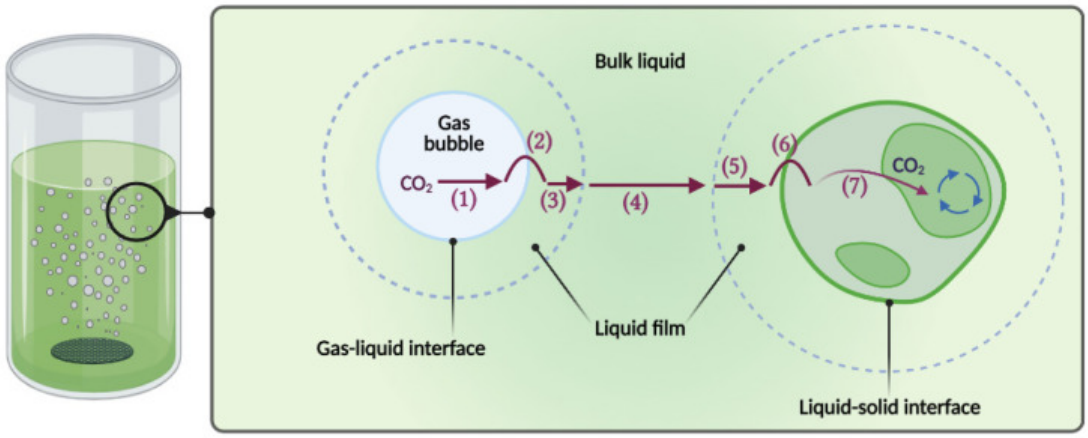

Figure 34: *Steps for CO_2 transfer from gas bubble to cell. (1) Transfer from the interior of the bubble to the gas–liquid interface. (2) Movement across the gas–liquid interface. (3) Diffusion through relatively stagnant film surrounding the bubble. (4) Transport through the bulk liquid. (5) Diffusion through the relatively thick film surrounding the microalgae. (6) Transport into the microalgae. (7) Transport through the cytoplasm to the site of the reaction. [112].*

The transfer of the gas to the liquid phase is a multi step process as shown in **Figure 34**. In a homogeneous regime, the rate at which mass is transferred through a given volume increases proportionally with the superficial gas velocity due to the formation of a greater number of bubbles. In this scenario, there is no interaction between the bubbles. However, when the superficial gas velocity is further increased, the rate of increase in the mass transfer coefficient becomes less than linear. This is because the smaller bubbles join together to form bigger bubbles in the process of coalescence. Since the volume and surface of a sphere of radius R are expressed respectively as:

$$V = \frac{4}{3}\pi R^3 \tag{22}$$

$$S = 4\pi R^2 \tag{23}$$

their ratio will be :

$$S/V = \frac{3}{R} \tag{24}$$

It can be easily understood that if the radius of the bubble increase, the surface to volume ratio will decrease leading to changes in the interfacial area per unit volume of gas and so to a smaller gas-liquid exchange. Smaller bubbles are therefore beneficial for the enhancement of the gas-liquid exchange [99]. Despite this, cells could also undergo damages due to both the shear stress of bursting bubbles and by the hydrodynamic forces which creates at the air sparger when the bubble leave the nozzle. In a optimization approach, a critical gas velocity should be found for the desire strain also considering the dimension of the turbulent eddies which should always be greater than the cell size in order to diminish the stress on the cell walls [99], [111].

5.3.2 Flow and gas–liquid mass transfer

It has already been explained how the design of a photobioreactor should take into account the gas-liquid mass transfer and hydrodynamics. Both the carbon dioxide assimilation and the oxygen production by microalgae play a role in the design of the system which must be capable of providing carbon at a specific rate proportional to the intensity of photosynthesis and at the same time to remove the generated oxygen. By applying a mass balance in different zones of the reactor it is possible to model these two fundamental aspects. The relation between the gas-liquid mass transfer rate and the generation/consumption rates can be expressed as follow:

$$Q_L d[O_2] = K_L aO_2([O_2]^* - [O_2])Sdx + RO_2(1-\epsilon)Sdx \tag{25}$$

$$Q_L d[C_T] = K_L aCO_2([CO_2]^* - [CO_2])Sdx + RCO_2(1-\epsilon)Sdx \tag{26}$$

where: $K_L aO_2$ and $K_L aCO_2$ denote the volumetric gas–liquid mass transfer coefficient for the two gas components; dx is the differential distance along the direction of flow; $[O_2]$, $[C_T]$ and $[CO_2]$ are the liquid-phase concentrations of oxygen, inorganic carbon and carbon dioxide; ϵ is the gas holdup, defined as the ratio between the cross section of the tube occupied by gas in respect to the total cross section; S is the cross-sectional area of the tube; RO_2 and RCO_2 are the volumetric generation and consumption rate of oxygen and carbon dioxide; Q_L is the volumetric flow rate of the liquid. The maximum possible liquid-phase concentration of the component in contact with the gas phase is the so called equilibrium concentration and are marked with asterisk [111]. As previously explained in **Section** 4.5.3 the dissolution of carbon dioxide generates carbonate and bicarbonate species into the medium, respectively $CO_3^=$ and HCO_3. Because of this, the mass balance considers the total inorganic carbon concentration C_T and not only the carbon dioxide. The components of the gas can also be modeled through a mass balance as follows:

$$dF_{O_2} = -K_L aO_2([O_2]^* - [O_2])Sdx \tag{27}$$

$$dF_{CO_2} = -K_L aCO_2([CO_2]^* - [CO_2])Sdx \tag{28}$$

where dF_{O_2} and dF_{CO_2} are respectively the molar flow rates of the 2 components in the gas phase [111]. The equilibrium concentrations of the gas phases can be expressed by using Henry's law as follows:

$$[O_2]^* = H_{O_2} P_{O_2} = H_{O_2}(P_T - P_V)\frac{F_{O_2}}{F_{O_2} + F_{CO_2}} \tag{29}$$

$$[CO_2]^* = H_{CO_2} P_{CO_2} = H_{CO_2}(P_T - P_V)\frac{F_{CO_2}}{F_{O_2} + F_{CO_2}} \tag{30}$$

where P_T and P_V are respectively the total pressure and the water vapour pressure. The integration of equations 25 - 30, together with proper initial conditions of the system allow the determination of carbon dioxide and oxygen concentration profiles along the tubular loop of the reactor. Camacho Rubio et al. (1999) verified the accuracy of these equations for the estimation of the behaviour of a tubular photobioreactor during the day as shown in **Figure 35** [113]. Being the mean error for the entire set of variable less than 15%, the model can be used as a scale up tool for any type of photobioreactor. The model is moreover very adaptable to different setups, being dependent of the gas holdup, on the volumetric flow rate, on the reactor mass transfer coefficient and on the generation and consumption rate of oxygen and carbon dioxide of the selected microalgae strain [111].

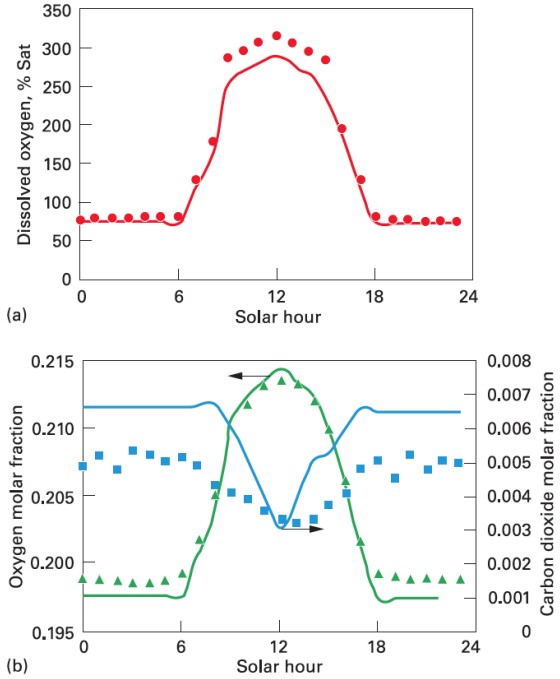

Figure 35: *Comparison between experimental (symbols) and simulated (lines) data of pH, total inorganic carbon, oxygen and carbon dioxide in the liquid and gas phase, on an outdoor tubular photobioreactor (0.22 m) [113].*

While having a look at **equation 30** it is possible to notice that the equilibrium concentration of carbon dioxide can be enhanced by increasing its partial pressure. However, the more CO_2 is dissolved into the medium, the lower will be the pH. The ultimate choice of CO_2 partial pressure should be done taking into account the carbon uptake capability of the microalgae in order to build a constant equilibrium in the photobioreactor. If the carbon dioxide injection is therefore driven by the uptake capability and pH, the while gas stream rate is instead dictated by the required mixing regime, which in turn also depends on the type of photobioreactor in use [4].

5.3.3 Carbon dioxide fixation yield

One of the most significant parameter to evaluate the efficiency of the system in the optic of carbon capture and utilization is the fixation yield of carbon dioxide (ηCO_2). This parameter evaluate the amount of carbon accumulated into the algal biomass in respect to the carbon supplied to the culture. The fixation yield is expressed as:

$$\eta CO_2 = \frac{W_{Cbiomass}}{W_{Cin}} * 100 \tag{31}$$

$W_{Cbiomass}$ and W_{Cin} are derived respectively as:

$$W_{Cbiomass} = W_{biomass} * C_{Cbiomass} \tag{32}$$

and

$$W_{Cin} = (W_{CO_2in} - W_{CO_2water}) * (M_C / M_{CO_2}) \tag{33}$$

where $W_{Cbiomass}$ indicates the kg of carbon accumulated in the biomass; $W_{biomass}$ are the kg of the biomass produced during the cultivation cycle; $C_{Cbiomass}$ is the fraction of carbon inside the cell that can be quantified through elemental analysis of the selected algae strain, W_{Cin} are the kg of carbon injected into the reactor as flow of carbon dioxide; $W\mathrm{CO}_{2i}n$ are the kg of carbon dioxide injected; W_{CO_2water} are the kg of carbon dioxide which remain dissolved in water at the end of the batch; M_C and M_CO_2 are the molar mass of carbon and carbon dioxide, respectively $12gmol^-1$ and $44gmol^-1$. The carbon dioxide fixation yield stricly depends on the type of microalgae and also varies according to the cultivation conditions. Typical values for photobioreactor cultivations are in the range between 50 and 90% [3]. This range is significantly lower for open pond cultivation being dispersion in the atmosphere almost immediate after the injection into the medium.

5.4 Choosing the plant technology and experimental data selection

Now that a wide overview of cultivation systems and techniques has been given, all necessary information are available to justify the choice of a precise technology between all cited ones. The choice is justified by several consideration.
First of all, if industrial cultivation of microalgae in raceway pond systems is neglected, few plants worldwide are able to economically sustain them self using flat panel, tubular and column reactor types. As pointed out in **Section 4.5.1**, among these plants even less of them are trying to use CO_2 captured from flue gases, independently if these gases come from a power plant, a cement industry or incineration plants. Only one

plant in Saga-city, Japan, is currently able to capture and use CO_2 coming from an incineration plant at commercial scale. Plus, a strong robustness of technologies like flat panel systems and tubular photobioreactors has not been fully reached at industrial scales. As a consequence, very few information are available about the operational parameters of commercial plants and because of this it is difficult to precisely orient with safety on a single technology.
Another consideration is that the extrapolation and use of results obtained during lab experiments conducted over a short period of time can be problematic since the productivity of microalgae is also linked to solar irradiation which varies, together with temperature, along the year. In this perspective, few year-round productivity data are available in literature for PBR [67]. Always on this side, productiveness values obtained in lab experiment should be taken with uncertainty and caution. The extrapolation of daily productiveness obtained in lab, for example during an experiment conducted in conical flask reactors, in fermenter or similar cannot be followed by an application of these data in a different type of reactors or in different illumination condition. Moreover, it is impossible to assume the application of these technologies in large scales as they are used mainly in laboratory for research purpose and not for commercial production. Even considering the same reactor type, single modules could perform differently in respect to a whole industrial plant because of the mutual shading of the modules or because of different flow conditions required fot a large scale cultivation [67]. Therefore, the coherent approach that will be used in this work is to strictly attain to those daily productiveness data conducted in condition that are the nearest possible to outdoor industrial cultivation. Following these considerations, priority of importance is given to experiments with illumination intensity and Light/Dark cycle similar to the natural ones and more important to those experiments conducted in systems that can be industrially scaled up with safety. Among the experiments previously cited in **Table 8 Section 5.1.2** which were already selected according to the illumination criteria, the one of *Scenedesmus obliquus* will therefore be neglected because conducted in Erlenmeyer flask while all the others are well applicable for the scope of this work because conducted in Bubble Column Photobioreactor (BCPB). Data of the cited experiments concerning the parameters needed for the best growing conditions are reported in **Table 10**. As a consequence to these consideration the final chose of the type of reactor to use will fall on bubble column photobioreactor, BCPB from here over.

Species	**Reactor type**	**V (l)**	**Light Intensity**	**Light/dark (h)**	**Outdoor**	**T(C°)**	**CO_2 (%)**	**pH**	**CO_2 fixation rate (g l-1 d-1)**	**Biomass production**			**Ref**
										Value	U. of measure	g l-1 d-1	
Anabaena sp.	BCPB	5	250 [b]	12:12	no	35	10	5.9	1.01	2.09	g/d	0.418	[6]
Chlorella sp.	BCPB	1	84 [b]	12:12	no	18	10	6	0.5	0.27	g l-1 d-1	0.268	[76]
Euglena gracilis	PB	1000	-	-	yes	28	7.5	3.5	-	0.710	g/l (5 days)	0.142	[56]

Table 10: *Growing condition parameters for the selected microalgae strain according to cut-off criteria listed in* ***Section 5.4***

As already pointed out in **Section 5.2.2**, in BCPB the mixing is provided by the bubbling of the gas from the lower part of the column. On the upper part, a gas outlet releases the mix of oxygen and unconsumed carbon dioxide. In general terms, vertical-column photobioreactors accounts for high gas to liquid mass transfer, a good mixing with low shear stress (even if this striclty depends on the gas inlet velocity), low energy

consumption and high potentials for scalability. They are moreover easy to sterilize and already largely used in commercial production of microalgae. Despite these advantages, their construction require sophisticated materials and due to their shape microalgae experience a decrease of illumination surface area upon scale-up [110]. Commercial application of vertical photobioreactor is already on the run from several years. For instance, several bubble column photobioreactor producers are selling their systems worldwide. Annular columns in volumes ranging from 30 to 230 liters are available through Fotosintetica & Microbiologica (F&M) Srl, an Italian company (femonline.it/products, 9 August 2023). Exenia Group Srl (Padova, Italy) produces microalgae for aquaculture facilities, cosmetic and food integration using column type photobioreactor in Pinerolo, Italy (exeniagroup.it, 9 August 2023). Same for Microalgaetech Srl (Salerno, Italy) which uses vertical photobioreactors for food integration and cosmetic purposes (microalgaetech.com/, 19 August 2023). Now that the choice of the technology has been made, it is time to collect a range of design parameter and operative parameters of these reactors

5.4.1 Bubble Column Reactor design parameters

Despite some range of flexibility exist for the dimensioning of BCPB, on average their size varies around some standing still values. The diameter of a BCPB for algae culture should not exceed about 0.2 m in order to guarantee light availability along the radial direction even to the portion of the medium standing in the inner region. For what concerns the height of the reactor, it should not exceed 4 m for structural reason and to reduce the mitual shading of single modules in a multicolumn facility. As in any other reactor, the aeration rate should provide a good mixing of the medium but not damage the cells due to shear stress on their membrane. Finally, the gas holdup and the overall gas-liquid mass transfer coefficient should be enough to provide a good exchange of carbon and the removal of excess produced oxygen [117].

5.4.2 Mass transfer coefficient and gas holdup in bubble column reactor

Mubarak et al (2019) conducted several experiment to characterize a 20 l, 90 cm height 18 cm diameter cylindrical BCPB. In their configuration, holes in the air sparger were arranged in star-shaped manner so that the plate would not experience weeping phenomena and uniform homogeneous bubble distribution will be achieved in microalgae culture without causing any shear stress to algal cells. Their experimental results showed a volumetric mass transfer coefficient $k_L a_L(s-1)$ ranging from 0.01 to 0.07 depending on the gas velocity at the air sparger (from 0.01 to 0.05 m/s) while a gas holdup ϵ from 0.01 to 0.06 always depending on the same range of gas velocity at the inlet [115]. Miròn et al. (2000) evaluated several configuration of column photobioreactor among which the bubble column finding values of gas holdup between 0.015 and 0.1 according to a specific power input ranging from 40 to 500 W/m^3 and a mass transfer coefficient between 0.002 and 0.030 depending on the gas outlet speed (from 0.002 to 0.033 m/s) [117]. Khoo et al. (2015) investigated a pilot-scale semi-continuous cultivation of microalgae Chlorella vulgaris in bubble column photobioreactor finding the best optimum growing condition for the microalgae at compressed-air aeration rate of 0.16 VVM, with superficial velocity of 0.185 m s-1. In this set-up, the experimental

volumetric gas-liquid mass transfer coefficient was calculated as 0.0045 s-1 [116]. Multiple models have been proposed to theoretically express the gas holdup and the mass transfer coefficient, where the first strictly depends on superficial gas velocity and the latter on superficial gas velocity, depth of the column and effective gassed area [118]. Desing parameters for these experimental setups are collected in **Table 11**.

Working Volume (l)	**Dimension (HxD in meters)**	**Gas velocity (m/s)**	**Gas Holdup (-)**	$k_L a_L(s^-1)$	**Reference**
13	1.5x0.13	0.005-0.082	-	0.0017-0.0047	[119]
56	2x0.19	0.002-0.033	0.015-0.1	0.002-0.030	[117]
20	0.9x0.18	0.01-0.05	0.01-0.06	0.01-0.07	[115]
56	2x0.2	0.185	0.012	0.0045	[116]

Table 11: *Design parameter of some experimental Bubble Column Photobioreactor setups where H is the height of the reactor and D its diameter.*

6 Dimensioning of the cultivation plant in Macchiareddu

6.1 Biomass production

In this chapter, a simplified model for biomass production estimation for a bubble column reactor based on natural light availability is presented and applied in Tecnocasic municipal waste incinerator's location. The model simplifies the cross section of a bubble column reactor as representative for its whole volume. Uses the Lambert-Beer law to compute the light penetration inside of it and the Molina growth model for an estimation of the specific growing rate. It then computes the required carbon dioxide and macro nutrients as well. For this purpose A MATLAB code was developed by the author and reported into the **Annex 8.1**.

6.1.1 Growth modelling on light availability

Several studies have tried to develop a model to link the growing rate of microalgae to the irradiance. As pointed out in **Section 4.3.2**, light intensity and growth rate show a linear relationship only if the first is less than the saturation light intensity, quantity above which photosynthesis is slowed down because of the saturation of the photosystems. Despite, this linear behaviour, linking illumination and growth rate with a linear relationship is not recommended. In an accurate analysis on light intensity the correct approach would be to use a model to express the distribution of irradiance inside the reactor. This is fundamental since as microalgae grow, their concentration and therefore optical density of the medium increases as well, causing a mutual shading between fluctuating cells. In this way, as shown in **Figure 36** cells staying on the outern layers could for example receive a saturating irradiance during the brightest hours of the day while cells laying on the inside region of the reactor could be in a different region of the light-photosynthetic activity path.

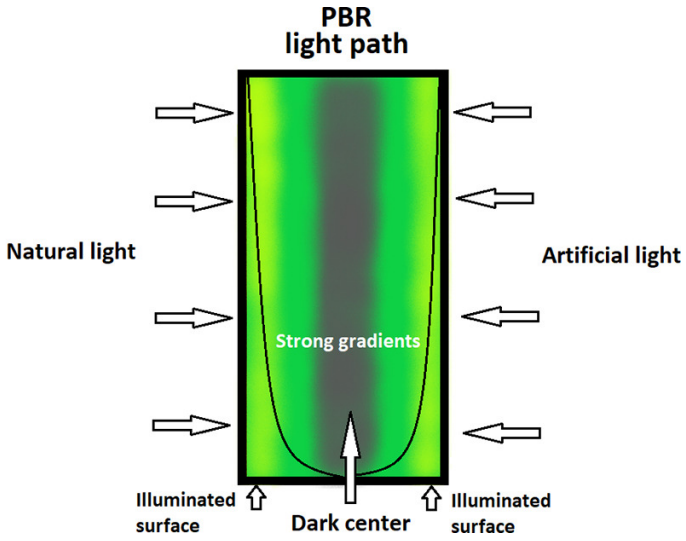

Figure 36: *Schematic representation of light attenuation inside a column photobioreactor [122]*

The steps in order to link light intensity with biomass production on a particular reactor type is to first express the incoming radiation inside the reactor with a proper model which considers the attenuation of light by the cells itself as a function of the type of algae and its concentration, the incoming solar radiation intensity and the path it has to take inside the reactor. Secondly, this radiation can be linked to the growing rate of algae according to different models. As a first approach, Lambert-Beer law can be used to express the incoming radiation that has to cross a certain path inside a certain medium. The law states that the radiation intensity attenuation when going thought a medium is expressed as:

$$dI = -K_a C dx \tag{34}$$

where:

- K_a is the attenuation coefficient measured in squared length over grams of biomass m^2/g
- C is the concentration of the biomass into the medium g/m^3
- dx is the infinitesimal increase in the light path in meters

By integrating the equation 34 between a path of length "l" and by isolating the radiation it is possible to obtain the irradiance at any point of distance "l" from the incident point as:

$$I_1 = \eta_{transmission} * I_0 \exp -K_a C l \tag{35}$$

In the equation above, $\eta_{transmission}$ is the trasmissivity coefficient of light of the chosen material. The Coefficient of attenuation of microalgae species K_a depends on their shape pigmentation and on the incoming light wavelength. Despite this, for the scope of this work there won't be distinction between wavelength nor dependency on the chlorophyll content. Unfortunately, at the knowledge of the authors the only values that could be found in literature regarded Chlorella pyrenoidosa and Anabaena. Moreover, since Anabaena attenuation coefficient is given in square centimeter over filament and there are no data in literature regarding the weight of a single Anabaena filament, the only remaining species suitable for following calculation is Chlorella sp **Table 12**.

Species	**Attenuation Coefficient**	**Reference**
Anabaena sp	$5.2x10^{-}6cm^2 filament^{-}1$	[120]
Chlorella Pyrenoidosa	0.200 m^2/g	[121]
Euglena	-	-

Table 12: *Light attenuation coefficient of selected species*

According to the coefficient of attenuation, molar or dry weight concentration can be used in **equation 34**. Light penetration models, in this case the Lambert-Beer law can be used to check the light availability of the species in the different points of the reactor during specific time intervals of the day. Since in this work a continuous culture is assumed, once working the reactor will approximately have always the same concentration of biomass. For instance it is necessary to collect data relative to the

Species	**Saturation irradiance** ($\mu molm^2s^-1$)	**Reference**
Anabaena sp	118	[123]
Chlorella sp	270	Polito Lab
Euglena gracilis	178	[56]

Table 13: *Half saturation constant for the selected species*

saturation irradiance of these species. These data are available in literature and listed in **Table 13**

Once the irradiation profile along the reactor thickness is defined, a growth model can be used to express specific growth rate as a function of irradiance. Despite the scientific literature offers several of these models, one of the easiest to apply is the one developed by Molina et al. (1994) [125]. The local specific growth rate in a point "p" of the reactor can be expressed as:

$$\mu_{i,p} = \frac{\mu_{max} I_{i,p}^n}{I_k^n + I_{i,p}^n} \tag{36}$$

where:

- μ_{max} is the maximum specific growing rate, a characteristic of each algae species.
- I is the average incoming irradiance
- I_k is the saturation irradiance for the specific algae species
- n is a parameter which takes into account the mutual shading between the cells and depends on the shape of the organism, in this case n=1.7 [136].
- "p" is the index of the considered point inside the reactor and "i" is the hour of the day index.

The cited model is quite simplified. It does not takes into account nutrient depletion, temperature effects, growth inhibition because of excess oxygen and other factors influencing the growth. Moreover, since in this work the model will be applied every hour, it is necessary to have an hourly maximum growing rate. This value is found dividing by 24 the daily maximum growing rate provided by Zhao et al. 2015 [76]. Therefore:

$$\mu_{max,h} = \frac{\mu_{max,d}}{24} = \frac{0.372}{24} = 0.0155h^-1 \tag{37}$$

Except for irradiance, to which the following section will be dedicated, all other the parameters concerning the application of **equation 36** are listed in **Table 14**.

6.1.2 Incoming irradiance in the selected cultivation site

In order to proceed with the calculation of the specific growing rate, the first step is to obtain irradiance data on the site where the cultivation is expected to be built.
The radiation incident on the surface of a photobioreactor consists of direct sunlight,

Parameter	Value	U. measure	Ref
Specific growing rate μ_{max}	0.0155	h-1	[76]
Attenuation coefficient K	0.2	m^2/g	[121]
Concentration C	0.8	g/l	Author
Saturation Irradiance I_{sat}	270	$\mu mol/m^2 s$	Polito Lab
Light Trasmissivity (glass)	95	%	[133]
Shape parameter n	1.7	-	[134]

Table 14: *Culture parameters for the application of Molina model*

reflected radiation from the surroundings, and diffuse radiation due to particulate matter in the atmosphere and clouds all these components together make the Global Horizontal Irradiance (GHI). Irradiation data for Macchiareddu site (39.185033, 9.011559) can be easily obtained from PVGIS portal, the Photovoltaic Geographical Information System provided by the Joint Research Center of EU [38]. Since a BCPB is not horizontally placed but vertically, a correction is needed in order to compute the Global Tilted Irradiance. Moreover, not all solar radiation is useful for the photosynthesis. A theoretical maximum photosynthetic efficiency as been calculated between 8 and 10% of the total irradiance received by microalgae. However it has been showed that average values for photosynthetic efficiency mostly fall between 0.5 and 3% of the received irradiance converted into biomass. This reduction takes into account several processes such as photorespiration, cellular metabolic activity and heat losses [43]. For what concerns the solar radiation components, if the Global Horizontal Irradiance is considered, the following correction are needed in order to find its component on a vertical surface:

$$I_T = I_H \frac{cos\theta}{cos\theta_z} \tag{38}$$

where:
θ is the angle of incidence estimated as:

$$\begin{aligned} \theta = \cos^{-}1(&sin\delta \cdot sin\phi \cdot cos\beta \\ &-sin\delta \cdot cos\phi \cdot sin\beta \cdot cos\gamma \\ &+cos\delta \cdot cos\phi \cdot cos\beta \cdot cos\omega \\ &+cos\delta \cdot cos\phi \cdot sin\beta \cdot cos\gamma \cdot cos\omega \\ &+cos\delta \cdot sin\beta \cdot sin\gamma \cdot sin\omega) \end{aligned} \tag{39}$$

and

$$\theta_z = \arccos(cos\gamma \cdot cos\phi \cdot cos\omega + sin\delta \cdot sin\phi) \tag{40}$$

- β is the surface slope, or the angle between the photobioreactor's surface and the horizontal. For vertical photobioreactor this value is equal to 90°
- γ is the surface azimuth angle, or the deviation of the projection on a horizontal plane of the normal to the surface from the local meridian.
- ϕ is the latitude of the site.

- δ is the solar declination angle which depends on the day of the year "N" and is expressed as:

$$\delta = 23.45 \cdot sin(\frac{360(284+N)}{365}) \tag{41}$$

- ω is the solar angle which depends on the solar hour expressed as local standard time in 24hours format and is expressed as:

$$\omega = 15(12-h) \tag{42}$$

A representation of these useful angles has been provided by Molina et al. (1998) and it's shown in **Figure 37**. PVGIS portal automatically implements these calculation, therefore by setting a slope angle of 90° and an azimuth of 0°, hourly Global Tilted Irradiance is given in W/m2. There values has then to be converted to micro moles of photon per second. But, as previously said, not all the solar radiation is photosintetically active. Microalgae and plants in general utilize only specific spectral range for their metabolism. Photosynthetically active radiation (PAR) wavelenghts are those which falls in the range between 4.0 to 7.0 μm. In general, only 45% of the energy of solar radiation falls in this range. Therefore, according to literature, a conversion factor of 2.02 is used to convert W/m2 to micro moles of PAR photons per m2 per second [126].

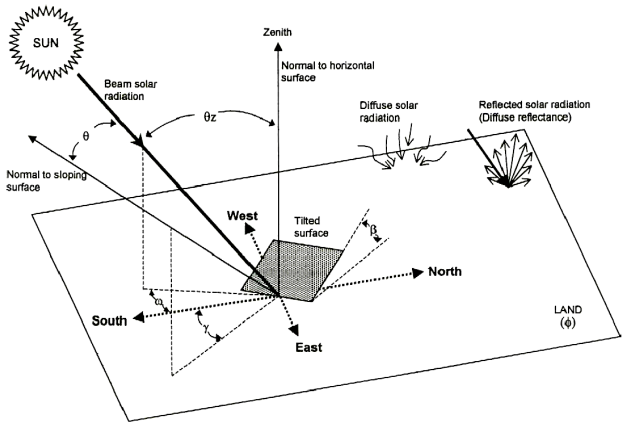

Figure 37: *The various angles relevant to estimation of solar radiation level incident on the flat surface of a photobioreactor with any general orientation relative to the land [125].*

Radiation data were therefore obtained from PVGIS-SARAH2 database for the year 2020 at the selected location (9.185033, 9.011559) at 0° and 90° degree slope. Consequently, they were converted as follow:

$$1\frac{W}{m^2} = 2.02\frac{\mu mol}{m^2 s} \tag{43}$$

Figure 38 shows the radiation component profile along the year for a vertical and horizontal surface.

While having a look at the vertical surface scenario, it is possible to notice how the profile of direct irradiance follows a convex shape while the opposite happens for

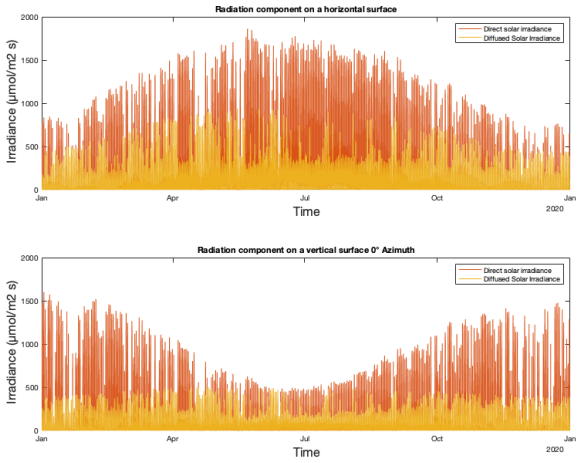

Figure 38: *Irradiance component along the year for an horizontal and vertical surface*

the horizontal surface. This behaviour is clearly linked to the solar angle development along the seasons. Another important consideration to point out is that the irradiance is almost always above the saturation level of *Chlorella*. This means that the first layer of medium inside the reactor will likely be saturated and therefore not productive along most of the year. In order to overcome this issue, a shading system made by white, light diffusive nets is assumed to be adopted. The system consists in a series of nets which spread above the cultivation thanks to the work of a cable system driven by electrical motors. These types of systems are widely adopted in greenhouses for regular plants to overcome the limit of saturation irradiance and to enhance the diffusive component, which penetrates along the plant leaf structure more easily and provides a more widespred source of light for the cultivation [114]. The shading nets can be seen partially open above the industrial PBR in Roquette Klötze GmbH & Co. KG Chlorella vulgaris cultivation plant [32] as shown in **Figure 39**.

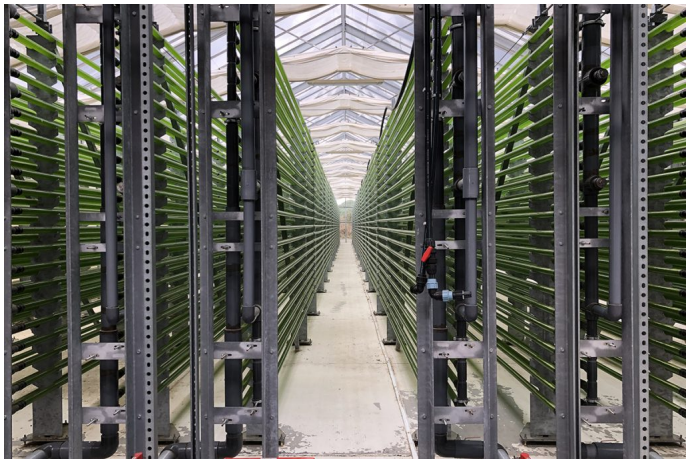

Figure 39: *Partially open shading system above the PBR in Roquette Klötze GmbH & Co. KG Chlorella vulgaris cultivation plant [32]*

When the sum of direct and diffuse irradiance is above the saturation level of the selected microalgae strain, the shading system is activated. **Figure 40** shows how the plastic film would modify the radiation component when the system is active.

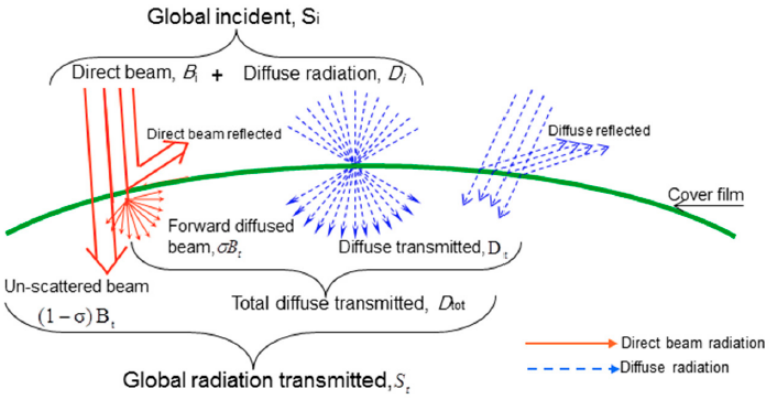

Figure 40: *Schematic representation of the transmission and diffusion mechanisms of solar radiation components when they pass through a plastic film [114]*

As can be seen form the figure, two main modification happens when the shading system is active. First, part of the direct and diffuse incoming irradiance on the horizontal film is reflected, the remaining portion is transmitted from the net into the greenhouse according to the transmittance τ. Secondly, a part of the direct irradiance which is not reflected is diffused according to the diffusion coefficient σ (-), the remaining penetrates as direct according to a factor (1-σ). Therefore, when nets are active, the direct and diffuse incoming irradiance will be partially reflected and the remaining intensities will be:

$$\begin{aligned} B_t &= \tau * Bh_i \\ D_t &= \tau * Dh_i \end{aligned} \tag{44}$$

where:

- the subscript "t" indicates transmitted and "i" means incident.
- Bh and Dh are respectively the direct beam and diffused irradiance on a horizontal surface.
- τ is the transmittance of the material(-)

As the irradiance component are transmitted into the greenhouse, or in general below the plastic film, the direct transmitted irradiance undergo an ulterior transformation thanks to the scattering properties of the plastic film. This component is scattered and diffused so that the total diffused and direct irradiance now becomes:

$$\begin{aligned} D &= \sigma * B_t + D_t \\ B &= (1-\sigma) * B_t \end{aligned} \tag{45}$$

where:

- "D" is the diffuse irradiance component below the plastic film
- "B" is the direct irradiance component below the plastic film
- σ is the diffusion coefficient (-) of the plastic film

The film provides a way to transform the direct irradiance in diffused irradiance and moreover it generally decreases the intensity of light transmitted into the greenhouse. In this way, more light is available for those part of the reactor which normally would be in shade and light intensity is evenly lowered along the seasons. The implementation of this solution is done by building a MATLAB model which, for every hour, works as follow:

- verify if the sum of direct and diffused radiation on a vertical surface is above the saturation level of *Chlorella* (270 $\frac{\mu mol}{m^2 s}$)
- if the previous is true, shading system is activated and radiation components are modified as shown in **Equation 44** and **45**
- if the first condition is not true, the shading system does not activate and the photobioreactor receives the direct and diffuse radiation component on a vertical surface.

For the purpose of this work, experimental data from Al-Helal et al. 2020 [114] regarding a particular plastic film produced by Napco Modern Plastic Products Company-Sack Division Ltd. (Dammam, Saudi Arabia) were used. According to the cited research, τ and σ of the selected film are respectively 0.77 and 0.43. As shown in **Figure 41**, the adoption of this system results in a modified irradiance profile along the year. Direct irradiance component is heavily lowered and spread more evenly, together with the diffused one, along all the seasons. In this way, despite summer being the brightest season, the irradiance level below the nets has less extreme seasonal oscillations.

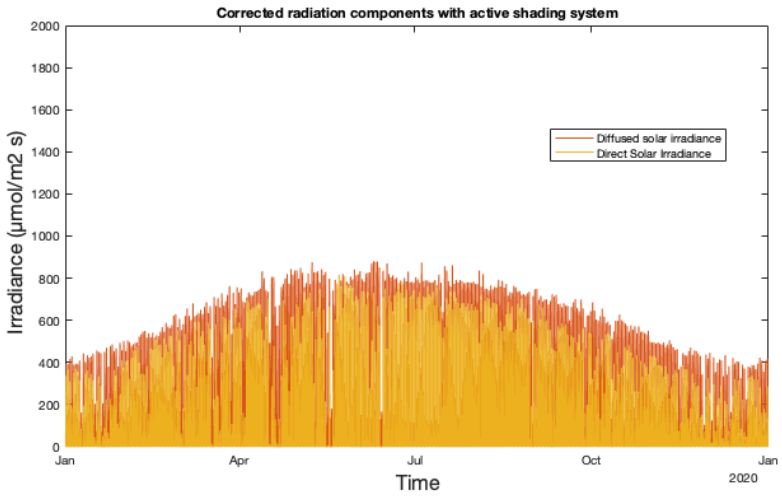

Figure 41: *Corrected irradiance component along the year when the shading system is active*

6.1.3 Reactor geometry and light penetration modelling

The following step in order to compute how much biomass could potentially be produced in a specific site is to model the reactor geometry and consequently, model the light penetration inside the reactor. In this case, two simplified bubble column reactors are presented. One is a standard Bubble Column with the entire volume available for medium circulation. The second one is a bubble column with an empty cylindrical volume inside. This last type of reactor tries optimize the volumetric productiveness of the reactor by making un-available for the medium regions of the reactor which would be under low illumination for the most part of the year. The technical difficulties of building, cleaning and in general maintaining such type of reactor are however not investigated here despite it is comprehensible that having such a complicated volume could present disadvantages in respect to a standard cylindrical column. Finally, for the simplicity of this work, the simplified reactors will be represented by a generic cross section of the reactor itself. The reactors dimension and capacity are reported in **Table 15**.

Reactor type	**Dimension (HxD) (m)**	**Volume (l)**
Bubble Column	2x0.05	7.85
Bubble Column empty volume inside	2x0.1 (outer cylinder), 2x0.05 (inner cylinder)	23.56

Table 15: *Reactor dimensions and volume where H=height, D=base diameter*

Inside the cross section of the bubble column a fine grid of control points is created. The number of points was 1876 for the Bubble column with full volume available and 1408 for the Bubble column with the empty volume inside. Each point is representative of a small portion of medium volume equal to:

$$volume = \frac{Reactor\,volume}{number\,of\,points} \tag{46}$$

For what concern the irradiance, the southern point of the reactor, indicated in **Figure 42** by a red dot, is assumed to be an approximation of the sun position. Therefore, direct irradiance will be coming from this point while diffused irradiance will be penetrates from all all around the reactor's surface. A schematic representation of the reactors cross section together with control points is given in **Figure 42** and **Figure 43**

Clearly, a more precise analysis would better define the sun position as the equation system provided by Molina et al. 1996 [125] indicates. The sun elevation angle and therefore the light penetration at different height of the reactor should be taken into account in a 3D approach. Nevertheless, being the scope of this work a first dimensioning of a plant and not a fine modelling of bubble column reactors, the purposed 2D simplification will be taken as acceptable. It is however important to point out that having the sun position approximated at the surface could cause an overestimation of the amount of direct light which penetrates into the reactor for two main reasons. The first is that the amount of medium that direct radiation travels increases when the elevation angle of the sun increases. When the sun is high above the horizon, part of the reactor volume near to the ground could be in shade. Moreover, in a real industrial

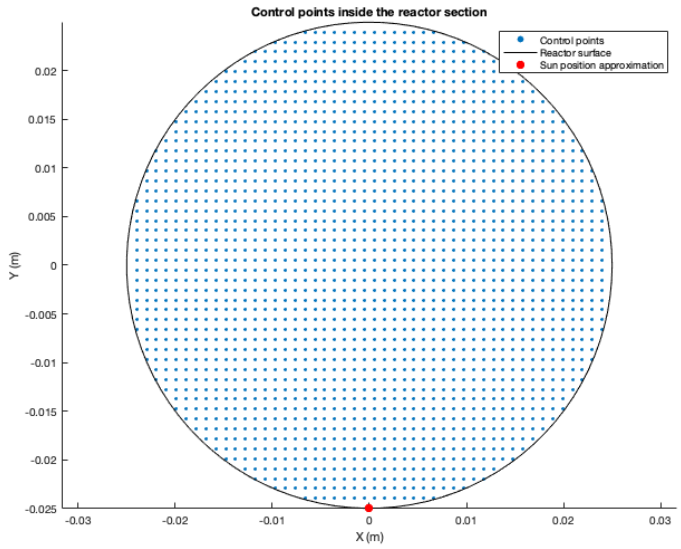

Figure 42: *Cross section of the simplified Bubble Column reactor with control points. The red dot represents the approximation of sun's position.*

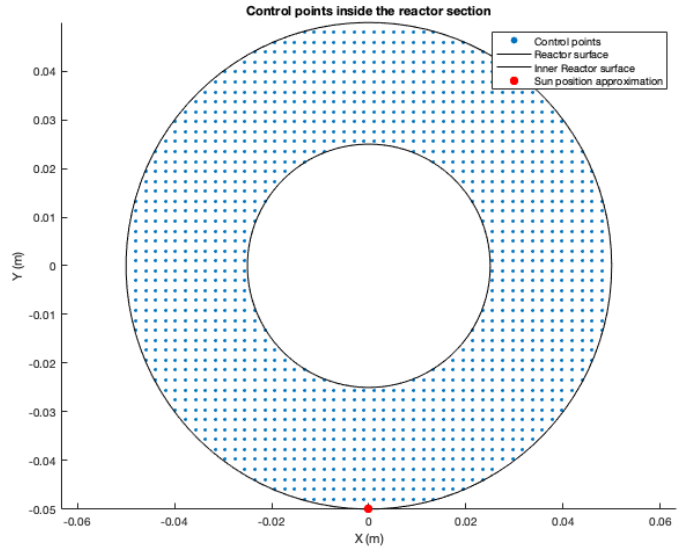

Figure 43: *Cross section of the simplified Bubble Column reactor with empty volume inside and control points. The red dot represents the approximation of sun's position.*

plant the relative position PBR modules will influence the amount of mutual shading between them. Here instead, this phenomenon will be neglected.

Once the control points grid is enstablished inside the cross section, 2 main para-

menter are computed for each point:

- the distance "s" of each point from the approximated sun position
- the distance "d" of each point from the surface of the reactor, or depth

These two parameters are respectively found as:

$$\begin{aligned} d_p &= r - \sqrt{y_p^2 + x_p^2} \\ s_p &= \sqrt{(r + y_p^2) + x_p^2} \end{aligned} \tag{47}$$

where:

- x_p and y_p are the coordinates of the generic point "p" inside the cross section
- "r" is the reactor radius

Once all distances are found, the Lambert-Beer light penetration law can be applied. More specifically, for a precise hour, the irradiance received by a generic point "p" inside the reactor cross section will be found as:

$$I_p = \eta_t * [B * exp{-K_a} * C * s_p + D * exp{-K_a} * C * d_p] \tag{48}$$

where:

- η_t is the transmission coefficient of the PBR material, in this case 0.95 for glass.
- "B" and "D" are respectively the direct and diffuse component of irradiance after the active shading system correction made in the previous section
- K_a and C are the light attenuation coefficient and the constant biomass concentration inside the reactor, respectively 0.2 m^2/g and 0.5 g/l

In order to appreciate the results from the application of Lambert-Beer law in the simplified cross section, the brightest hour of the year is found as the 22nd of May 2020 at 12 pm (noon) and used as example for the Bubble column reactor with and without the active shading system in **Figure 44**. As can be seen from the figure, during this specific hour, which should not be forgotten to be the brightest of the year, a significant portion of the reactor experiences irradiance above the saturation level. This clearly happens in the first millimeters of depth from the reactor surface. The reactor volumes near the approximated sun position are slightly more influenced due to the direct irradiance. Despite this, a uniform, diffused light is present around all the reactor surface penetrating a providing energy to a large volume of medium. The situation for the very same hour is completely different if no active shading system was provided as shown in the lower part of **Figure 44**. Here the saturated part of the reactor is the one south oriented while the rest of the volume experience lower irradiance. The lower diffused light is responsible for this effect. This is why the active shading system could possibly provide an advantage for an outdoor cultivation plant. A different situation is presented when an empty volume is located inside the reactor. In this case, shown in

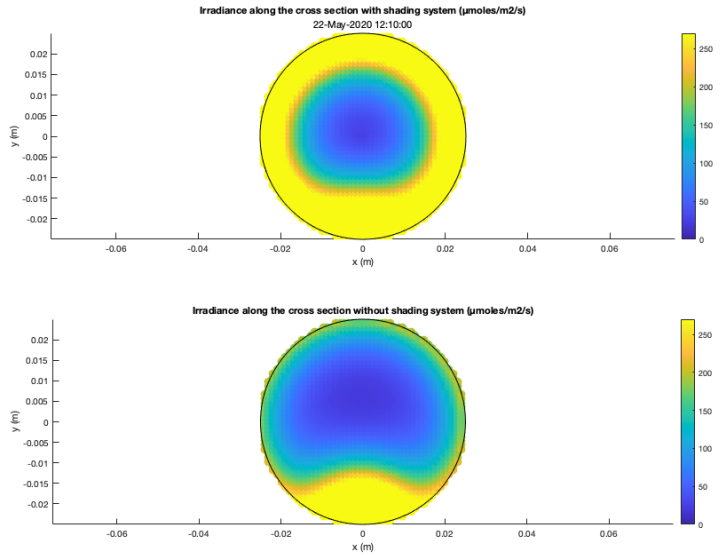

Figure 44: *Irradiance inside the cross section of the reactor during the brightest hour of the year, 22nd of May 2020 at 12 pm (noon) with (upper) and without (lower) the active shading system*

.

Figure 45, much of the reactor in the active shading system scenario experience an irradiance equal or above the saturation level while where no shading system is adopted, the irradiance along the cross section follows lower values. It is however important to remember how these results are referred to the brightest day of the year and therefore no conclusion can be pointed out before an assessment of the real productivity. Having less volume of medium to penetrate as happens when a second cylinder is located inside the reactor could be a disadvantage during the brightest hours but an advantage in all those periods when illumination is lower.

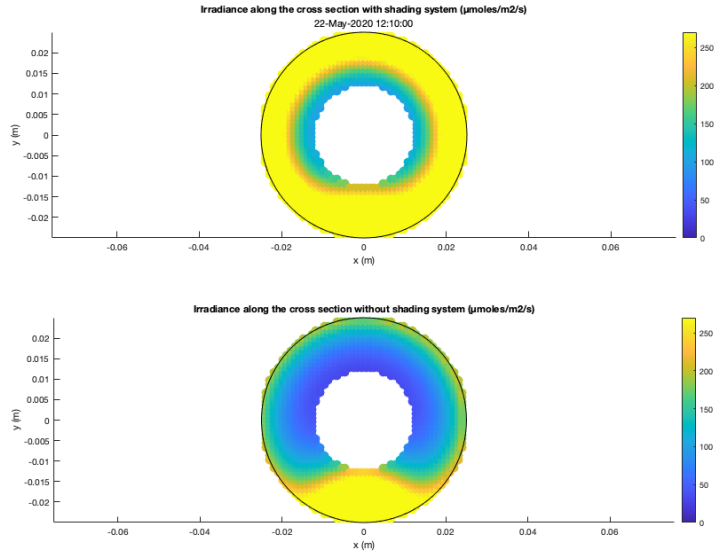

Figure 45: *Irradiance inside the cross section of the reactor with an empty volume inside during the brightest hour of the year, 22nd of May 2020 at 12 pm (noon) with (upper) and without (lower) the active shading system.*

6.1.4 Biomass productivity

Once the **equation 48** is applied for every point in every hour of the year, the Molina model **equation 36** reported in **Section 6.1.1** can be used. By doing so, a hourly growing rate is computed for each one of the points inside the cross section. Each point is representative of a volume of the reactor volume as stated before, therefore, the biomass grown inside each one of these volumes for a certain hour can be found as:

$$biomass_{(i,p)}(g) = \mu_{(i,p)} * C * volume_{(p)} \tag{49}$$

- "i" is the hour of the day index
- "p" the index of the selected point or volume inside the reactor simplified cross section
- $\mu_{(i,p)}$ is the local growing rate, computed at the hour "i" in the point "p" with the Molina model
- "C" is the biomass concentration settled to 0.8 g/l.
- "volume" is 1/1876th of the reactor volume for the standard Bubble column and 1/1408th of the reactor volume for the Bubble column with an inner empty volume.

The sum of each volume "p" contribution gives as result the total biomass produced every hour "i" inside the reactor.

$$biomass_i(g) = \sum_{p=1}^{1876} biomass_{(i,p)} \tag{50}$$

Once the hourly biomass production of a single reactor module has been computed, by normalizing it for the reactor volume, an hourly biomass productivity can be found. In this case it was multiplied by 1000 in order to thow the mg/l produced.

$$biomass_i(\frac{mg}{lh}) = 1000 * (1 - loss) * \frac{biomass_i}{Vol} \tag{51}$$

where:

- "i" is the hour of the day index
- "loss" is the biomass loss due to respiration and photorespiration equal to 30% [43]
- "Vol" is the volume of the reactor.

The profile of biomass productivity for the standard Bubble column can be seen in **Figure 46**. For completeness, the hourly biomass production of the same reactor if no active shading system was used is also given. The profile of biomass productivity for the Bubble column with the inner empty volume is instead shown in **Figure 47** From the figure is easy to identify that the major biomass production occurs in summer when light availability, both in terms of sunshine hours and radiance intensity, is higher. If

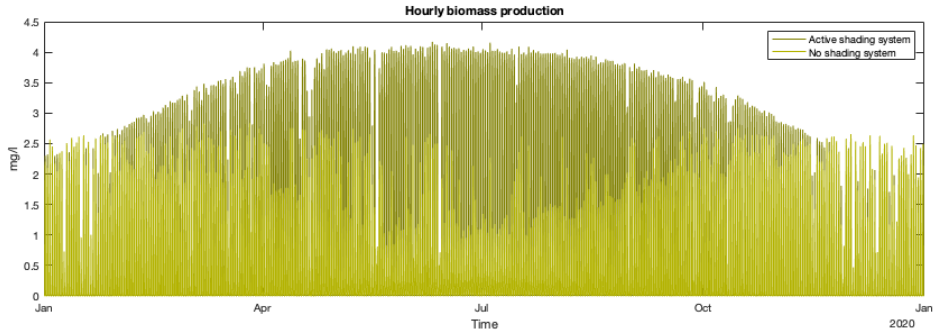

Figure 46: *Hourly biomass production. Standard Bubble column, comparison between scenarios with and without active shading system*

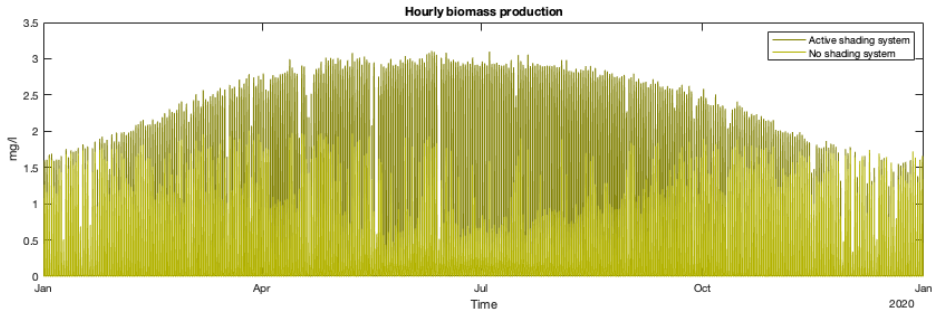

Figure 47: *Hourly biomass production. Bubble column with empty volume inside. Comparison between scenarios with and without active shading system*

no active shading system was in use, the biomass production profile would be lower and different in shape, with higher biomass production outside summer since the direct radiation component received for a vertical surface is lower in this last season and higher in winter. Overall, the active shading system is expected to provide significant advantages to the cultivation.
Figure 48 shows another comparison between the two scenarios for the standard bubble column (with and without active shade system) in 2 different day, the 1st of January and the first of June 2020. The figure shows clear differences between the two scenarios. Starting from the upper couple of figures, where the shading system is active, it is possible to appreciate how, independently from the season, direct and indirect radiation intensities are much more similar between each other in respect to the lower figures where no shading system is adopted and the direct component always overcome the diffused one. Regarding to the lower couple of figure where the shading system is not adopted, being the PBR vertical, much of the high intensity radiation during a summer day (lower right figure) is lost as the sun elevation is high and the PBR does not receive it. In contrast, the same configuration in winter (lower left) receives much more direct radiation as the sun elevation is lower in winter. Without shading system the biomass productivity is paradoxically higher in winter than in summer while the opposite happens if the shading nets are used. Slightly lower productivity but a similar behaviour is seen in **Figure 49** for the Bubble column with inner volume inside.

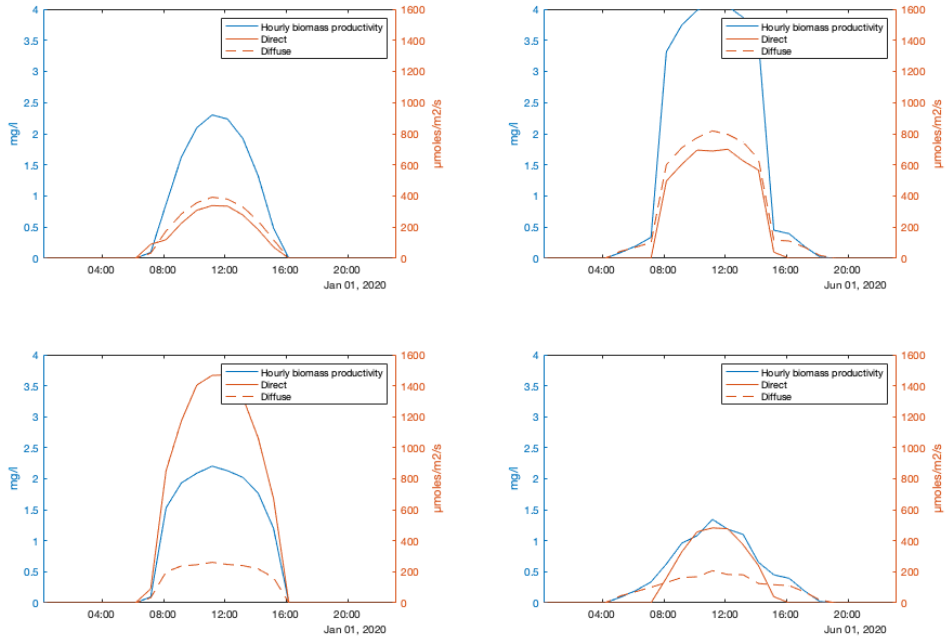

Figure 48: *Hourly productivity and radiation components for a winter and summer day with (upper) and without (lower) active shading system. Standard bubble column*

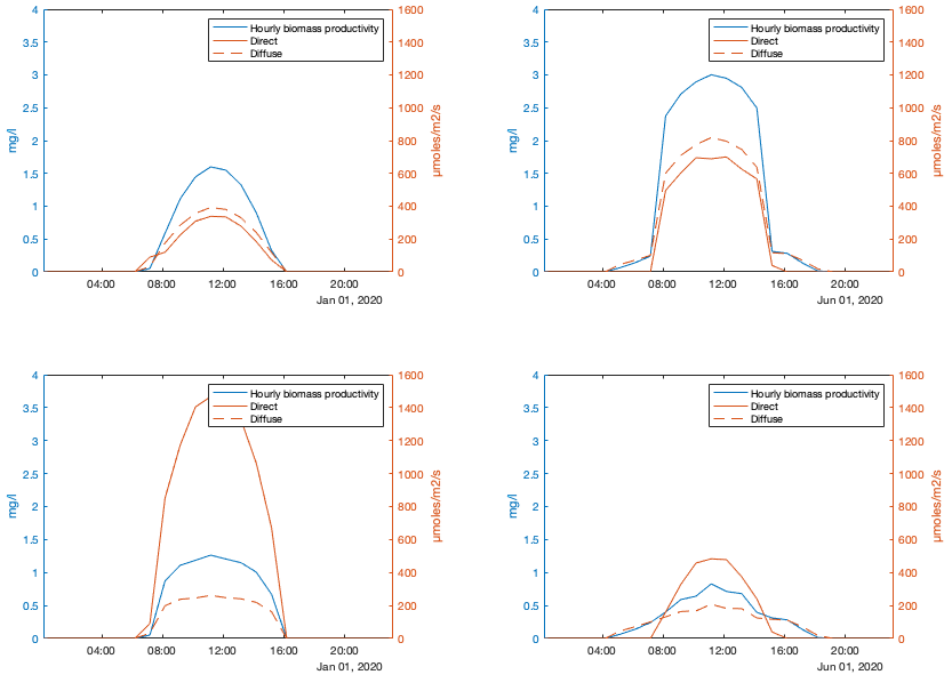

Figure 49: *Hourly productivity and radiation components for a winter and summer day with (upper) and without (lower) active shading system. Bubble column with inner empty volume.*

In order to have a comparable daily volumetric productivity, a sum of the hourly biomass produced by one single module is done, corrected considering the 30% of losses, divided by 365 days and normalized on the reactor volume, giving as result an averaged daily biomass productivity per liter.

$$biomass(\frac{g}{l \cdot d}) = (1 - loss) * \frac{\sum_{i=1}^{8760} biomass_i}{365 \cdot Vol} \tag{52}$$

where:

- "i" is the hour of the day index
- "loss" is the biomass loss due to respiration and photorespiration equal to 30% [43]
- "Vol" is the volume of the reactor.

The result of this operation done considering the scenarios with and without the active shading system are reported in **Table 16**. The Productivity with the irradiance control system is almost doubled in respect to the other one.

	Biomass Productivity (g/l d)	
Scenario	**Standard Bubble Column**	**Bubble Column empty inner volume**
Active shading system	0.0210	0.0151
No shading system	0.0127	0.0081

Table 16: *Average biomass productivity with and without active shading system*

6.1.5 Plant volume estimation

As already pointed out in **Section 5.1**, the volume necessary to harvest biomass continuously at a certain flow rate in a given concentration is a function of the specific growing rate. All the expected volume estimations made in **Section 5.1** where done by considering the maximum specific growing rate as the growing rate of the culture. Since this was a strong and overestimating approximation, a more precise estimation of the specific growing rate has to be done. Once the growing rate was computed for each hour in each one of the points inside the reactors, an average hourly growing rate can be computed. Results of this average are reported in **Table 17**.

	Growing rate μ (h-1)	
Scenario	**Standard Bubble Column**	**Bubble Column empty inner volume**
Active shading system	0.0016	0.0011
No shading system	0.00094	0.00060

Table 17: *Average hourly growing rates with and without active shading system*

Once the average hourly growing rate are given, the **equation 17** reported in **Section 5.1** can be again applied and it is therefore possible to obtain the required plant volume in the real case scenario.

$$V = F/\mu \tag{53}$$

where: μ ($1h^{-}1$) is the specific growing rate and F ($lh^{-}1$) the harvesting flow rate. Results from these computation are reported in **Table 18**. These results demonstrate that quite a large plant would be necessary for such an industrial application and depends on several factors. The major dependence is on chosen harvesting rate and chosen PBR radius. A continuous harvesting for 16h day at 500 l/h certainly represent a challenge. As shown in **equation 53** and already explained in **Section 5.1** the plant volume is proportional to the harvesting rate and inversely proportional to the specific growing rate. Therefore, the choice of harvesting rate given the solar irradiance of a precise location should undergo ulterior technical-economical analysis which however are not the scope of this work.
For what concerns the radius, the shorter the optical path, the better light penetrates in the medium. However, a too short optical path could result in too much light arriving at the cells during the highest radiation peaks. Moreover, the number of required modules, and therefore the capital cost of the plant, would increase as the single reactor volume decreases.

	Plant Volume (m3)	
Scenario	**Standard Bubble Column**	**Bubble Column empty inner volume**
Active shading system	5 125	7 139
No shading system	8 481	13 313

Table 18: *Computed plant volumes necessary for harvesting continuously for 16 h at 500 l/h, 0.8 g/l biomass concentration.*

Given these plant volume (Vol_{plant}) and the volume of one reactor module ($Vol_{reactor}$), the number of total modules per plant is computed as:

$$N_{modules} = \frac{Vol_{plant}}{Vol_{reactor}} \tag{54}$$

and reported in **Table 19**

	Number of modules	
Scenario	**Standard Bubble Column**	**Bubble Column empty inner volume**
Active shading system	652 580	303 000
No shading system	1 079 900	565 000

Table 19: *Estimated number of modules necessary for harvesting at 500l/h continuously*

The total biomass production of one year is found by summing the hourly biomass production of each module for all the hours of the year and by then multiplying it for the required number of modules. This value is adjusted as before with a 30% biomass loss parameter [43].

$$biomass_{annual} = (1 - loss) * \sum_{i=1}^{8760} biomass_{(i)} * N_{modules} \tag{55}$$

- "i" is the hour of the day index
- "loss" is the biomass loss due to respiration and photorespiration equal to 30%

- "$biomass_{(i)}$" is the biomass produced in the hour "i".
- $N_{modules}$ is the required number of modules.

Since the number of modules is computed in such a way to provide a constant biomass flow to the harvesting centrifuge in both scenarios, the annual biomass production will be equal for both of them. All computation done, the plant is expected to produce about 40 tons of biomass per year. This value is lower than the production of Klötze, Chlorella production plant in Germany, which claims to collect 130-150 tons of biomass per year in a 700 000 liters tubular photobioreactor. Literature data regarding outdoor *Chlorella* cultivations in vertical photobioreactor show however results on the same order of magnitude of the results obtained in the active shading system scenario (while still being higher). Sarker et al. 2019 obtained a biomass productivity between 0.0960 and 0.0618 g/ld during an outdoor experiment where *Chlorella Vulgaris* was grown in 16.5 cm diameter vertical PBR [131] with biomass concentrations below 0.4 g/l. Lopes et al. 2020 [130] found an hourly productivity between 2.3 and 5 x $10^{-}3$ g/l h, equivalent to 0.0552 and 0.12 g/l d for an outdoor cultivation of *Chlorella Vulgaris*, values higher than those found in this work. The experiment was however conducted in a 40 l PBR of 4.6 cm diameter, therefore with a slightly shorter optical path than the one used in this work.

6.2 Carbon and nutrient requirement

Now that the expected biomass production has been calculated it is possible to make a further step and investigate the carbon and macro nutrient requirement for the algae. All previous calculations and reasoning have been made by supposing that no limiting factor was preventing the algae to grow apart from the excessive light. In reality, temperature, pH swings due to carbon dioxide injection, inhibition due to excessive oxygen production are all limiting factors which have to be carefully monitored along the growth. The assumption of a perfect growing environment, although strong, can be intended as an approach to the correct cultivation practices. Nutrient have to be dosed and their availability in the culture medium should always be on a slight excess.
In order to understand how much nutrient is required, some elemental computation are needed. The first step is to use the elemental composition of *Chlorella sp* to compute how much, in moles or grams, is each element contained in a mole of *Chlorella*. The elemental composition of *Chlorella sp* normalized for carbon is [135]

$$C_1 H_{1.861} O_{0.339} N_{0.182} P_{0.016} S_{0.003} \tag{56}$$

Table 20 reports moles and weight of each element normalized for carbon. One mole of biomass weight approximately 22.4488 grams. The following step is to understand how these elements are given to the cultivation. While carbon is mostly provided through carbon dioxide injection as pointed out in **sectio 4.5.3**, several other nutrients have to be provided in solution. An example of traditional growing media was already listed in **table 5**. Among these, BG11 is one of the most utilized for *Chlorella* cultivation [76]. From here over, only macro nutrient will be considered, therefore among those: NaNO3, which provides nitrogen, K2HPO4 which provides potassium, MgSO4,

Element	Atomic mass (g/mol)	Moles in Chlorella sp (mol)	Total atomic weight (g)
C	12.0107	1	12.0107
H	1.0079	1.861	1.8757
O	15.9940	0.339	5.4220
N	14.0067	0.182	2.5492
P	30.9378	0.016	0.4950
S	32.0650	0.003	0.962
			22.4488

Table 20: *Elemental composition of Chlorella sp and respective atomic weights*

which provides sulphur and CO_2 which provides carbon. Considering these nutrients, a simplified photosynthesis equation can be re-written as:

$$CO_2 + 0.182NaNO_3 + 0.016K_2PO_4 + 0.003MgSO_4 + 1.032H_2O =$$
$$C_1H_{1.861}O_{0.339}P_{0.016}S_{0.003} + 0.182NaOH + 0.003Mg(OH)_2 + 0.032KOH + 1.5475O_2$$

The equation states how many moles of each macro nutrient is required to form one mole of biomass.

6.2.1 Nitrogen requirement

Nitrogen is provided to the microalgae as sodium nitrate $NaNO_3$. According to **Table 20**, For 1 mol of biomass of atomic weight 22.4488 grams, 0.182 moles sodium nitrate $NaNO_3$ are required. The atomic weight of 0.182 moles of sodium nitrate is:

$$\begin{aligned} aw_{NaNO3} = am_{NaNO3} * mol_{NaNO3} = (am_{Na} + am_N + 3 * am_O) * mol_{NaNO3} = \\ = (22.9897g/mol + 14.0067g/mol + 3 * 15.9940g/mol) * 0.182mol = \\ = 84.9784g/mol * 0.182mol = 15.4661g \end{aligned}$$

where "am" is the atomic mass in g/mol. 15.4661 g of sodium nitrate are necessary for 22.4488 grams of biomass, meaning that the grams of sodium nitrate required for 1 g of biomass are

$$\frac{aw_{NaNO3}}{aw_{biomass}} = \frac{15.4661g}{22.4488g} = 0.6889\frac{g_{NaNO3}}{g_{biomass}} \tag{57}$$

The weight percentage of Nitrogen in 0.182 moles (15.4661 g) of sodium nitrate $NaNO_3$ is:

$$\frac{am_N * mol_{NaNO3}}{g_{NaNO3}} * 100 = \frac{14.0067g/mol * 0.182mol}{15.4661g} * 100 = 16.48\% \tag{58}$$

Therefore, Nitrogen required for 1 gram of biomass is:

$$g_N = 0.1648 * 0.6889g = 0.1136\frac{g_N}{g_{biomass}} \tag{59}$$

6.2.2 Phosphorus requirement

Phosphorus is provided to the microagranism as dipotassium phosphate For 1 mol of biomass of atomic weight 22.4488 grams, 0.016 moles of dipotassium phosphate K_2HPO_4 are required. The atomic weight of 0.016 moles of sodium nitrate is:

$$aw_{K_2HPO_4} = am_{K_2HPO_4} * mol_{K_2HPO_4} = (2 * am_K + am_H + + am_P + 4 * am_O) * mol_{K_2HPO_4} =$$
$$= (2 * 39.0983g/mol + 1.0079g/mol + 30.9378g/mol + 4 * 15.9940g/mol) * 0.016mol =$$
$$= 174.1183g/mol * 0.016mol = 2.7859g$$

where "am" is the atomic mass in g/mol. 2.7859 g of dipotassium phosphate are necessary for 22.4488 grams of biomass, meaning that the grams of dipotassium phosphate required for 1 g of biomass are

$$\frac{aw_{K_2HPO_4}}{aw_{biomass}} = \frac{2.7859g}{22.4488g} = 0.1241\frac{g_{K_2HPO_4}}{g_{biomass}} \tag{60}$$

The weight percentage of phosphorus in 0.016 moles (2.7859 g) of dipotassium phosphate K_2HPO_4 is:

$$\frac{am_P * mol_{K_2HPO_4}}{g_{K_2HPO_4}} * 100 = \frac{30.9378g/mol * 0.016mol}{2.7859g} * 100 = 17.76\% \tag{61}$$

Therefore, phosphate required for 1 gram of biomass is:

$$g_P = 0.1776 * 0.1241g = 0.0221\frac{g_P}{g_{biomass}} \tag{62}$$

6.2.3 Sulphur requirement

Sulphur is provided to the microorganism as magnesium sulphate. For 1 mol of biomass of atomic weight 22.4488 grams, 0.003 moles of magnesium sulphate $MgSO_4$ are required. The atomic weight of 0.003 moles of magnesium sulphate is:

$$aw_{MgSO_4} = am_{MgSO_4} * mol_{MgSO_4} = (am_{Mg} + am_S + 4 * am_O) * mol_{MgSO_4} =$$
$$= (24.305g/mol + 32.0650g/mol + 4 * 15.9940g/mol) * 0.003mol =$$
$$= 120.346g/mol * 0.003mol = 0.3610g$$

where "am" is the atomic mass in g/mol. 0.3610 g of magnesium sulphate are necessary for 22.4488 grams of biomass, meaning that the grams of magnesium sulphate required for 1 g of biomass are

$$\frac{aw_{MgSO_4}}{aw_{biomass}} = \frac{0.3610g}{22.4488g} = 0.0161\frac{g_{MgSO_4}}{g_{biomass}} \tag{63}$$

The weight percentage of sulphur in 0.016 moles (2.7859 g) of magnesium sulphate $MgSO_4$ is:

$$\frac{am_S * mol_{MgSO_4}}{g_{MgSO_4}} * 100 = \frac{32.0650g/mol * 0.003mol}{0.3610g} * 100 = 26.64\% \tag{64}$$

Therefore, Sulphur required for 1 gram of biomass is:

$$g_S = 0.2664 * 0.0161g = 0.0043\frac{g_S}{g_{biomass}} \tag{65}$$

6.2.4 Carbon requirement

Carbon is provided to the microorganism as carbon dioxide at food grade. For 1 mol of biomass of atomic weight 22.4488 grams, 1 mole of carbon dioxide CO_2 are required. The atomic weight of 0.003 moles of magnesium sulphate is:

$$\begin{aligned} aw_{CO_2} = am_{CO_2} * mol_{CO_2} = (am_C + 2 * am_O) * mol_{CO_2} = \\ = (12.010g/mol + 2 * 15.9940g/mol) * 1mol = \\ = 43.9987g/mol * 1mol = 43.9987g \end{aligned}$$

where "am" is the atomic mass in g/mol. 43.9987 g of magnesium sulphate are necessary for 22.4488 grams of biomass, meaning that the grams of magnesium sulphate required for 1 g of biomass are

$$\frac{aw_{CO_2}}{aw_{biomass}} = \frac{43.9987g}{22.4488g} = 1.960\frac{g_{CO_2}}{g_{biomass}} \tag{66}$$

This value is near the 1.8 gram of CO_2 per gram of biomass found by Li et al. [105]. The weight percentage of carbon in 1 moles (43.9987 g) of carbon dioxide CO_2 is:

$$\frac{am_C * mol_{CO_2}}{g_{CO_2}} * 100 = \frac{12.010g/mol * 1mol}{43.9987g} * 100 = 27.29\% \tag{67}$$

Therefore, carbon required for 1 gram of biomass is:

$$g_P = 0.2729 * 1.9g = 0.5350\frac{g_C}{g_{biomass}} \tag{68}$$

Results of this and of the previous computation on all other macronutrients considered are resumed in **Table 21**.

Element	Macronutrient	Grams of macronutrient per gram of biomass	Grams of element per gram of biomass
C	CO_2	1.960	0.5350
N	$NaNO_3$	0.6889	0.1136
P	K_2HPO_4	0.1241	0.0221
S	$MgSO_4$	0.0161	0.0043

Table 21: *Grams of macronutrients and grams of element required for 1 gram of biomass*

6.2.5 Annual nutrient requirement

Now that the required mass of each macronutrient are known, it is possible to find the annual requirement of each one of those. Considering the annual production of 40 tons as stated in **Section 6.1.5** and the ratio gram of element to gram of biomass listed in **Table 21**, the annual requirement of each element can be found by multiplying the annual production for this ratio. Then, by knowing the weight percentage of each

element in its respective macronutrient, it is possible to retrieve the annual weight requirement of macronutrients. As example for nitrogen:

$$N_{year} = \frac{g_N}{g_{biomass}} * biomass_{year} = 0.1136 * 40ton = 4.46ton$$
$$NaNO3_{year} = \frac{g_{NaNO_3}}{g_{biomass}} * biomass_{year} = 0.6889 * 40ton = 27.1ton$$

These calculation have been repeated for all other macronutrient and the results are listed in **Table 22**

	Annual production (tons)		
Biomass	40		
Element	**Macronutrient**	**Macronutrient requirement per year (tons)**	**Element requirement per year (tons)**
C	CO_2	77.12	21.05
N	$NaNO_3$	27.1	4.46
P	K_2HPO_4	4.48	0.86
S	$MgSO_4$	0.632	0.168

Table 22: *Annual biomass production and annual requirement of macronutrients*

6.3 Carbon Capture

Now that the annual carbon dioxide requirement is finally determined, the following step is to understand and describe which kind of technology is most suitable for this application. Among the various method for capturing carbon dioxide from a stream of flue gasses, the amine absorption is one of the most widely used.

6.3.1 Flue gas composition

As previously said, one important parameter which determines the energy requirement of the carbon capture process is the volumetric concentration of CO_2 in the flue gasses. The higher the molar fraction, higher will be the efficiency of the capture. Data regarding precise emission components of the waste incinerator flue gases were extracted from the annual relation published by Tecnocasic relative to the year 2021 [137].

The document reports the emission into the atmosphere of several different gas components in grams per year, the volume of flue gasses emitted in cubic meters and the cumulative hours of functioning of the plant. These information are collected in **Table 24**. Since the plant account for 4 different waste incineration lines conveying into 2 chimneys, the cumulative hours of emission are more than the hours in one year. Moreover, temperature and pressure of the flue gases are also reported. The amount of each emitted compound are reported in **Table 24**. Here, substances emitted in amount lower than than 1 kg per year were neglected for simplicity. PM10 and non methanic hydrocarbons were neglected too from the analysis. **Table 23** shows instead the physical parameters related to the flue gas.

Hours of emission [h]	10 963
Yearly emitted volume [m3/year]	532 622 220
Hourly emitted volume [m3/hour]	48 584
Temperature at chimney [C°]	120
Pressure [Pa]	101325
Yearly emitted moles	$1,65 * 10^{10}$
Hourly emitted moles	$1,50 * 10^{6}$

Table 23: *Physical parameter of the flue gasses according to Tecnocasic 2021 annual relation [137]*

In order to obtain the CO_2 volumetric concentration at the chimney, the first step is to compute how many moles of each gas are released every hour. The released moles can be found by dividing the emitted grams/hour by the molecular mass (g/mol) of each gas. By doing so, the released mol/hour are found for each component.

$$mol/h = \frac{g/h}{u} \tag{69}$$

where:

- "g/h" are the grams of gas component emitted in 1 hour.
- "u" is the molecular mass of the gas component in g/mol.

Once the moles of each gas component emitted every hours are found, by applying the law of ideal gas it is possible to retrieve the volume of each single component emitted per hour.

$$V_i = \frac{n_i RT}{p} \tag{70}$$

where:

- "i" is the index of the gas ith component.
- "p" is the pressure of the gas in Pa, in this case 101325 equal to 1atm
- "T" is the temperature of the gas in Kelvin, in this case 393.15
- "R" is the universal costant of gasses equal to 8.314 J/mol K
- "n" is the number of hourly emitted moles of the gas component

In this way, partial volume of each gas component is found and reported in **Table 24**. Once this procedure is done, the volumetric percentage of each gas component is obtained by dividing its partial volume by the total volume of gas emitted in one hour. These results are once again reported on the last column of **Table 24**.

The aware reader will notice that the sum of all partial volume reported in **Table 24** does not coincide with the total volume of hourly emitted gas reported in **Table 23**.

Compound	Molecular mass	Emission in atmosphere			X molar	Partial	Concentration
	g/mol	[g/year]	g/h	mol/h	fraction	volume [m3/h]	in flue gas [%]
Hydrofluoric acid	20,00	7370	0,67	0,03	0,00000002	0,001	0,000002
Total organic carbon	12,01	8670	0,79	0,07	0,00000004	0,002	0,000004
Ammonia	17,01	81800	7,46	0,44	0,00000029	0,014	0,00003
Sulphur oxide	48,06	179490	16,37	0,34	0,00000023	0,011	0,00002
Hydrochloric acid	36,46	350540	31,97	0,88	0,00000058	0,028	0,00006
Carbon Oxide	28,01	1393000	127,06	4,54	0,00000301	0,146	0,00030
Nitrogen Oxide	30,01	54136000	4938,06	164,57	0,00010927	5,309	0,0109
Carbon dioxide	44,09	79012000000	7207151,33	163464,53	0,1085	5273	10,85

Table 24: *Flue gas composition according to Tecnocasic 2021 annual report [137]*

This is because among the emitted and not reported gas there still is an high contribution of water vapour , nitrogen, air and oxygen. Given these considerations, results from previous calcuations state a volumetric concentration of CO_2 around 11 %V. This value is in line with average volumetric concentration of power plant flue gases.

6.3.2 Carbon capture technology

Once the concentration of carbon dioxide in flue gasses is known, it is finally possible to compute how much energy will be necessary to capture the required amount of annual CO_2 necessary to provide the right amount of carbon to the microalgae cultivation. Before doing so, it is worth to take a moment to analyse how carbon dioxide can be captured from flue gases. Carbon capture and Utilisation or Carbon capture and Storage, respectively CCU and CCS are common practices adopted now days all over the world. Carbon capure can be done both before the combustion or after it. From here over we will ony refer to the latter case. There are several methods to separate the carbon dioxide from a general gaseous mix. These methods can be re-assumed in adsorption, absorption and membrane separation. The differences between these method lays in where the gaseous molecule will be hosted during the capture. In absorption, a molecule transfer from a gas phase into a liquid phase while in adsorption molecules are fixed in a solid surface. Overall, all CO_2 capture processes require a regenerative two-step process where the carbon dioxide is first captured into a solvent or a solid and then released. The capture usually requires low temperatures and high pressure, while the release is done by lowering the pressure and increasing the temperature. These method is often referred as temperature-pressure swings and can be done in batch using several reactor in series. One of the most common absorption method is the amine absorption. This technology is based on the use of amine, weak basic compounds which tend to react with acid gases forming chemical bonds. These bonds can then be broken, as said before by heat or pressure drops. Several types of alkanolamines exists while the most commonly diffused for CC purposes are monoethanolamine MEA, diethanolamine DEA and triethanolamine TEA. Structure of these molecules are given in **Figure 50**.

The capture process, as said previously, works in two steps: absorption of the carbon dioxide and desorption of it. **Figure 51** shows a schematic representation of a capture plant where two reactors, namely the absorber and the stripper/desorber are used in series. Starting from the right side of the figure, the flue gas is cooled in a column using water. The cooled gas is then pumped into the absorber by a fan. Here, a combined water-solvent is used to wash the gas from above while this latter is feed

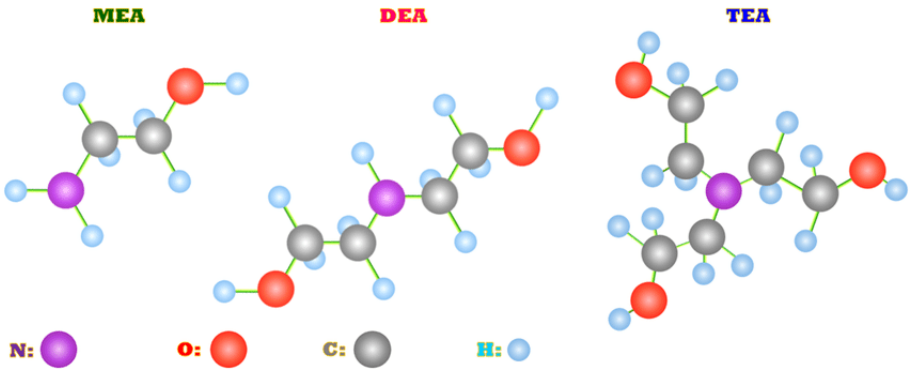

Figure 50: *Structure of MEA, DEA and TEA molecules [141]*

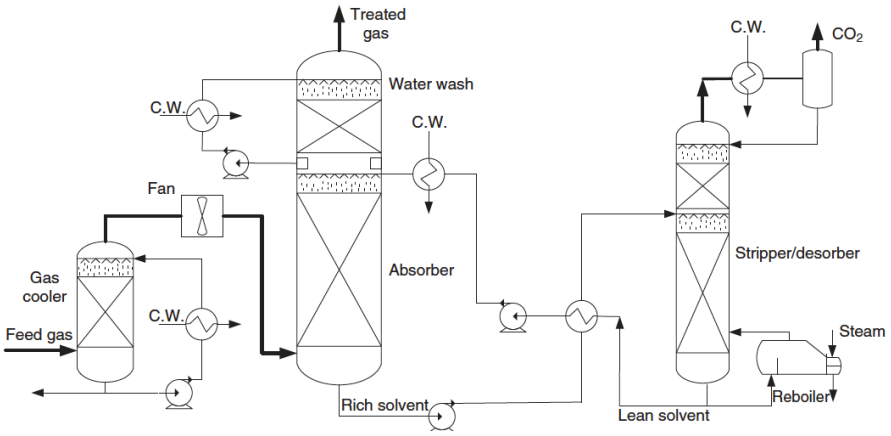

Figure 51: *Absorption/desorption process with temperature only and no pressure swings. The abbreviation C.W. denotes cooling water. [142]*

from below. The solvent capture the carbon dioxide and then collects at the bottom of the absorber. The remaining gas flows out through opportune valves. Once the rich solvent is collected at the bottom, it is pumped on the upper part of the stripper where hot steam is released on the bottom to enhance the temperature. By doing so, the solvent releases the previously captured CO_2 which now rises on the upper part of the stripped just to be cooled and collected in a buffer thank with the help of a compressor. The now clean solvent is then collected again ready to initiate another capturing cycle. Energy requirement for this type of process are mainly: the mechanical work to drive pumps used for cooling water and solvent circulation; the mechanical work needed for the pressure drops encountered by the gas during the gas cooling, water wash and all ducting between these; the steam for heating the reboiler of the desorber and the steam for reclaiming of amine.

6.3.3 Energy requirement

The amount of energy required to fix 1 kg of carbon dioxide with amines, but more in general with any carbon capture technology strictly depends on the partial pressure of CO_2 in the gaseous mix and therefore on its concentration. The higher is the partial pressure of CO_2, the easier will it be to capture. Overall, the energy re-

quirement for the capture of 1 ton of carbon dioxide with amines is between 3-5 GJ. To this, work requirement for blowers and compressor should be added. Husebye et al. [143] evaluated the energy requirement of carbon capture in several cases using, mostly differentiated by the molar concentration of CO_2 and by the flue gas flowrates, using MEA. A diagram in **Figure 52** shows the energy consumption of the desorber and of the blowers for different CO_2 concentrations at fixed operation parameters.

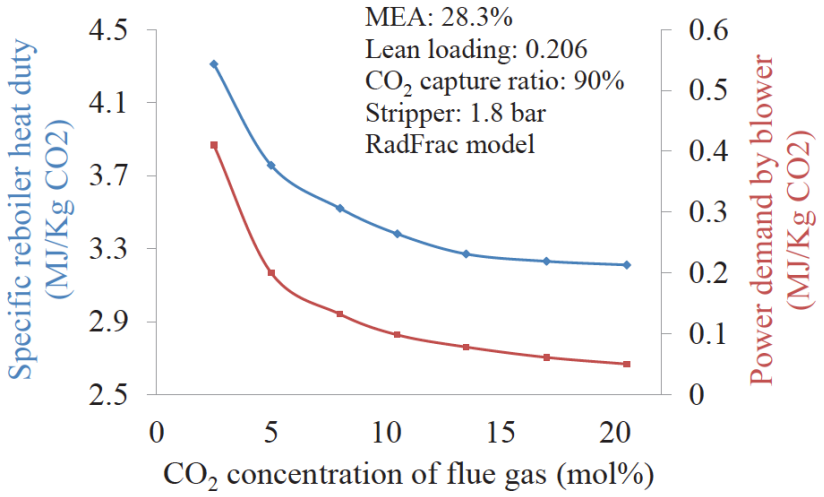

Figure 52: *Energy consumption of stripper and gas blowers at different CO_2 concentration and fixed operational parameters using MEA. [143]*

As previously said, the higher is the carbon dioxide concentration, the lower will be the work necessary to capture a fixed amount of CO_2 and less will be the heat required for the stripper duty cycle.
All information are now available to have a rough estimation of the energy requirement necessary to capture the desired amount of CO_2 stated in **Section 21** as 77.12 tons/year.
This amount was computed considering a fixation efficiency of 100%. A more reasonable estimation would consider this last parameter as 90%, meaning that 10% of what comes into the PBR as carbon dioxide is not fixed and lost while the reactor degases. Therefore, the annual CO_2 requirement should be increased by 10%, becoming in this way **84.8 tons/year**.
Given the CO_2 concentration in the flue gases of the waste incinerator of 10.8% as previously computed and reported in **Table 24**, the Specific reboiler heat duty and power demand by blowers can be retrieved from Husebye et al. [143] proposed diagram.
A conservative estimation of 2.9 MJ/kgCO_2 for the stripper duty cycle and 0.1 MJ/kgCO_2 for the blowers are respectively given. These energy amount can also be expressed in kWh respectively as 0.80 kWh/kgCO_2 in the form of heat and 0.0278 kWh/kgCO_2 in the form of electricity according to the conversion

$$1MJ = 0,278kWh \tag{71}$$

. Considering the annual carbon dioxide requirement, the cumulative energy of the

stripper duty cycle is given as:

$$E_{stripper} = 0.80 * 84800 = 67840 kWh \tag{72}$$

while the annual energy demand for blowers and fans is computed as:

$$E_{fan\&blowers} = 0.0278 * 84800 = 2357 kWh \tag{73}$$

Another step is nevertheless necessary to store the captured CO_2 in a buffer thank and this step is a ulterior compression of the gas. Once stored in the tank, the CO_2 can be utilised according to the hourly need of the cultivation through an appropriate feeding system as described in **Section 5.2**. The work necessary for a polytropic compression of a real gas is expressed as follow:

$$\dot{W}_{compr} = \dot{m} c_p T_1 \left(\left(\frac{p_2}{p_1} \right)^{\frac{k-1}{k\eta_p}} - 1 \right) \tag{74}$$

where:

- $\dot{W}_{compr}$ is the power necessary for the compression in kW
- $\dot{m}$ is the mass flow rate in kg/s
- c_p is the specific heat capacity at constant pressure in kJ/(kg K)
- T_1 is the temperature of the gas at the inlet of the compressor
- p_2 and p_1 are respectively the outlet and inlet gas pressure
- k is ratio of specific heats at constant pressure and constant volume, cp/cv
- η_p is the compressor polytropic efficiency

In the analysed case, the CO_2 leaves the condenser at 40°C and 1.8 bar as stated by Husebye et al. [143], therefore:
$T_1 = 273.15 + 40 = 313.15$ K and
$p_1 = 1.8$ bar.
Since the specific heat capacity is a function of pressure and temperature, at this state it can be assumed:
$c_p = 0.85$ as shown in **Figure 53**.

For what concerns η_p, the compressor polytropic efficiency, it can be assumed:
$\eta_p = 0.80$ according to literature [142].
The exponent k can be set equal to 1.30 for CO_2. The final pressure of the gas depends on the storing system in use. Operational pressure for commercial storing tanks of CO_2 varies between 20 and 30 bar, therefore the final pressure of the captured carbon dioxide will here be assumed as:
$p_2 = 25$ bar and

$$\frac{p_2}{p_1} = \frac{25}{1.8} = 13.8. \tag{75}$$

A recap of the chosen paramenters is given here below as:

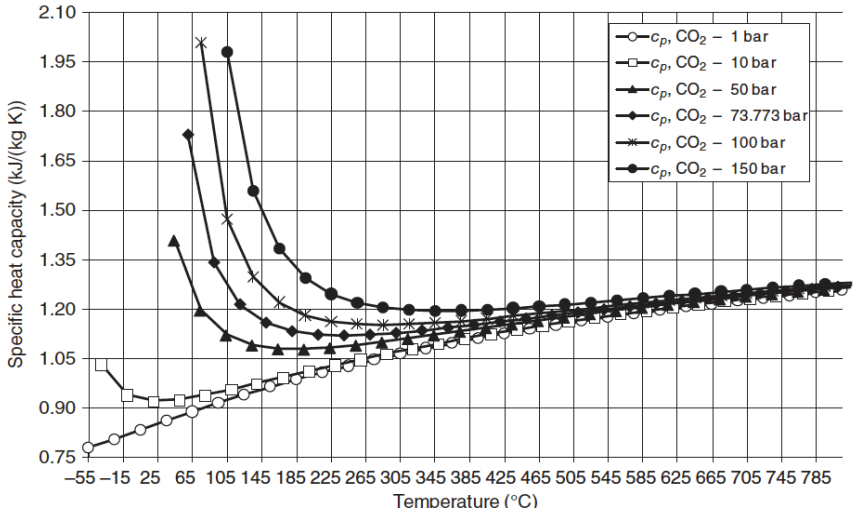

Figure 53: *Pure carbon dioxide Specific heat capacity with varying pressure and temperature [142].*

- $c_p = 0.85$ kJ/(kg K)
- $T_1 = 313.15$ K
- $p_2 = 25$ bar and $p_1 = 1.8$ bar
- k = 1.30
- $\eta_p = 0.80$

Before continuing with the calculation it is necessary to fix a flow rate at which the carbon dioxide can be captured. Despite the most correct approach would be to accurately select an already existing and commercialised CO_2 amine absorber reactor, it is also possible to make some calculation considering a low flow rate. For example, the Carbon Capture system built by Toshiba in Saga City waste incineration plant cited in **Section 4.5.1** is capable of capturing 10 tons of CO_2 every day. At this pase, the annual requirement of 84.8 tons previously obtained would be fullfilled in 9 days, leaving the reactor unused for the remaining 356 days per year. This would mean that the capacity factor of the reactor would not even reach 2%. Therefore, in this specific case, what could be called a micro scale, or laboratory scale capture system would be necessary. In order to compute a plausible flow rate, it is possible to assume a capacity factor of 80%. This would mean that the reactor is in use for 80% of the days in one year, in other words:

$$days = 0.8 * 365 = 292 days/year \tag{76}$$

or in hours:

$$hours = 292 * 24 = 7008 h/year \tag{77}$$

Considering therefore the annual CO_2 requirement previously computed, an hourly flow rate is given as:

$$\dot{m} = 84800 kg/7008 h = 12.10 kg/h = 0.0034 kg/s \tag{78}$$

Therefore, 0.0034 kg/s would be the flow rate of the carbon capture reactor in order to have a capacity factor of 80%. It is necessary to specify how this method is an indirect method. A more precise estimation would dimension the system on the maximum hourly amount of needed carbon dioxide. Nevertheless, for the purpose of this work, a rough estimation based on average is enough. Given this flow rate, it is finally possible to compute the power requirement necessary to compress and store the captured CO_2 at 25 bar in a buffer tank as stated in **Equation 74**.

$$\dot{W}_{compr} = \dot{m} c_p T_1 \left(\left(\frac{p_2}{p_1} \right)^{\frac{k-1}{k\eta_p}} - 1 \right) = \\ = 0.0034 * 0.85 * 313.15 * \left((13.8)^{\frac{1.30-1}{1.30*0.80}} - 1 \right) = 1.02 kW \tag{79}$$

The annual cumulative energy requirement will consequently be the power requirement multiplied by the hours of functioning, therefore

$$E_{compression} = 1.02 * 7008 = 7148 kWh \tag{80}$$

Now every major energy requirement is computed and listes in **Table 25**.

Phase	Energy (MWh)	Form
Stripper duty cycle	67.8	Heat
Fan and blowers	2.3	Electricity
Compressor	7.1	Electricity

Table 25: *Cumulative energy requirements for the capture and compression of 84.8 annual ton of CO_2 .*

6.3.4 Downside effect on Tecnocasic plant energy production

Once the energy requirements have been computed, the last necessary step is to analyse what could possibly be the downside effect of this required energy on the electricity production of Tecnocasic waste incineration plant. If energy requirement listed in **Table 25** are normalised over the cumulative tons of CO_2 required, a MWh/ton_{CO_2} is obtained as listed in **Table 26**. For simplicity, processes requiring heat and electricity were divided in order to consider two major energy requirements only.

According to Tecnocasic annual relation [137], 1.40 tons of CO_2 are released for every ton of waste being burned. At the same time, 3.21 MWh of thermal energy and 0.42 MWh of electricity are produced per ton of waste. Moreover, the cumulative CO_2

Phase	Normalised energy (MWh/t_{CO_2})	Form
Stripper duty cycle	0.79	Heat
Fan&Blowers&Compressor	0.11	Electricity

Table 26: *Energy requirements normalised per ton of captured CO_2*

emission, heat and pelectricity production are respectively 79 012 ton, 204649 MWh and 29.998 MWh These information are listed in **Table 27**

	Specific production	**Unit of measure**	**Cumulative production**	**Unit of measure**
CO_2	1.4	t/t	79012	t
Heat	3.21	MWh/t	204649	MWh
Electricity	0.42	MWh/t	26998	MWh

Table 27: *Normalised CO_2 emission, heat and electricity production per ton of burned waste on the left and cumulative CO_2 emission, heat and electricity production on the right.*

The 84.8 tons of CO_2 required as carbon source for the cultivation represent the 0.11% of the cumulative 79 012 tons of Carbon dioxide emitted every year by the plant. This means that if carbon capture was adopted in the proposed way, the specific emission per ton of burned waste would be decreased by an almost negligible amount. More precisely, given the specific emission of 1.4 ton CO_2/ton of waste, capturing 0.11% of every ton of CO_2 emitted would mean to capture

$$1.4 * 0.0011 = 0.0015 t_{CO_2} / t_{waste} \tag{81}$$

In order to capture $0.0015 t_{CO_2} / t_{waste}$, the specific energy requirements per ton of burned waste would be:

$$Heat = 0.8 MWh / t_{CO_2} * 0.0015 t_{CO_2} / t_{waste} = 0.0012 MWh / t_{waste} \tag{82}$$

and

$$Electricity = 0.11 MWh / t_{CO_2} * 0.0015 t_{CO_2} / t_{waste} = 0.000165 MWh / t_{waste} \tag{83}$$

Therefore, approximately 1.2 kWh of heat and 0.16 kWh of electricity would be necessary to capture the required amount of carbon dioxide per ton of burned waste while using a small scale MEA capture system at 80% capacity factor. These results are reported in **Table 28**.

Phase	**Subtracted energy** (MWh / t_{waste})	**Form**
Stripper duty cycle	0.0012	Heat
Fan&Blowers&Compressor	0.000165	Electricity

Table 28: *Energy subtraction per ton of waste in order to capture the required CO_2*

As can be easily understood by comparison with the specific energy production listed in **Table 27**, being these requirement orders of magnitude lower than the production, they will have almost no considerable effect on both the specific heat and electricity production per ton of burned waste, In conclusion, capturing the required amount of carbon dioxide from the flue gas of the waste incinerator through an amine technology would be feasible from an energetic point of view with almost no downside effect on the energy production of the plant.

7 Conclusion

The objective of this work was to provide a rapid and elementary method to forecast how much an outdoor, naturally illuminated microalgae production plant would produce annually in Macchiareddu, south Sardinia. The second objective was to understand what would be the energy requirement in order to provide the necessary carbon dioxide to the cultivation if all the carbon was provided by capturing the CO_2 from the flue gases of a nearby municipal waste incineration plant.
At first, a literature review on lab and pilot scale experiment was done in order to select the most promising microalgae species according to their capability to withstand both high percentages of CO_2 in the feed gas and low pH of the cultivation medium. The former condition was settled in order to promote the absorption of gasseous CO_2 directly by the microalgae. *Anabaena sp, Euglena gracilis, Scenedesmus obliquus* and *Chlorella sp* were selected as the most promising species. An ulterior selection on these experiment was done based on the illumination strategy. Only those experiments were illumination was natural or followed dark/light cycle which would resent natural illumination (12:12) were kept. After all these selection, the only remaining species among those previously cited was *Chlorella sp*.
Hourly solar radiation data for the selected location were acquired from PVGIS European Portal. A model to consider the adoption of automatic shading nets for irradiance control and irradiance diffusion was also adopted. The irradiance was accordingly modified when it was above the saturation limit of *Chlorella*. The Lamber-Beer light dispersion law was then applied in order to model the hourly irradiation profile along numerous points inside a generalized cross section of a vertical, bubble column photobioreactor of 5 cm diameter and 2 meter height. For comparison, a second bubble bolumn photobioreactor with an empty cylindrical volume inside was also considered. The dimension of this last one were 2 meter height, outer cylinder of 10 cm diameter an inner cylinder of 5 cm diameter. A static harvesting concentration of 0.8 g/l was settled as a conservative value for industrial harvesting and 500 l/h for 16 hours per day was adopted as harvesting flow rate. Consequently, the irradiation profiles were incorporated into Molina growth model in order to have an estimation of the specific growing rate of the selected microalgae. Overall, the system with active shading nets performed better. Among the two reactor design, the one with 5 cm diameter without inner empty volume was found as the better one. The 5 cm diameter reactor performed similarly to those found in literature. The hourly specific growing rate with and without the active shading system of this reactor were found respectively as $0.0016h-1$ and $9.4x10^{-}4h-1$. For what concerns the productivity, it was found as 0.0210 and 0.0127 g/l d for respectively the scenario with and without active shading system. The reactor with an empty cylindrical volume inside was less productive. The hourly specific growing rate with and without the active shading system of this last reactor design were found respectively as $0.0011h-1$ and $6x10^{-}4h-1$ and its productivity was found as 0.0151 and 0.0081 g/l d for respectively the scenario with and without active shading system. The results suggest that the adoption of a system to control irradiance would double the productivity and be beneficial for the cultivation. The specific growing rate and productivity values were lower than those found in literature for outdoor, naturally illuminated cultivation. This lower productivity could be linked to an higher harvesting concentration and an higher diameter assumed for the bubble column, both

factors which influence light penetration across the cultivation medium and therefore have an effect on productivity.
Later, while considering a continuous centrifugation flow rate of 500 l/h for 16 hours per day, the theoretical plant volumes for the standard, 5 cm diameter bubble column were found as 5 and 8 thousand cubic meters for respectively the active shading system and no shading system scenarios. Theoretical plant volumes for the second type of reactor were higher.
The technical and economical feasibily of the adoption of such types of reactor on an industrial scale was not object of investigation for this works and was therefore not studied. It is however possible to declare that adopting several thousand of this type of reactor at industrial scale could present serious difficulties and would probably have high mantainance costs. The final choice of what technology to adopt should also consider the required volume and value of the final biomass, or eventually the consequent processes which this biomass would undergo. Overall, an annual theoretical biomass production of 40 tons was found.
Given this biomass production and by using the elemental composition of *Chlorella sp*, the carbon, nitrogen, phosphorus and sulphur annual requirement were found. The cultivation medium was assumed as BG11, being this one already largely used for *Chlorella*. Sodium nitrate was considered as the source of nitrogen, dipotassium phosphate as the source of phosphorous and magnesium sulphate as the source of sulphur. Annual requirements of 27.1, 4.48 and 0.63 tons were respectively found for these compounds. These requirement would represent a significant expense for the plant. One way to lower the mineral nutrient requirement could be the use of waste flows from various sources. Macchiareddu industrial district accounts for several of those potential flows. Among the possible sources one is Ichnusa brewery, whose wastewater are remarkably rich in sugars and other compounds which can be used in microalgae production plant [138]. Another possible source of nutrient could be the neraby anaerobic digestor which is in these object of a refurbishment and expansion [139]. Finally, CACIP itself, the consortium which owns Tecnocasic waste incinerator plant, has a dedicated line for the treatment of industrial wastewater which is then sold for agriculture field irrigation thanks to its high content of nutrient [140]. All these options could represent concrete alternatives for the nutrient supply of the cultivation.
The carbon dioxide requirement of 77.12 tons was instead prospected to be entirely full filled by gaseous carbon dioxide. This amount was increased by a 10% in order to consider the lost of gaseous CO_2 during the de-gasing of the photobioreactors reaching in this way an annual requirement of 84,8 tons.
All this carbon dioxide was assumed to be provided by capturing the CO_2 from the flue gases of Tecnocasic municipal waste incineration plant whose CO_2 concentration reaches a volumetric concentration of about 11%. The annual requirement of carbon dioxide was found as the 0.11% of what is currently emitted by the incineration plant. This results indicates that while microalgae are surely a promising tool to use some of the CO_2 emitted by these plants, it would be quite unreasonable to think that they could also be responsible for of entirely capture and use all the emitted carbon dioxide. A further abatement of emission could be achieved if this biomass was used to synthesize products that now days are still fossil based. Monoethanolamine capture system was assumed as the carbon dioxide capture method followed by a compression of the gas at 25 bar in order to have a temporary storage of CO_2 . An annual energy require-

ment of 67.8 MWh and 9.4 MWh were found for respectively the heat and electricity consumption of the capture and compression.
Finally, using these annual cumulative energy consumption, specific energy requirement per tons of burned waste were found in order to asses the eventual downside of the carbon capture on the energy production of Tecnocasic incineration plant. Results showed that capturing and compressing the required CO_2 to 25 bar for storage purposes would have an almost negligible effect on the energy production of the waste incineration plant being the heat and electricity subtraction per ton of burned waste orders of magnitude lower than what is generated for the same unit weight of waste.

References

[1] Livegreen Società Agricola Srl website, accessible at:https://livegreen.bio/en

[2] Wang, B., Li, Y., Wu, N.: CO2 bio-mitigation using microalgae. Appl. Microbiol. Biotechnol. 79(5), 707–718 (2008)

[3] Vuppaladadiyam AK, Yao JG, Florin N, George A, Wang X, Labeeuw L, Jiang Y, Davis RW, Abbas A, Ralph P, Fennell PS, Zhao M. Impact of Flue Gas Compounds on Microalgae and Mechanisms for Carbon Assimilation and Utilization. ChemSusChem. 2018 Jan 23;11(2):334-355. doi: 10.1002/cssc.201701611. Epub 2018 Jan 15. PMID: 29165921.

[4] Schediwy K, Trautmann A, Steinweg C, Posten C. Microalgal kinetics — a guideline for photobioreactor design and process development. Eng Life Sci. 2019; 19: 830–843. https://doi.org/10.1002/elsc.201900107

[5] Roh Pin Lee, Bernd Meyer, Qiuliang Huang, Raoul Voss, Sustainable waste management for zero waste cities in China: potential, challenges and opportunities, Clean Energy, Volume 4, Issue 3, September 2020, Pages 169–201, https://doi.org/10.1093/ce/zkaa013

[6] Chang-Ling Chiang, Chi-Mei Lee, Pei-Chung Chen, Utilization of the cyanobacteria Anabaena sp. CH1 in biological carbon dioxide mitigation processes, Bioresource Technology, Volume 102, Issue 9, 2011, Pages 5400-5405, ISSN 0960-8524, https://doi.org/10.1016/j.biortech.2010.10.089.

[7] CO2 Algaefix project report, accessible at: https://www.co2algaefix.es/?q=documentacion

[8] Sofie Van Den Hende, Han Vervaeren, Nico Boon, Flue gas compounds and microalgae: (Bio-)chemical interactions leading to biotechnological opportunities, Biotechnology Advances, Volume 30, Issue 6, 2012, Pages 1405-1424, ISSN 0734-9750, https://doi.org/10.1016/j.biotechadv.2012.02.015.

[9] Lam, Man & Lee, Keat Teong & Mohamed, Abdul. (2012). Current status and challenges on microalgae-based capture. International Journal of Greenhouse Gas Control. 10. 456-469. 10.1016/j.ijggc.2012.07.010.

[10] Drzizga, D., et al. Biodegradation of the aminopolyphosphonate DTPMP by the cyanobacterium Anabaena variabilis proceeds via a C–P lyase-independent pathway. Environmental microbiology, 2017, 19.3: 1065-1076.

[11] Qian-lin Wang, Yong-ding Liu, Yin-wu Shen, Chuan-yin Jin, Jin-shu Lu, Jiamin Zhu, Shang-hao Li, Studies on mixed mass cultivation of Anabaena spp. (nitrogen-fixing blue-green algae, cyanobacteria) on a large scale, Bioresource Technology, Volume 38, Issues 2–3, 1991, Pages 221-228, ISSN 0960-8524, https://doi.org/10.1016/0960-8524(91)90158-G.

[12] Yaming Ge, Junzhi Liu, Guangming Tian, Growth characteristics of Botryococcus braunii 765 under high CO2 concentration in photobioreactor, Bioresource Technology, Volume 102, Issue 1, 2011, Pages 130-134, ISSN 0960-8524, https://doi.org/10.1016/j.biortech.2010.06.051.

[13] Thomas, D.M., Mechery, J. Paulose, S.V. Carbon dioxide capture strategies from flue gas using microalgae: a review. Environ Sci Pollut Res 23, 16926–16940 (2016). https://doi.org/10.1007/s11356-016-7158-3

[14] Dahai Tang, Wei Han, Penglin Li, Xiaoling Miao, Jianjiang Zhong, CO2 biofixation and fatty acid composition of Scenedesmus obliquus and Chlorella pyrenoidosa in response to different CO2 levels, Bioresource Technology, Volume 102, Issue 3, 2011, Pages 3071-3076, ISSN 0960-8524, https://doi.org/10.1016/j.biortech.2010.10.047.

[15] Bito, T.; Okumura, E.; Fujishima, M.; Watanabe, F. Potential of Chlorella as a Dietary Supplement to Promote Human Health. Nutrients 2020, 12, 2524. https://doi.org/10.3390/nu12092524

[16] Jun Cheng, Yun Huang, Jia Feng, Jing Sun, Junhu Zhou, Kefa Cen, Improving CO2 fixation efficiency by optimizing Chlorella PY-ZU1 culture conditions in sequential bioreactors, Bioresource Technology, Volume 144, 2013, Pages 321-327, ISSN 0960-8524, https://doi.org/10.1016/j.biortech.2013.06.122.

[17] Xiaojun Yan, Roger R. Ruan, High-value chemicals from Botryococcus braunii and their current applications – A review, Bioresource Technology, Volume 291, 2019, 121911, ISSN 0960-8524, https://doi.org/10.1016/j.biortech.2019.121911.

[18] Yaming Ge, Junzhi Liu, Guangming Tian, Growth characteristics of Botryococcus braunii 765 under high CO2 concentration in photobioreactor, Bioresource Technology, Volume 102, Issue 1, 2011, Pages 130-134, ISSN 0960-8524, https://doi.org/10.1016/j.biortech.2010.06.051.

[19] Minxi Wan, Zhen Zhang, Ruixuan Wang, Wenmin Bai, Jianke Huang, Weiliang Wang, Guomin Shen, Anquan Yu, Yuanguang Li, High-yield cultivation of Botryococcus braunii for biomass and hydrocarbons, Biomass and Bioenergy, Volume 131, 2019, 105399, ISSN 0961-9534

[20] Gouveais, João Diogo Guimarães. “Botryococcus braunii for the production of hydrocarbons and exopolysaccharides and the role of associated bacteria.” (2017).

[21] Salih, Fadhil M. "Microalgae tolerance to high concentrations of carbon dioxide: a review." Journal of Environmental Protection 2.05 (2011): 648.

[22] Chen, Cong Huang, Maoqiang Zhang, Weijuan Yang, Jun Cheng, CO2 gradient domestication improved high-concentration CO2 tolerance and photoautotrophic growth of Euglena gracilis, Science of The Total Environment, Volume 868, 2023, 161629, ISSN 0048-9697

[23] Takeyama H, Kanamaru A, Yoshino Y, Kakuta H, Kawamura Y, Matsunaga T. Production of antioxidant vitamins, beta-carotene, vitamin C, and vitamin E, by two-step culture of Euglena gracilis Z. Biotechnol Bioeng. 1997 Jan 20;53(2):185-90. doi: 10.1002/(SICI)1097-0290(19970120)53:2<185::AID-BIT8>3.0.CO;2-K. PMID: 18633963.

[24] Eurostat waste statistics, accessible at: https://ec.europa.eu/eurostat/databrowser/view/env$_{w}asm$

[25] Suzuki K., Large scale cultivation of Euglena. Adv Med Biol. 2017; 285-293. doi:10.1007/978-3-319-54910-1-14.

[26] EFSA Panel on Nutrition, Novel Foods and Food Allergens (NDA), et al. "Safety of dried whole cell Euglena gracilis as a novel food pursuant to Regulation (EU) 2015/2283." EFSA Journal 18.5 (2020): e06100.

[27] Euglena, a Gravitactic Flagellate of Multiple UsagesScientific Figure on ResearchGate. Available from: Häder, Donat & Hemmersbach, Ruth. (2022). Euglena, a Gravitactic Flagellate of Multiple Usages. Life. 12. 1522. 10.3390/life12101522

[28] Gissibl A, Sun A, Care A, Nevalainen H and Sunna A (2019) Bioproducts From Euglena gracilis: Synthesis and Applications. Front. Bioeng. Biotechnol. 7:108. doi: 10.3389/fbioe.2019.00108

[29] Barsanti, L., Vismara, R., Passarelli, V. et al. Paramylon (β-1,3-glucan) content in wild type and WZSL mutant of Euglena gracilis. Effects of growth conditions. Journal of Applied Phycology 13, 59–65 (2001). https://doi.org/10.1023/A:1008105416065

[30] Mafruha T. Hasan, Angela Sun, Mehdi Mirzaei, Junior Te'o, Graham Hobba, Anwar Sunna, Helena Nevalainen, A comprehensive assessment of the biosynthetic pathways of ascorbate, α-tocopherol and free amino acids in Euglena gracilis var. saccharophila, Algal Research, Volume 27, 2017, Pages 140-151, ISSN 2211-9264,

[31] Chun-Dan Zhang, Wei Li, Yun-Hai Shi, Yuan-Guang Li, Jian-Ke Huang, Hong-Xia Li, A new technology of CO2 supplementary for microalgae cultivation on large scale – A spraying absorption tower coupled with an outdoor open runway pond, Bioresource Technology, Volume 209, 2016, Pages 351-359, ISSN 0960-8524, https://doi.org/10.1016/j.biortech.2016.03.007.

[32] Michael Bader Fotografie, accessible at: https://mbader.com/blog/spirulina/, last access 31/03/2023

[33] Al Hoqani, Umaima & Young, Rosanna & Purton, Saul. (2016). The biotechnological potential of Nannochloropsis. Perspectives in Phycology. 4. 10.1127/pip/2016/0065.

[34] Microalgae of the genus Nannochloropsis: Chemical composition and functional implications for human nutrition - Scientific Figure on ResearchGate. Available from: Zanella, Lorenzo & Vianello, Fabio. (2020). Microalgae of the genus Nannochloropsis: Chemical composition and functional implications for human nutrition. Journal of Functional Foods. 68. 10.1016/j.jff.2020.103919.

[35] Ana F. Esteves, José C.M. Pires, Ana L. Gonçalves, Chapter 8 - Current utilization of microalgae in the food industry beyond direct human consumption, Editor(s): Tomás Lafarga, Gabriel Acién, Cultured Microalgae for the Food Industry, Academic Press, 2021, Pages 199-248, ISBN 9780128210802, https://doi.org/10.1016/B978-0-12-821080-2.00005-8.

[36] Enzing, Christien, et al. "Microalgae-based products for the food and feed sector: an outlook for Europe." JRC Scientific and policy reports (2014): 19-37.

[37] Araújo R, Vázquez Calderón F, Sánchez López J, Azevedo IC, Bruhn A, Fluch S, Garcia Tasende M, Ghaderiardakani F, Ilmjärv T, Laurans M, Mac Monagail M, Mangini S, Peteiro C, Rebours C, Stefansson T and Ullmann J (2021) Current Status of the Algae Production Industry in Europe: An Emerging Sector of the Blue Bioeconomy. Front. Mar. Sci. 7:626389. doi: 10.3389/fmars.2020.626389

[38] Huld, T., Müller, R. and Gambardella, A., 2012. "A new solar radiation database for estimating PV performance in Europe and Africa". Solar Energy, 86, 1803-1815.

[39] Anna L Stephenson, John S Dennis, Christopher J Howe, Stuart A Scott & Alison G Smith (2010) Influence of nitrogen-limitation regime on the production by Chlorella vulgaris of lipids for biodiesel feedstocks, Biofuels, 1:1, 47-58, DOI: 10.4155/bfs.09.1

[40] Pond Technologies Holdings Inc. website, accessible at: ttps://pondtech.com

[41] Sung, Y.J., Lee, J.S., Yoon, H.K. et al. Outdoor cultivation of microalgae in a coal-fired power plant for conversion of flue gas CO2 into microalgal direct combustion fuels. Syst Microbiol and Biomanuf 1, 90–99 (2021). https://doi.org/10.1007/s43393-020-00007-7

[42] Negoro M, Shioji N, Miyamoto K, Miura Y. Growth of microalgae in high CO2 gas and effects of SOX and NOX. Appl Biochem Biotechnol. 1991 Spring;28-29:877-86. doi: 10.1007/BF02922657. PMID: 1929389.

[43] Anastasios Melis, Solar energy conversion efficiencies in photosynthesis: Minimizing the chlorophyll antennae to maximize efficiency, Plant Science, Volume 177, Issue 4, 2009, Pages 272-280, ISSN 0168-9452, https://doi.org/10.1016/j.plantsci.2009.06.005.

[44] F.G. Acién Fernández, José María Fernández Sevilla, Emilio Molina Grima, Chapter 21 - Costs analysis of microalgae production, Editor(s): Ashok Pandey, Jo-Shu Chang, Carlos Ricardo Soccol, Duu-Jong Lee, Yusuf Chisti, In Biomass, Biofuels, Biochemicals, Biofuels from Algae (Second Edition), Elsevier, 2019, Pages 551-566, ISBN 9780444641922, https://doi.org/10.1016/B978-0-444-64192-2.00021-4.

[45] Microalgal removal of CO2 from flue gases: CO2 capture from a coal combustor - Scientific Figure on ResearchGate. Available from: Olaizola, Miguel & Bridges, T & Flores, S & Griswold, L & Morency, J & Nakamura, Toshitaka. (2003). Microalgal removal of CO2 from flue gases: CO2 capture from a coal combustor.

[46] Giving CO2 an Economic Value: Carbon Capture Technology Helps Recycle Waste into Resources, accessible at https://asia.toshiba.com/highlights/giving-co2-an-economic-value-carbon-capture-technology-helps-recycle-waste-into-resources/

[47] Nano- and Microplastics Hetero-aggregation by a Microalgal-based Biopolymer: An Industrial Solution - Scientific Figure on ResearchGate. Available from: Cunha, César & Silva, Laura & Paulo, Jorge & Faria, Marisa & Quintana, Antera & Nogueira, Natacha & Cordeiro, Nereida. (2019). Nano- and Microplastics Hetero-aggregation by a Microalgal-based Biopolymer: An Industrial Solution

[48] Tipawan Thawechai, Benjamas Cheirsilp, Yasmi Louhasakul, Piyarat Boonsawang, Poonsuk Prasertsan, Mitigation of carbon dioxide by oleaginous microalgae for lipids and pigments production: Effect of light illumination and carbon dioxide feeding strategies, Bioresource Technology, Volume 219, 2016, Pages 139-149, ISSN 0960-8524, https://doi.org/10.1016/j.biortech.2016.07.109.

[49] Fang-Fang Li, Zhong-Hua Yang, Rong Zeng, Gai Yang, Xu Chang, Jia-Bao Yan, and Ya-Li Hou, Microalgae Capture of CO2 from Actual Flue Gas Discharged from a Combustion Chamber Industrial & Engineering Chemistry Research 2011 50 (10), 6496-6502 DOI: 10.1021/ie200040q

[50] Samarpita Basu, Abhijit Sarma Roy, Kaustubha Mohanty, Aloke K. Ghoshal, Enhanced CO2 sequestration by a novel microalga: Scenedesmus obliquus SA1 isolated from biodiversity hotspot region of Assam, India, Bioresource Technology, Volume 143, 2013, Pages 369-377, ISSN 0960-8524, https://doi.org/10.1016/j.biortech.2013.06.010.

[51] Potential and properties of marine microalgae Nannochloropsis oculata as biomass fuel feedstock - Scientific Figure on ResearchGate. Available from: Sukarni, Sukarni & Soeparman, Sudjito & Hamidi, Nurkholis & Yanuhar, Uun & Wardana, (2014). Potential and properties of marine microalgae Nannochloropsis oculata as biomass fuel feedstock. International Journal of Energy and Environmental Engineering. 10.1007/s40095-014-0138-9.

[52] Italian Istituto Nazionale di Statistica actualization tool for money, accessible at: https://rivaluta.istat.it/Rivaluta/

[53] Niels-Henrik Norsker, Maria J. Barbosa, Marian H. Vermuë, René H. Wijffels, Microalgal production — A close look at the economics, Biotechnology Advances, Volume 29, Issue 1, 2011, Pages 24-27, ISSN 0734-9750, https://doi.org/10.1016/j.biotechadv.2010.08.005.

[54] Ana L. Gonçalves, Carla M. Rodrigues, José C.M. Pires, Manuel Simões, The effect of increasing CO2 concentrations on its capture, biomass production and wastewater bioremediation by microalgae and cyanobacteria, Algal Research, Volume 14, 2016, Pages 127-136, ISSN 2211-9264, https://doi.org/10.1016/j.algal.2016.01.008.

[55] Khattar, J.I.S., Kaur, S., Kaushal, S., Singh, Y., Singh, D.P., Rana, S., Gulati, A., 2015. Hyperproduction of phycobiliproteins by the cyanobacterium Anabaena fertilissima PUPCCC 410.5 under optimized culture conditions. Algal Res. 12, 463–469. https://doi.org/10.1016/j.algal.2015.10.007.

[56] Chae SR, Hwang EJ, Shin HS. Single cell protein production of Euglena gracilis and carbon dioxide fixation in an innovative photo-bioreactor. Bioresour Technol.

2006 Jan;97(2):322-9. doi: 10.1016/j.biortech.2005.02.037. Epub 2005 Apr 18. PMID: 16171688.

[57] C-Phycocyanin from Spirulina sp. by Sigma-Alrich, accessible at: https://www.sigmaaldrich.com/IT/it/product/sigma/p2172, last access 25/03/2023.

[58] Moslavac S. Outer membrane proteins of Anabaena sp. strain PCC 7120 (Doctoral dissertation, lmu).

[59] Fernando Pagels, A. Catarina Guedes, Helena M. Amaro, Anake Kijjoa, Vitor Vasconcelos, Phycobiliproteins from cyanobacteria: Chemistry and biotechnological applications, Biotechnology Advances, Volume 37, Issue 3, 2019, Pages 422-443, ISSN 0734-9750, https://doi.org/10.1016/j.biotechadv.2019.02.010.

[60] Dinesh Kumar Saini, Dinesh Yadav, Sunil Pabbi, Deepak Chhabra, Pratyoosh Shukla, Phycobiliproteins from Anabaena variabilis CCC421 and its production enhancement strategies using combinatory evolutionary algorithm approach, Bioresource Technology, Volume 309, 2020, 123347, ISSN 0960-8524, https://doi.org/10.1016/j.biortech.2020.123347.

[61] Program on Technology Innovation: A Case Study of Seambiotic's Research on Utility-Connected Algae Systems, Electric Power Research Institute,2010 accessible at: https://www.epri.com/research/products/1020807, last access 24/03/2023.

[62] B. Simoneit, W. Rogge, Q. Lang, R. Jaff8, Chemosphere 2001, 2, 107 – 122.

[63] Dahai Tang, Wei Han, Penglin Li, Xiaoling Miao, Jianjiang Zhong, CO2 biofixation and fatty acid composition of Scenedesmus obliquus and Chlorella pyrenoidosa in response to different CO2 levels, Bioresource Technology, Volume 102, Issue 3, 2011, Pages 3071-3076, ISSN 0960-8524, https://doi.org/10.1016/j.biortech.2010.10.047.

[64] Raquel Guidetti Vendruscolo, Mariany Costa Deprá, Pricila Nass Pinheiro, Valcenir Junior Mendes Furlan, Juliano Smanioto Barin, Alexandre José Cichoski, Cristiano Ragagnin de Menezes, Leila Queiroz Zepka, Eduardo Jacob-Lopes, Roger Wagner, Food potential of Scenedesmus obliquus biomasses obtained from photosynthetic cultivations associated with carbon dioxide mitigation, Food Research International, Volume 160, 2022, 111590, ISSN 0963-9969, https://doi.org/10.1016/j.foodres.2022.111590.

[65] Sheng-Yi Chiu, Chien-Ya Kao, Ming-Ta Tsai, Seow-Chin Ong, Chiun-Hsun Chen, Chih-Sheng Lin, Lipid accumulation and CO2 utilization of Nannochloropsis oculata in response to CO2 aeration, Bioresource Technology, Volume 100, Issue 2, 2009, Pages 833-838, ISSN 0960-8524, https://doi.org/10.1016/j.biortech.2008.06.061.

[66] Rodolfi L, Chini Zittelli G, Bassi N, Padovani G, Biondi N, Bonini G, Tredici MR. Microalgae for oil: strain selection, induction of lipid synthesis and outdoor mass cultivation in a low-cost photobioreactor. Biotechnol Bioeng. 2009 Jan 1;102(1):100-12. doi: 10.1002/bit.22033. PMID: 18683258.

[67] Chini Zittelli, Graziella & Biondi, Natascia & Rodolfi, Liliana & Tredici, Mario. (2013). Photobioreactors for Mass Production of Microalgae. 10.1002/9781118567166.ch13.

[68] Allmicroalgae – Natural Products S.A official website: https://www.allmicroalgae.com/en/microalgae/

[69] Laura Barsanti, Paolo Gualtieri, Is exploitation of microalgae economically and energetically sustainable?, Algal Research, Volume 31, 2018, Pages 107-115, ISSN 2211-9264, https://doi.org/10.1016/j.algal.2018.02.001.

[70] Bo Huang, Ying Shan, Tao Yi, Tao Tang, Wei Wei, Nigel W.T. Quinn, Study on high-CO2 tolerant Scenedesmus sp. and its mechanism via comparative transcriptomic analysis, Journal of CO2 Utilization, Volume 42, 2020, 101331, ISSN 2212-9820, https://doi.org/10.1016/j.jcou.2020.101331.

[71] Underwater Photosynthesis of Submerged Plants – Recent Advances and Methods - Scientific Figure on ResearchGate. Available from: Pedersen, Ole & Colmer, Timothy & Sand-Jensen, Kaj. (2013). Underwater Photosynthesis of Submerged Plants – Recent Advances and Methods. Frontiers in plant science. 4. 140. 10.3389/fpls.2013.00140.

[72] THE Niederraussen Coal Innovation Centre, 2009. Accessible at https://braunkohle.de/wp-content/uploads/2019/04/Das-Innovationszentrum-Kohle-englisch.pdf. Last access 24/03/2023.

[73] Comprehensive evaluation of microalgal based dairy effluent treatment process for clean water generation and other value added products - Scientific Figure on ResearchGate. Accessible at: Kiran Kumar, Adepu & Sharma, Shaishav & Patel, Aesha & Dixit, Gaurav & Shah, Ekta. (2019). Comprehensive evaluation of microalgal based dairy effluent treatment process for clean water generation and other value added products. International Journal of Phytoremediation. 21. 1-12. 10.1080/15226514.2018.1537248.

[74] Zawar P, Javalkote V, Burnap R, Mahulikar P, Puranik P. CO2 capture using limestone for cultivation of the freshwater microalga Chlorella sorokiniana PAZ and the cyanobacterium Arthrospira sp. VSJ. Bioresour Technol. 2016 Dec;221:498-509. doi: 10.1016/j.biortech.2016.09.079. Epub 2016 Sep 20. PMID: 27677152.

[75] Choi W, Kim G, Lee K. Influence of the CO2 absorbent monoethanolamine on growth and carbon fixation by the green alga Scenedesmus sp. Bioresour Technol. 2012 Sep;120:295-9. doi: 10.1016/j.biortech.2012.06.010. Epub 2012 Jun 16. PMID: 22771020.

[76] Bingtao Zhao, Yaxin Su, Yixin Zhang, Guomin Cui, Carbon dioxide fixation and biomass production from combustion flue gas using energy microalgae, Energy, Volume 89, 2015, Pages 347-357, ISSN 0360-5442, https://doi.org/10.1016/j.energy.2015.05.123.

[77] Park, J., Kumar, G., Bakonyi, P. et al. Comparative Evaluation of CO2 Fixation of Microalgae Strains at Various CO2 Aeration Conditions. Waste Biomass Valor 12, 2999–3007 (2021). https://doi.org/10.1007/s12649-020-01226-8

[78] Johnson, Tylor & Katuwal, Sarmila & Anderson, Gary & Gu, Liping & Zhou, Ruanbao & Gibbons, William. (2018). Photobioreactor Cultivation Strategies for Microalgae and Cyanobacteria. Biotechnology Progress. 34. 10.1002/btpr.2628.

[79] Stefano Cernuschi, Mario Grosso, Federico Viganò, Maria Chiara Zanetti, Deborah Panepinto, Marco Ragazzi, Libro bianco sull'incenerimento dei rifiuti urbani. Joint working group between Politecnico di Torino, Politecnico di Milano, Università di Trento. September 2020.

[80] Huang, G., Chen, F., Kuang, Y. et al. Current Techniques of Growing Algae Using Flue Gas from Exhaust Gas Industry: a Review. Appl Biochem Biotechnol 178, 1220–1238 (2016). https://doi.org/10.1007/s12010-015-1940-4

[81] Jeffery West Design, Deltaway Energy CC, 2011.

[82] Garam Kim, Wookjin Choi, Chang-Hee Lee, Kisay Lee, Enhancement of dissolved inorganic carbon and carbon fixation by green alga Scenedesmus sp. in the presence of alkanolamine CO2 absorbents, Biochemical Engineering Journal, Volume 78, 2013, Pages 18-23, ISSN 1369-703X

[83] Asthary, Prima & Saepulloh, & Pramono, Kristaufan & Rachmanto, Toni & Setiawan, Yusup. (2019). Cultivation of Spirulina platensis using WWTP effluent and CO2 emission of papermill in tubular photobioreactor. AIP Conference Proceedings. 2120. 040031. 10.1063/1.5115669.

[84] Chen HW, Yang TS, Chen MJ, Chang YC, Lin CY, Wang EI, Ho CL, Huang KM, Yu CC, Yang FL, Wu SH, Lu YC, Chao LK. Application of power plant flue gas in a photobioreactor to grow Spirulina algae, and a bioactivity analysis of the algal water-soluble polysaccharides. Bioresour Technol. 2012 Sep;120:256-63. doi: 10.1016/j.biortech.2012.04.106. Epub 2012 Jun 27. PMID: 22820115.

[85] Ben-Amotz, A. (1995) New mode of Dunaliella biotechnology: two-phase growth for b-carotene production. J. Appl. Phycol., 7, 65–68.

[86] Skalska K, Miller JS, Ledakowicz S. Trends in NO(x) abatement: a review. Sci Total Environ. 2010 Sep 1;408(19):3976-89. doi: 10.1016/j.scitotenv.2010.06.001. Epub 2010 Jun 26. PMID: 20580060.

[87] Nord, L.O; Bolland, O. Carbon Dioxide Emission Management in Power Generation, John Wiley & Sons, 2020

[88] McGinn PJ, Dickinson KE, Bhatti S, Frigon JC, Guiot SR, O'Leary SJ. Integration of microalgae cultivation with industrial waste remediation for biofuel and bioenergy production: opportunities and limitations. Photosynth Res. 2011 Sep;109(1-3):231-47. doi: 10.1007/s11120-011-9638-0. Epub 2011 Mar 9. Erratum in: Photosynth Res. 2011 Sep;109(1-3):249. PMID: 21461850.

[89] Aslam A, carbon dioxide capture-Hall SR, Mughal TA, Schenk PM. Selection and adaptation of microalgae to growth in 100% unfiltered coal-fired flue gas. Bioresour Technol. 2017 Jun;233:271-283. doi: 10.1016/j.biortech.2017.02.111. Epub 2017 Mar 1. PMID: 28285218.

[90] https://commons.wikimedia.org/w/index.php?curid=35450226

[91] Bleeke, F., Milas, M., Winckelmann, D. et al. Optimization of freshwater microalgal biomass harvest using polymeric flocculants. Int Aquat Res 7, 235–244 (2015).

[92] By FarmerOnMars - Own work, CC BY-SA 3.0, https://commons.wikimedia.org/w/index.php?curid=19

[93] Ramos, Ana & Polle, Jürgen & Tran, Duc & Cushman, John & Jin, Eonseon & Varela, João. (2011). The unicellular green alga Dunaliella salina Teod. as a model for abiotic stress tolerance: Genetic advances and future perspectives. Algae. 26. 3-20. 10.4490/algae.2011.26.1.003.

[94] By Environmental Protection Agency, https://commons.wikimedia.org/w/index.php?curid=2779560

[95] By Anatoly Mikhaltsov - Own work, CC BY 4.0, https://commons.wikimedia.org/w/index.php?curid=10

[96] Sun, XM., Ren, LJ., Zhao, QY. et al. Microalgae for the production of lipid and carotenoids: a review with focus on stress regulation and adaptation. Biotechnol Biofuels 11, 272 (2018). https://doi.org/10.1186/s13068-018-1275-9

[97] Italian Emission Inventory Informative report 1990 - 2021. Istituto Superiore per la Protezione e la Ricerca Ambientale, 2023. Accessible at: https://www.isprambiente.gov.it/files2023/pubblicazioni/rapporti/rapporto-$385_2023_iir2023.pdf$

[98] Amos Richmond, Handbook of Microalgal Culture: Biotechnology and Applied Phycology. First Edition, Blackwell Publishing Ltd, 2004.

[99] Barbosa, M. J. (2003). Microalgal photobioreactors: Scale-up and optimisation. [internal PhD, WU, Wageningen University].

[100] Lim, Y. A., Chong, M. N., Foo, S. C., & Ilankoon, I. M. S. K. (2021). Analysis of direct and indirect quantification methods of CO2 fixation via microalgae cultivation in photobioreactors: A critical review.

[101] V. Bhola, F. Swalaha, R. Ranjith Kumar, M. Singh, F. Bux, Overview of the potential of microalgae for CO2 sequestration, 2014

[102] X. Xu, X. Gu, Z. Wang, W. Shatner, Z. Wang, Progress, challenges and solutions of research on photosynthetic carbon sequestration efficiency of microalgae, 2019

[103] M. Collotta, P. Champagne, W. Mabee, G. Tomasoni, Wastewater and waste CO2 for sustainable biofuels from microalgae, 2018

[104] Sabariswaran Kandasamy, Bo Zhang, Zhixia He, Narayanamoorthy Bhuvanendran, Ahmed I. EL-Seesy, Qian Wang, Mathiyazhagan Narayanan, Palaniswamy Thangavel, Mudasir A. Dar, Microalgae as a multipotential role in commercial applications: Current scenario and future perspectives, 2022

[105] Li, Yan & Markley, Brandie & Mohan, Arun & Rodriguez-Santiago, Victor & Thompson, David & Van Niekerk, Daniel. (2006). Utilization of carbon dioxide from coalfired power plant for the production of value-added products. 23rd Annual International Pittsburgh Coal Conference, PCC - Coal-Energy, Environment and Sustainable Development.

[106] Han T, Lu H F, Ma S S, Zhang Y H, Liu Z D, Duan N. Progress in microalgae cultivation photobioreactors and applications in wastewater treatment: A review. Int J Agric & Biol Eng, 2017; 10(1): 1–29.

[107] Oeschger, Linda and Posten, Clemens. "11 Construction and assessment parameters of photobioreactors". Microalgal Biotechnology: Potential and Production, edited by Clemens Posten and Christian Walter, Berlin, Boston: De Gruyter, 2013, pp. 225-236. https://doi.org/10.1515/9783110225020.225

[108] Anand V. Kulkarni, Shrikant V. Badgandi, Jyeshtharaj B. Joshi, Design of ring and spider type spargers for bubble column reactor: Experimental measurements and CFD simulation of flow and weeping, Chemical Engineering Research and Design, Volume 87, Issue 12, 2009, Pages 1612-1630, ISSN 0263-8762, https://doi.org/10.1016/j.cherd.2009.06.003.

[109] Michele Carone, Davis Alpe, Valentina Costantino, Clara Derossi, Andrea Occhipinti, Mariachiara Zanetti, Vincenzo A. Riggio, Design and characterization of a new pressurized flat panel photobioreactor for microalgae cultivation and CO2 bio-fixation, Chemosphere, Volume 307, Part 2, 2022, 135755, ISSN 0045-6535, https://doi.org/10.1016/j.chemosphere.2022.135755.

[110] C.U. Ugwu, H. Aoyagi, H. Uchiyama, Photobioreactors for mass cultivation of algae, Bioresource Technology, Volume 99, Issue 10, 2008, Pages 4021-4028, ISSN 0960-8524, https://doi.org/10.1016/j.biortech.2007.01.046.

[111] Posten, Clemens, and Christian Walter. 2012. Microalgal biotechnology: potential and production. Berlin: De Gruyter

[112] Rodas-Zuluaga LI, Castillo-Zacarías C, Núñez-Goitia G, Martínez-Prado MA, Rodríguez-Rodríguez J, López-Pacheco IY, Sosa-Hernández JE, Iqbal HMN, Parra-Saldívar R. Implementation of kLa-Based Strategy for Scaling Up Porphyridium purpureum (Red Marine Microalga) to Produce High-Value Phycoerythrin, Fatty Acids, and Proteins. Mar Drugs. 2021 May 21;19(6):290. doi: 10.3390/md19060290. PMID: 34064032; PMCID: PMC8224092.

[113] F., Camacho, Rubio., F.G., Acién, Fernández., J.A., Sánchez, Pérez., F., García, Camacho., E., Molina, Grima. (1999). Prediction of dissolved oxygen and carbon dioxide concentration profiles in tubular photobioreactors for microalgal culture. Biotechnology and Bioengineering, 62(1):71-86. doi: 10.1002/(SICI)1097-0290(19990105)62:1<71::AID-BIT9>3.0.CO;2-T

[114] Al-Helal, Ibrahim, Abdullah Alsadon, Mohamed Shady, Abdullah Ibrahim, and Ahmed Abdel-Ghany. 2020. "Diffusion Characteristics of Solar Beams Radiation Transmitting through Greenhouse Covers in Arid Climates" Energies 13, no. 2: 472. https://doi.org/10.3390/en13020472

[115] Mubarak M., Shaija A. & Prashanth P. (2019): Bubble column photobioreactor for Chlorella pyrenoidosa cultivation and validating gas hold up and volumetric mass transfer coefficient, Energy Sources, Part A: Recovery, Utilization, and Environmental Effects, DOI: 10.1080/15567036.2019.1680769

[116] Choon Gek Khoo, Man Kee Lam, Keat Teong Lee, Pilot-scale semi-continuous cultivation of microalgae Chlorella vulgaris in bubble column photobioreactor (BC-PBR): Hydrodynamics and gas–liquid mass transfer study, Algal Research, Volume 15, 2016, Pages 65-76, ISSN 2211-9264, https://doi.org/10.1016/j.algal.2016.02.001.

[117] Sánchez Mirón, A., García Camacho, F., Contreras Gómez, A., Grima, E.M. and Chisti, Y. (2000), Bubble-column and airlift photobioreactors for algal culture. AIChE J., 46: 1872-1887. https://doi.org/10.1002/aic.690460915

[118] J. Dudley, Mass transfer in bubble columns: A comparison of correlations, Water Research, Volume 29, Issue 4, 1995, Pages 1129-1138, ISSN 0043-1354, https://doi.org/10.1016/0043-1354(94)00253-4.

[119] Merchuk, Jose C. et al. “Comparison of photobioreactors for cultivation of the red microalga Porphyridium sp.” Journal of Chemical Technology Biotechnology 75 (2000): 1119-1126.

[120] Litchman, Elena. "Competition and coexistence of phytoplankton under fluctuating light: experiments with two cyanobacteria." Aquatic Microbial Ecology 31.3 (2003): 241-248.

[121] Ogbonna, James C., Hirokazu Yada, and Hideo Tanaka. "Light supply coefficient: a new engineering parameter for photobioreactor design." Journal of fermentation and bioengineering 80.4 (1995): 369-376.

[122] J. González-Camejo, A. Viruela, M.V. Ruano, R. Barat, A. Seco, J. Ferrer, Effect of light intensity, light duration and photoperiods in the performance of an outdoor photobioreactor for urban wastewater treatment, Algal Research, Volume 40, 2019, 101511, ISSN 2211-9264, https://doi.org/10.1016/j.algal.2019.101511.

[123] Berberoglu H, Barra N, Pilon L, Jay J. Growth, CO2 consumption and H2 production of Anabaena variabilis ATCC 29413-U under different irradiances and CO2 concentrations. J Appl Microbiol. 2008;104(1):105-121. doi:10.1111/j.1365-2672.2007.03559.x

[124] Hempel, N., Petrick, I. & Behrendt, F. Biomass productivity and productivity of fatty acids and amino acids of microalgae strains as key characteristics of suitability for biodiesel production. J Appl Phycol 24, 1407–1418 (2012). https://doi.org/10.1007/s10811-012-9795-3

[125] E. Molina Grima, F.G. Acién Fernández, F. García Camacho, Yusuf Chisti, Photobioreactors: light regime, mass transfer, and scaleup, Editor(s): R. Osinga, J. Tramper, J.G. Burgess, R.H. Wijffels, Progress in Industrial Microbiology, Elsevier, Volume 35, 1999, Pages 231-247, ISSN 0079-6352, ISBN 9780444503879, https://doi.org/10.1016/S0079-6352(99)80118-0.

[126] Reis, Mariana & Ribeiro, Aristides. (2020). Conversion factors and general equations applied in agricultural and forest meteorology. 27. 227-258. 10.31062/agrom.v27i2.26527.

[127] Simulation of the Light Distribution in a Solar Photocatalytic Bubble Column Reactor Using the Monte Carlo Method John Akach, John Kabuba, and Aoyi Ochieng Industrial & Engineering Chemistry Research 2020 59 (40), 17708-17719 DOI: 10.1021/acs.iecr.0c02124

[128] Marko Popovic, Thermodynamic properties of microorganisms: determination and analysis of enthalpy, entropy, and Gibbs free energy of biomass, cells and colonies of 32 microorganism species, Heliyon, Volume 5, Issue 6, 2019, e01950, ISSN 2405-8440, https://doi.org/10.1016/j.heliyon.2019.e01950

[129] Zhi Guo, Wei Boon Alfred Phooi, Zi Jian Lim, Yen Wah Tong, Control of CO2 input conditions during outdoor culture of Chlorella vulgaris in bubble column photobioreactors, Bioresource Technology, Volume 186, 2015, Pages 238-245, ISSN 0960-8524, https://doi.org/10.1016/j.biortech.2015.03.065.

[130] Lopes, Alcinda P., Francisca M. Santos, Tânia F. C. V. Silva, Vítor J. P. Vilar, and José C. M. Pires. 2020. "Outdoor Cultivation of the Microalga Chlorella vulgaris in a New Photobioreactor Configuration: The Effect of Ultraviolet and Visible Radiation" Energies 13, no. 8: 1962. https://doi.org/10.3390/en13081962

[131] Sarker, N.K., Salam, P.A. Indoor and outdoor cultivation of Chlorella vulgaris and its application in wastewater treatment in a tropical city—Bangkok, Thailand. SN Appl. Sci. 1, 1645 (2019). https://doi.org/10.1007/s42452-019-1704-9

[132] Marta E. Clares, José Moreno, Miguel G. Guerrero, Mercedes García-González, Assessment of the CO2 fixation capacity of Anabaena sp. ATCC 33047 outdoor cultures in vertical flat-panel reactors, Journal of Biotechnology, Volume 187, 2014, Pages 51-55, ISSN 0168-1656, https://doi.org/10.1016/j.jbiotec.2014.07.014.

[133] Katuwal, Sarmila, "Designing and Development of a Photobioreactor for Optimizing the Growth of Micro Algae and Studying Its Growth Parameters" (2017). Electronic Theses and Dissertations. 2161. https://openprairie.sdstate.edu/etd/2161

[134] Ambica Koushik Pegallapati, Nagamany Nirmalakhandan, Modeling algal growth in bubble columns under sparging with CO2-enriched air, Bioresource Technology, Volume 124, 2012, Pages 137-145, ISSN 0960-8524, https://doi.org/10.1016/j.biortech.2012.08.026.

[135] Picardo, Marta & de Medeiros, José & Monteiro, Juliana & Chaloub, Ricardo & Giordano, Mario & Araujo, Ofelia. (2013). A methodology for screening of microalgae as a decision making tool for energy and green chemical process applications. Clean Technologies and Environmental Policy. 15. 275-291. 10.1007/s10098-012-0508-z.

[136] Concas, Alessandro & Pisu, Massimo & Cao, Giacomo. (2010). Novel simulation model of the solar collector of BIOCOIL photobioreactors for CO2 sequestration with microalgae. Chemical Engineering Journal. 157. 297-303. 10.1016/j.cej.2009.10.059.

[137] Relazione annuale 2021 relativa al funzionamento e alla sorveglianza degli impianti. Tecnonasic 2021, accessible at https://tecnocasic.societatrasparente.it/18/generic/26122/02-%20Relazione%20termovalorizzatore.pdf

[138] Elena Barbera, Alberto Bertucco, Sandeep Kumar, Nutrients recovery and recycling in algae processing for biofuels production, Renewable and Sustainable Energy Reviews, Volume 90, 2018, Pages 28-42, ISSN 1364-0321, https://doi.org/10.1016/j.rser.2018.03.004.

[139] “Efficiency and adaptation of the plant composting site at the Macchiareddu environmental platform" https://cacip.it/wp-content/uploads/Contenuti-per-sito-web-1.pdf

[140] The Macchiareddu industrial zone. https://cacip.it/en/what-we-do/the-macchiareddu-industrial-zone/

[141] Effect of chelating agents on the surface parameters and optical constant of CZO thin films by sol–gel process - Scientific Figure on ResearchGate. 10.1007/s10854-019-00894-0

[142] Nord, Lars O., and Olav Bolland. Carbon dioxide emission management in power generation. John Wiley & Sons, 2020.

[143] Jo Husebye, Amy L. Brunsvold, Simon Roussanaly, Xiangping Zhang, Techno Economic Evaluation of Amine based CO2 Capture: Impact of CO2 Concentration and Steam Supply, Energy Procedia, Volume 23, 2012, Pages 381-390, ISSN 1876-6102, https://doi.org/10.1016/j.egypro.2012.06.053.

8 Annex 1

8.1 Matlab Code

```
clear all
close all
clc


%create time vectors
t1=datetime(2020,01,01,00,10,00);
t2=datetime(2020,12,31,23,10,00);
tC=t1:1/24:t2;

% Load solar data previously downloaded from PVGIS
% Direct and diffused radiation on horizontal surface
data_horiz = readmatrix('Timeseries_39.185_9.019_SA2_0deg_0deg_2020_2020.csv');

%direct radiation Conversion from W/m2 to  moles /m2/s PAR
%Reis et al. 2020 (10.31062/agrom.v27i2.26527)
GTI_d_horiz= data_horiz(1:size(tC,2),2)*2.02;
%diffused radiation PAR
GTI_diff_horiz=data_horiz(1:size(tC,2),3)*2.02;

%Direct and diffused radiation on vetical surface
data_vert = readmatrix('Timeseries_39.185_9.019_SA2_90deg_0deg_2020_2020.csv');
%direct radiation Conversion from W/m2 to  moles /m2/s PAR;
GTI_d_vert= data_vert(1:size(tC,2),2)*2.02;
%diffused radiation
GTI_diff_vert=data_vert(1:size(tC,2),3)*2.02;

%import solar angle for vertical surface
solar_angle_vert=data_vert(1:size(tC,2),5);
%import solar angle for horizontal surface
solar_angle_horiz=data_horiz(1:size(tC,2),5);

%irradiance vector,
%first column direct second column diffuse
Irradiance=zeros(size(tC,2),2);
%irradiance vectorwithout shading,
Irradiance_no_s=zeros(size(tC,2),2);


%Irradiance component without shading
%are the direct and diffused
%ones as downloaded from PVGIS
```

```
%for a vertical surface
Irradiance_no_s(:,1)=GTI_d_vert(:);
Irradiance_no_s(:,2)=GTI_diff_vert(:);

%% Plot solar data

figure
subplot(2,1,1)
plot(tC,GTI_d_horiz,'-','Color',[0.8500 0.3250 0.0980])
hold on
plot(tC,GTI_diff_horiz,'-','Color',[0.9290 0.6940 0.1250])
title('Radiation component on a horizontal surface')
xlabel('Time','FontSize', 16);
ylabel(' Irradiance ( mol /m2 s)','FontSize', 16);
legend('Direct solar irradiance', 'Diffused Solar Irradiance')
ylim([0 , 2000])

subplot(2,1,2)
plot(tC,GTI_d_vert,'-','Color',[0.8500 0.3250 0.0980])
hold on
plot(tC,GTI_diff_vert,'-','Color',[0.9290 0.6940 0.1250])
title('Radiation component on a vertical surface 0   Azimuth')
xlabel('Time','FontSize', 16);
ylabel(' Irradiance ( mol /m2 s)','FontSize', 16);
legend('Direct solar irradiance', 'Diffused Solar Irradiance')
ylim([0 , 2000])

%
%% Culture parameters
%harvesting flow rate (l/d) based on polito centrifugue
%500 l/h x 16 hours operation/day
fr=500*16;

%shape parameter (Pegallapati et al. 2012)
m=1.7;

%h-1 max specific growing rate for chlorella (Zhao et al. 2015)
mu_max= 0.372/24;
%light attenuation parameter for Chlorella (Ogbonna et al. 1995)
K_coeff = 0.2; %m2/g

%g/m3 industrial harvesting concentration
C=500;
C_L=C/1000; %g/l
%micro moles/m2 s saturation irradiance for Chlorella (Polito Labs)
irr_sat=270;
```

```
% PBR material

%remaining light intensity
%after transmission loss due to PB material (glass).
trans_material_PBR = 0.95;

% shading parameters (Al-Helal et al. 2020)

%direct-to-diffuse light coefficient when shading is on
sigma=0.43;
%trasmissivity of shading
tau_shading=0.77;

% loss of biomass (%) due to respiration (Melis et al. 2009)
loss=0.30;


%%%%%% shading nets for irradiance control
% The nets are activated in those hours
% where the irradiance is above the saturation level.
% The light diffusion model with shading net is provided
% by Al-Helal et al. 2020,
% Energies https://doi.org/10.3390/en13020472

%counter of how many hours in one year is the shading system active
h_count=0;

for i=1:size(tC,2)
    dummy= GTI_d_vert(i) + GTI_diff_vert(i);
     % verify if the irradiance over the PBR surface
     % is above the saturation irradiance of chlorella
    if dummy > irr_sat
        h_count=h_count+1;
       %direct irradiance
       Irradiance(i,1)= (1-sigma)*GTI_d_horiz(i)*tau_shading;
       %diffused irradiance
       Irradiance(i,2)= sigma*GTI_d_horiz(i)*tau_shading +...
           GTI_diff_horiz(i)*tau_shading ;

    else %if irradiance is below saturation, nets are off
         %and the PBR receives as a vertical surface
        Irradiance(i,1)=GTI_d_vert(i);
        Irradiance(i,2)=GTI_diff_vert(i);
    end
end

%%% Plot the corrected irradiance
```

```
%
% figure
% plot(tC,Irradiance(:,2),'-','Color',[0.8500 0.3250 0.0980])
% hold on
% plot(tC,Irradiance(:,1),'-','Color',[0.9290 0.6940 0.1250])
% title('Corrected radiation components with active shading system')
% xlabel('Time','FontSize', 16);
% ylabel(' Irradiance ( mol /m2 s)','FontSize', 16);
% legend('Diffused solar irradiance', 'Direct Solar Irradiance')
% ylim([0 , 2000])
%
%%% %%% %max solar irradiance with shading %micromol/m2s

% Find the hour with the highest direct irradiance
[Irradiance_d_max,i_max]=max(Irradiance(:,1));
% Find the corresponding diffused irradiance
Irradiance_diff_max=Irradiance(i_max,2);


%%% %%% %max solar irradiance without shading

% Find the hour with the highest direct irradiance
[Irradiance_d_max_no_s,i_max_no_s]=max(GTI_d_vert(:,1));
% Find the corresponding diffused irradiance
Irradiance_diff_max_no_s=GTI_diff_vert(i_max_no_s);

%% Bubble column reactor geometry

% Paramenters
radius = 0.05; % in m
radius_inner=radius; %radius of the inner cylinder
height=2; % m

%reactor volume in m3

if radius>radius_inner
reactor_volume_BC=height*2*pi*radius^2 - height*2*pi*radius_inner^2 ;


else if radius == radius_inner
reactor_volume_BC=height*2*pi*radius^2; %reactor volume in m3

    end
end

reactor_volume_BC_L=reactor_volume_BC*1000; %reactor volume in l
```

```
% reactor circunference
theta = linspace(0, 2*pi, 100);

% points on the circunference
x_circle = radius * cos(theta);
y_circle = radius * sin(theta);

x_circle_inner = radius_inner * cos(theta);
y_circle_inner = radius_inner * sin(theta);

% create a fine point grid which approximates
% the generic cross section of the reactor
num_points_x = 50;
num_points_y = 50;
[x, y] = meshgrid(linspace(-radius, radius, num_points_x),...
    linspace(-radius, radius, num_points_y));

% Select only the points inside the cross section
if radius>radius_inner
    index_of_internal_points = (x.^2 + y.^2) <= radius^2 &...
        (x.^2 + y.^2) >= (radius_inner)^2  ;

else if radius == radius_inner
    index_of_internal_points = (x.^2 + y.^2) <= radius^2 ;

    end
end

x_internal = x(index_of_internal_points);
y_internal = y(index_of_internal_points);

coordinates=zeros(size(x_internal,1),2);
coordinates(:,1)=x_internal;
coordinates(:,2)=y_internal;

if radius>radius_inner
% Plot of points inside the cross section of the Bubble Column
figure;
scatter(x_internal(:), y_internal(:), 10, 'filled');
axis equal;
hold on
plot(x_circle, y_circle, 'k', 'LineWidth', 1);
plot(x_circle_inner, y_circle_inner, 'k', 'LineWidth', 1);
plot(0,-radius,'r*','LineWidth', 4);
xlabel('X (m)');
ylabel('Y (m)');
legend('Control points', 'Reactor surface',...
```

```
    'Inner Reactor surface','Sun position approximation')
title('Control points inside the reactor section');

else if radius == radius_inner
   % Plot of points inside the cross section of the Bubble Column
figure;
scatter(x_internal(:), y_internal(:), 10, 'filled');
axis equal;
hold on
plot(x_circle, y_circle, 'k', 'LineWidth', 1);
plot(0,-radius,'r*','LineWidth', 4);
xlabel('X (m)');
ylabel('Y (m)');
legend('Control points', 'Reactor surface',...
    'Sun position approximation')
title('Control points inside the reactor section');


    end
end


%calculate the depth of each point (distance from cylinder surface)
% and the distance of each point from the southern point
% which approximates the sun position
depth=ones(size(y_internal));
distance_from_S=ones(size(y_internal));

for j=1:size(x_internal)
            depth(j)= radius-sqrt(coordinates(j,1)^2 + ...
                coordinates(j,2)^2);
            distance_from_S(j)=sqrt((radius + y_internal(j))^2+ ...
            (x_internal(j))^2);
        end
%% Irradiance inside the reactor section
%labert beer law is applied considering that each point recieves:
%1) diffused irradiance that travels a distance equal
% to the point depth previously computed and
%2) direct irradiance from the southern point
% (approximation of the sun) which travels
% the distance_from_S previously computed.

irr=zeros(size(x_internal,1),size(tC,2));

for j=1:size(tC,2)
    for i=1:size(x_internal)
        irr(i,j)=trans_material_PBR*(Irradiance(j,2)*exp(-K_coeff*C*depth(i))+...
```

```
            Irradiance(j,1)*exp(-K_coeff*C*distance_from_S(i)));

    end
end

%% plot irradiance at brightest hour in the year

figure;
scatter(x_internal, y_internal,100, irr(:,i_max) , 'filled');
axis equal;
hold on
plot(x_circle, y_circle, 'k', 'LineWidth', 1);
xlabel('Asse x (cm)');
ylabel('Asse y (cm)');
title('Irradiance distribution inside the cross section of the PBR ');
colorbar;


%% Irradiance with no shading system

for j=1:size(tC,2)
    for i=1:size(x_internal)
        irr_no_s(i,j)=trans_material_PBR*(GTI_diff_vert(j)*...
            exp(-K_coeff*C*depth(i))+...
            GTI_d_vert(j)*exp(-K_coeff*C*distance_from_S(i)));
    end
end

%% plot irradiance at brightest day

figure;
subplot(2,1,1)
scatter(x_internal, y_internal, 100, irr(:,i_max), 'filled');
axis equal;
hold on
plot(x_circle, y_circle, 'k', 'LineWidth', 1);
xlabel('x (m)');
ylabel('y (m)');
title('Irradiance along the cross section with shading system ( moles /m2/s)',...
    datestr(tC(i_max)));
colorbar;
    caxis([0 270])


subplot(2,1,2)
scatter(x_internal, y_internal,100, irr_no_s(:,i_max_no_s) , 'filled');
axis equal;
```

```
hold on
plot(x_circle, y_circle, 'k', 'LineWidth', 1);
xlabel('x (m)');
ylabel('y (m)');
title('Irradiance along the cross section without shading system ( moles /m2/s)')
colorbar;
    caxis([0 270])

set(gcf, 'Position', get(0, 'Screensize'));

%% Biomass production with shading

growing_rate_BC= zeros(size(x_internal,1),size(tC,2)); %(h-1)

% dividing the reactor in as many volumes as points
% in the cross section (l)
volumes=reactor_volume_BC_L/size(x_internal,1);

Biomass_inside_volumes=zeros(size(x_internal,1),size(tC,2));

    %for every hour,the  Molina model is applied in every point.
    % Each point is representative of a volume portion of the reactor.
    % Each volume has a proper growing rate and therefore
    % a proper biomass production.
for k=1:size(tC,2)
    for i=1:size(x_internal,1)
        %growing rate in each point for each hour applying Molina
    growing_rate_BC(i,k) = (mu_max*irr(i,k)^m)/(irr_sat^m + irr(i,k)^m);
        %biomass production in each single volume for each hour in g/h
    Biomass_inside_volumes(i,k)=C_L*volumes*growing_rate_BC(i,k);
    end

end



% hourly bimass production in one single reactor
BC_hourly_biomass_production=sum(Biomass_inside_volumes,1);

% hourly bimass production in mg/l
BC_hourly_biomass_production_gl=1000*(1-loss)*...
    sum(Biomass_inside_volumes,1)/reactor_volume_BC_L;


% averaged daily productivity in g/d l
BC_avrg_daily_biomass_production=(1-loss)*...
    sum(BC_hourly_biomass_production)/(365*reactor_volume_BC_L);
```

```
% take the mean of growing rate of all the points for each hours then
% makes the mean over all year excluding null values.
BC_growing_rate_avrg= mean(nonzeros(mean(growing_rate_BC,2)));
% expected plant volume (l) to have continuous harvesting
% at desired flow rate fr
BC_plant_volume=fr/BC_growing_rate_avrg;
% expected number of Bubble Columns required
BC_n_reactors= BC_plant_volume/reactor_volume_BC_L;
% whole plant yearly biomass production in tons
BC_avrg_annual_production=((1-loss)*sum(BC_hourly_biomass_production)*...
    BC_n_reactors)*(10^-6);


%%%% Biomass production without shading system



growing_rate_BC_no_s= zeros(size(x_internal,1),size(tC,2)); %(h-1)

% dividing the reactor in as many volumes as points
% in the cross section (l)
volumes=reactor_volume_BC_L/size(x_internal,1);

Biomass_inside_volumes_no_s=zeros(size(x_internal,1),size(tC,2));

    %for every hour,the  Molina model is applied in every point.
    % Each point is representative of a volume portion of the reactor.
    % Each volume has a proper growing rate and therefore
    % a proper biomass production.
for k=1:size(tC,2)
    for i=1:size(x_internal,1)
        %growing rate in each point for each hour applying Molina
    growing_rate_BC_no_s(i,k) = (mu_max*irr_no_s(i,k)^m)/(irr_sat^m +...
        irr_no_s(i,k)^m);
        %biomass production in each single volume for each hour in g/h
    Biomass_inside_volumes_no_s(i,k)=C_L*volumes*growing_rate_BC_no_s(i,k);
    end

end


% hourly bimass production in one single reactor
BC_hourly_biomass_production_no_s=sum(Biomass_inside_volumes_no_s,1);

% hourly bimass production in mg/l
BC_hourly_biomass_production_gl_no_s=1000*(1-loss)*...
```

```
    sum(Biomass_inside_volumes_no_s,1)/reactor_volume_BC_L;

% averaged daily productivity in g/d l
BC_avrg_daily_biomass_production_no_s=(1-loss)*...
    sum(BC_hourly_biomass_production_no_s)/(365*reactor_volume_BC_L);
% take the mean of growing rate of all the points for each hours then
% makes the mean over all year excluding null values.
BC_growing_rate_avrg_no_s= mean(nonzeros(mean(growing_rate_BC_no_s,2)));
% expected plant volume (l) to have continuous harvesting
% at desired flow rate fr
BC_plant_volume_no_s=fr/BC_growing_rate_avrg_no_s;
% expected number of Bubble Columns required
BC_n_reactors_no_s= BC_plant_volume_no_s/reactor_volume_BC_L;
% whole plant yearly biomass production in tons
BC_avrg_annual_production_no_s=((1-loss)*...
    sum(BC_hourly_biomass_production_no_s)*...
    BC_n_reactors_no_s)*(10^-6);



%% plots
figure
plot(tC,BC_hourly_biomass_production_gl,'Color', [0.5, 0.5, 0],'LineWidth', 1)
hold on
plot(tC,BC_hourly_biomass_production_gl_no_s,'Color',[0.7, 0.7, 0],...
'LineWidth', 1)
xlabel('Time');
ylabel('mg/l');
title('Hourly biomass production');
legend('Active shading system','No shading system')
%%
figure
subplot(2,2,1)
yyaxis left
plot(tC,BC_hourly_biomass_production_gl,'LineWidth', 1)
ylabel('mg/l')
ylim([0 4])
hold on
yyaxis right
plot(tC,Irradiance(:,1),'LineWidth', 1);
plot(tC,Irradiance(:,2),'LineWidth', 1);
legend('Hourly biomass productivity','Direct','Diffuse')
ylabel(' moles /m2/s')
xlim([datetime(2020,01,01,00,10,00), datetime(2020,01,01,23,10,00)])
ylim([0 1600])

subplot(2,2,2)
```

```
yyaxis left
plot(tC,BC_hourly_biomass_production_gl,'LineWidth', 1)
ylabel('mg/l')
ylim([0 4])
hold on
yyaxis right
plot(tC,Irradiance(:,1),'LineWidth', 1);
plot(tC,Irradiance(:,2),'LineWidth', 1);
legend('Hourly biomass productivity','Direct','Diffuse')
ylabel(' moles /m2/s')
xlim([datetime(2020,06,01,00,10,00), datetime(2020,06,01,23,10,00)])
ylim([0 1600])


subplot(2,2,3)
yyaxis left
plot(tC,BC_hourly_biomass_production_gl_no_s,'LineWidth', 1)
ylabel('mg/l')
ylim([0 4])
hold on
yyaxis right
plot(tC,Irradiance_no_s(:,1),'LineWidth', 1);
plot(tC,Irradiance_no_s(:,2),'LineWidth', 1);
legend('Hourly biomass productivity','Direct','Diffuse')
ylabel(' moles /m2/s')
xlim([datetime(2020,01,01,00,10,00), datetime(2020,01,01,23,10,00)])
ylim([0 1600])

subplot(2,2,4)
yyaxis left
plot(tC,BC_hourly_biomass_production_gl_no_s,'LineWidth', 1)
ylabel('mg/l')
ylim([0 4])
hold on
yyaxis right
plot(tC,Irradiance_no_s(:,1),'LineWidth', 1);
plot(tC,Irradiance_no_s(:,2),'LineWidth', 1);
legend('Hourly biomass productivity','Direct','Diffuse')
ylabel(' moles /m2/s')
xlim([datetime(2020,06,01,00,10,00), datetime(2020,06,01,23,10,00)])
ylim([0 1600])



%%

%% %% nutrients requirement computation
```

```
%chlorella elemental composition
% C(1) N(0.182) O(0.339) P(0.016) S(0.003) H(1.861)
% CO2 + (0.182)NaNO3 + (0.016)K2PO4 + (0.003)MgSO4 + (1.032)H2O =
% C(1) N(0.182) O(0.339) P(0.016) S(0.003) H(1.861) +
% (0.182)NaOH + (0.003)Mg(OH)2 + (0.032)KOH + (1.5475)O2


%atomic mass (g/mol)
C_aw = 12.0107;
H_aw = 1.0079;
O_aw = 15.9940;
N_aw = 14.0067;
P_aw = 30.9378;
S_aw = 32.0650;
Na_aw = 22.9897;
K_aw = 39.0983;
Mg_aw = 24.305;

%moles in chlorella composition
C_mol = 1;
H_mol = 1.861;
O_mol = 0.339;
N_mol = 0.182;
P_mol = 0.016;
S_mol = 0.003;

%elemental weight in chlorella composition

C_w = C_aw*C_mol;
H_w = H_aw*H_mol;
O_w = O_aw*O_mol;
N_w = N_aw*N_mol;
P_w = P_aw*P_mol;
S_w = S_aw*S_mol;

chlo_aw= C_w + H_w + O_w + N_w + S_w + P_w; %(grams per mole of biomass)


%Nitrogen, given as NaNO3.
NaNO3_aw = Na_aw + N_aw + 3*O_aw; %(g/mol)
NaNO3_w = NaNO3_aw*N_mol; %(g)
% grams of NaNO3 per gram of biomass
NaNO3_req = NaNO3_w/chlo_aw;

%grams of N per gram of biomass
N_1gbiomass= (N_mol*N_aw)/(NaNO3_w)*NaNO3_req;
```

```
%Phosphorous, given as K2HPO4
K2HPO4_aw = K_aw*2 + H_aw + P_aw + O_aw*4; %(g/mol)
K2HPO4_w = K2HPO4_aw*P_mol; %(g)
% grams of K2HPO4 per gram of biomass
K2HPO4_req = K2HPO4_w/chlo_aw;
%grams of P per gram of biomass
P_1gbiomass = (P_mol*P_aw)/(K2HPO4_w)*K2HPO4_req;

%Sulphur, given as MgSO4
MgSO4_aw = Mg_aw + S_aw + O_aw*4;
MgSO4_w = MgSO4_aw*S_mol;
MgSO4_req = MgSO4_w/chlo_aw;

%grams of S per gram of biomass
S_1gbiomass = (S_mol*S_aw)/(MgSO4_w)*MgSO4_req;

%carbon dioxide
CO2_aw = C_aw + O_aw*2;
CO2_w = CO2_aw*C_mol;
CO2_req = CO2_w/chlo_aw;

%grams of C per gram of biomass
C_1gbiomass = (C_mol*C_aw)/(CO2_w)*CO2_req;

%annual requirements (tons/year)
%tons of CO2 required per year
CO2_annual_req = BC_avrg_annual_production*CO2_req;
%tons of C required per year
C_annual_req = BC_avrg_annual_production*C_1gbiomass;

%tons of NaNO3 required per year
NaNO3_annual_req = BC_avrg_annual_production*NaNO3_req;
%tons of N required per year
N_annual_req = BC_avrg_annual_production*N_1gbiomass;

%tons of MgSO4 required per year
MgSO4_annual_req = BC_avrg_annual_production*MgSO4_req;
%tons of S required per year
S_annual_req = BC_avrg_annual_production*S_1gbiomass;

%tons of K2HPO4 required per year
K2HPO4_annual_req = BC_avrg_annual_production*K2HPO4_req;
%tons of P required per year
P_annual_req = BC_avrg_annual_production*P_1gbiomass;
```